

**ESTABLISHMENT OF A REPEATABLE TEST
PROCEDURE FOR MEASURING ADHESION
STRENGTH OF PARTICULATES IN
CONTACT WITH SURFACES**

ERTAN ERMIS

A thesis submitted in partial fulfilment of the requirements of the
University of Greenwich for the Degree of Doctor of Philosophy

This research programme was carried out in collaboration with the Technical University
of Munich under 'Bio-Powders' Marie Curie RTN, EU 6th FP.

Project No: EU MRTN-CT-2004-512247

December 2011

DECLARATION

I certify that this work has not been accepted in substance for any degree, and is not concurrently being submitted for any degree other than that of Doctor of Philosophy (PhD) being studied at the University of Greenwich. I also declare that this work is the result of my own investigations except where otherwise identified by references and that I have not plagiarised the work of others.

Mr. Ertan Ermis,

PhD Candidate

Supported by

Prof Mike Bradley

First Supervisor

ACKNOWLEDGEMENTS

I would like to thank EU Marie-Curie Research Training Network ‘Biopowders’ programme and the Wolfson Centre for Bulk Solids Handling Technology at The University of Greenwich for financial support.

Special thanks go to my first and second supervisors, Prof Dr. Mike Bradley and Dr. Rob Berry for providing me with an interesting and challenging topic. I am also grateful to Mr. Richard Farnish for guidance, for valuable and constructive comments and inspiring discussions. Thanks also to Mrs. Caroline Chapman for her effort on doing paper work and for her support in terms of administration during my research period.

Thanks go to my research colleagues and friends for their support and warm conversations. Warm thanks go to Prof Dr. Karl Sommer and Dr. Elisabeth Kuschel for their warm welcome and support during my secondment period in Germany.

I would also like to express my gratefulness to all members of the ‘Biopowders’ research training network, especially the coordinator Dr. John Fitzpatrick from The University Collage Cork (UCC) for managing the whole project. My thanks also go to all my fellow PhD students, their supervisors, and the other people participating in the meetings, conferences and courses in Budapest, Tromso, and in Massy for sharing their scientific work and discussions.

I specially thank my wife for her pertinent advice, patience, and great support during the final year of my PhD programme.

Finally I would like to thank my parents and my siblings for their love, encouragement and constant support throughout my studies.

ABSTRACT

The firm adhesion of flavouring particles onto snack surfaces during coating processes is a major concern in the snack production industry. Detachment of flavouring powders from products during handling and production stages can lead to poor appearance and reduced taste of the product as well as substantial financial losses for the industry, in terms of variable flavour performance and extended cleaning down time of fugitive particle build-up on process equipment. Understanding the adhesion strength of applied bulk particulates used for flavouring formulations will help analysts to evaluate the efficiency of coating processes and potentially enable them to assess the adhesion strength of newly formulated flavouring powder prior to commitment to full scale plant trials.

Meeting this object has required the development of an over-arching review of the adhesion mechanisms as a primary step. Based on this overview to the work of previous researchers, technological gaps and promising techniques have been identified for further research and development. A prototype of a novel adhesion tester called an Impact Adhesion Tester (IAT) has been designed and constructed. The development of the overall tester design is presented, and details of its parts and the resulting tester are discussed.

The IAT and its experimental procedure were primarily designed and implemented for use in the snack industry, in particular, for the measurement and evaluation of the key factors affecting the adhesion behaviour of flavour powder onto snack surfaces qualitatively and quantitatively. This measurement can indicate the percent flavour powder loss within production stages (from coating to packing) and in package.

The instrument has been evaluated using different materials and substrates subjected to different coating conditions such as rotational speed of the drum, retention time in drum, the amount of surface oil and the amount of powder applied. By plotting the detachment versus impact force, the difference has been obtained between adhesion strength of different flavouring powders (which is a strong function of particle size, particle shape, particle density and surface oil content of the snack). In addition to the above work, ultra-centrifuge method was used as a reference for comparison.

The research work conducted using IAT on flavouring powders has proved the importance of particle adhesion strength and that the particle adhesion strength can reflect the changes in particle loss, based on particle characteristics as well as process conditions during snack production. It proved that bench size IAT would be a useful tester to measure adhesion strength of particles. The results obtained from experiments have confirmed that the tester may be able to usefully determine the variations between different powder materials. However the tester needs to be further evaluated by industrialists and researchers before possible use or commercialisation.

AUTHOR'S NOTE

Some parts of the work presented in this thesis have been published in the following articles:

Ermis, E., Farnish, R.J., Berry, R.J., Bradley, M.S.A. 2011. Centrifugal tester versus a novel design to measure particle adhesion strength and investigation of effect of physical characteristics (size, shape, density) of food particles on food surfaces. *Journal of Food Engineering* 104: 518-524.

Ermis, E., Farnish, R.J., Berry, R.J., Bradley, M.S.A. 2010. Centrifugal tester versus a novel design to measure particle adhesion strength and investigation of effect of physical characteristics (size, shape, density) of particles. *Bulk Solids Europe 2010 Conference*, Glasgow.

Ermis, E., Farnish, R.J., Berry, R.J., Bradley, M.S.A. 2009. Direct Measurement of Powder Flavor Adhesion onto a Crisp Surface Using a Novel Adhesion Tester. *Particulate Science and Technology*, 27: 362-372.

Ermis, E., Farnish, R.J., Berry, R.J., Bradley, M.S.A. 2007 Direct Measurement of Powder Flavour Adhesion onto a Food Surface Using a Novel Adhesion Tester. *Proceedings of International Symposium Reliable flow of Particulate Solids 4*, 803-810.

CONTENTS

DECLARATION.....	i
ACKNOWLEDGEMENTS	ii
ABSTRACT	iii
AUTHOR’S NOTE.....	v
CONTENTS	vi
LIST OF FIGURES	ix
LIST OF TABLES.....	xii
CHAPTER 1 INTRODUCTION AND LITERATURE REVIEW	1
1.1 Introduction.....	1
1.1.1 Motivation and objectives.....	3
1.2 Literature review	6
1.2.1 Snack foods	6
1.2.1.1 Common ingredients used for extruded snacks.....	7
1.2.1.2 Snack food production	10
1.2.1.2.1 Extrusion and dough formation techniques.....	11
1.2.1.2.2 Frying and Baking.....	12
1.2.1.3 Particulate ingredients in the snack industry	12
1.2.1.3.1 Application of snack seasoning	13
1.2.1.3.2 Methods of application.....	14
1.2.1.3.2.1 Blending drum application.....	16
1.2.1.3.2.2 Conveyor belt-type systems.....	18
1.2.1.3.2.3 Electrostatic powder coating.....	19
1.2.1.3.3 Factors influencing the coating efficiency	22
1.2.1.3.3.1 Flow of seasoning.....	22
1.2.1.3.3.2 Processing conditions	22
1.2.1.3.3.3 Adhesion mechanisms	26
1.2.2 Characterisation of food powders.....	29
1.2.2.1 Particle size.....	30
1.2.2.1.1 Dry Sieving.....	32
1.2.2.1.2 Laser diffraction (lasersizer).....	34
1.2.2.2 Powder density and porosity	35
1.2.2.3 Flowability.....	37

1.2.2.3.1	The Hausner ratio.....	38
1.2.2.3.2	Carr's compressibility index.....	39
1.2.2.3.3	Compressibility.....	39
1.2.2.3.4	Angle of repose.....	39
1.2.2.3.5	Friction.....	41
1.2.2.4	Methods for measuring particle adhesion.....	44
1.2.2.4.1	Atomic force microscope (AFM).....	44
1.2.2.4.2	Centrifugal detachment.....	45
1.2.2.4.3	Detachment field method.....	46
1.2.2.4.4	Ultrasonic vibration.....	46
1.2.2.4.5	Aerodynamic technique.....	47
1.2.2.4.6	Impact separation.....	48
1.2.2.4.7	Comparison of the techniques.....	48
1.2.3	Recent works on particle adhesion.....	52
1.2.3.1	Centrifuge technique.....	52
1.2.3.2	Liquid/gas flow.....	55
1.2.3.3	Atomic force microscope (AFM).....	56
1.2.3.4	Detachment field method.....	57
1.2.3.5	Vibration method.....	58
1.2.3.6	Summary of test procedures.....	59
1.2.4	Theoretical adhesion models.....	62
1.2.5	Texture analysis.....	63
1.2.6	Summary of the literature review.....	64
CHAPTER 2 MATERIAL AND METHODOLOGY		66
2.1	Introduction.....	66
2.2	Test Equipment.....	67
2.2.1	Evaluation of design of a novel adhesion tester.....	67
2.2.1.1	Development of Impact Adhesion Tester (IAT).....	68
2.2.1.2	Deceleration measurement of the IAT.....	73
2.2.1.2.1	Choosing the right accelerometer.....	73
2.2.1.2.2	Experimental set up for calibration.....	76
2.2.1.3	Tumbler mixer for powder coating.....	77
2.2.1.4	Vibratory flavour applicator.....	80
2.2.1.5	Experimental procedure of the IAT.....	84
2.2.2	Texture analyser.....	86

2.2.3	Pycnometer.....	87
2.2.4	Sieves.....	88
2.2.5	Centrifuge Tester.....	89
2.2.6	Balance.....	92
2.3	Test materials used for particle adhesion testing.....	92
2.3.1	SEM Image Analysis of Crisp Substrates.....	94
2.3.2	SEM Image Analysis of Flavouring Powders.....	99
2.3.3	Microscope image analysis of salt and glass particles.....	100
2.4	Problems and limitations.....	101
CHAPTER 3 THEORETICAL CALCULATIONS VERSUS EXPERIMENTAL RESULTS.....		102
3.1	Inferred total adhesion force from theoretical calculations.....	102
3.2	Total force acting on particles during deceleration of plate of IAT.....	106
3.3	Comparison of the theoretical adhesion force with the force acting on particles during deceleration.....	109
CHAPTER 4 RESULTS AND DISCUSSION		111
4.1	Results obtained.....	111
4.1.1	Fracture test.....	112
4.1.2	Impact force generation of IAT.....	114
4.1.3	Size analysis of the flavour powder systems.....	116
4.1.4	Particle density.....	117
4.1.5	Effect of particle size on adhesion strength.....	118
4.1.6	Effect of particle shape on adhesion strength.....	123
4.1.7	Effect of the amount of surface oil on particle adhesion strength.....	124
4.1.8	Effect of other process characteristics on particle detachment.....	125
4.1.9	Adhesion behaviour of different flavour powders.....	126
4.1.10	Reproducibility of the test procedure.....	127
4.2	Comparison of results to centrifugal tester.....	128
4.3	Discussion of different techniques and relevance of the data obtained to findings of this study.....	131
CHAPTER 5 CONCLUSIONS AND FUTURE WORK.....		134
5.1	Introduction.....	134
5.2	Development of an adhesion tester.....	135
5.3	Selection of a test substrate.....	135
5.4	Characterisation of flavour powders.....	136

5.5	Characterisation of adhesion strength of powders	136
5.6	Recommendations and Future Work.....	140
REFERENCES		142
APPENDICES.....		151
Appendix 1.	Dimensions of platen of IAT	151
Appendix 2.	Parts of IAT and their dimensions	152
Appendix 3.	Dimensions of IAT	153
Appendix 4.	Dimensions of tumbler mixer	154
Appendix 5.	Dimensions of vibratory feeder	155
Appendix 6.	Acceleration of dropped objects	156
Appendix 7.	Calibration certificate of IEPE accelerometer	162
Appendix 8.	Crisp production process flow diagram.....	163

LIST OF FIGURES

Figure 1-1.	Flavour particle built-up on the top of the packing unit	2
Figure 1-2.	A novel adhesion tester: Impact Adhesion Tester (IAT).....	4
Figure 1-3.	Examples to first, second and third generation snacks from left to right: potato chips, tortilla chips and fry type extruded snack.....	6
Figure 1-4.	Schematic cross section view of a typical loss-in-weight gravimetric feeder.....	14
Figure 1-5.	Tumbler for flavour coating on snack products.	16
Figure 1-6.	Schematic side view of fold-in action in drum	17
Figure 1-7.	Schematic diagram of typical flavour coating in tumbler mixer.....	18
Figure 1-8.	Schematic view of conveyor belt coating system.....	19
Figure 1-9.	Schematic view of a charged spray gun.....	20
Figure 1-10.	Electrostatic coating of tortilla chips, a) schematic view, b) a photo from production line.....	21
Figure 1-11.	Interaction forces acting on flavour powder (from 20 to 600 μm) particles on crisp surface.....	26
Figure 1-12.	Shematic view of a droplet resting on a solid surface.	29
Figure 1-13.	Classification of powder as a function of the particle size.....	31
Figure 1-14.	An example view of a laboratory test sieve	32
Figure 1-15.	Typical laser diffraction instrument layout.	34
Figure 1-16.	Angle of repose method.....	40
Figure 1-17.	Examples to methods to measure angle of repose.....	40

Figure 1-18. Schematic drawing of Jenike’s Shear Tester.....	42
Figure 1-19 a) Construction of a yield locus. S, shearing force reached during consolidation (N); F, unconfined yield strength (N); V, normal force applied to a shear cell during consolidation(N); b) flow functions (unconfined yield strength against maximum consolidation stress) of 4 different food powders (temperature of 20°C and 25% RH)	42
Figure 1-20. Wolfson Annular Shear Tester	43
Figure 1-21. Schematic view of the rotation.....	45
Figure 1-22. Adhesion testing by using air flow a) parallel and b) perpendicular to surface.	47
Figure 1-23. Pendulum shock testing machine	48
Figure 1-24. Schematic diagram of substrate housing in centrifuge rotor.....	53
Figure 1-25. Schematic diagram of substrate housing in the head of centrifuge.	54
Figure 1-26. Wind tunnel experimental setup and schematic drawing of rectangular channel	56
Figure 1-27. Colloidal probe technique in an atomic force microscope.....	57
Figure 1-28. Experimental setup of detachment field method for adhesion force measurements of particles	58
Figure 1-29. Schematic diagram of the vibration experimental apparatus	59
Figure 1-30. Support used to measure texture of potato chips.....	63
Figure 1-31. Typical force-deformation curve representing results by using Universal Testing Machine	63
Figure 2-1. Cross sections of main parts of the Impact Adhesion Tester (IAT).	69
Figure 2-2. Main parts of Impact Adhesion Tester (IAT).....	71
Figure 2-3. Sample holder.....	71
Figure 2-4. Specially designed placing tool and substrate placing.....	72
Figure 2-5. IEPE Accelerometer	74
Figure 2-6. G logger set	75
Figure 2-7. Acceleration data logger and coupler	76
Figure 2-8. Deceleration experimental set-up.....	77
Figure 2-9. Cross section and side view of tumbler mixer.	78
Figure 2-10. A sketch of the laboratory scale rotating drum.	79
Figure 2-11. Speed controlled Electrical drive unit.....	79
Figure 2-12. Vibratory feeder unit and placing in tumbler mixer	81
Figure 2-13. Vibratory feeding conveyor	82

Figure 2-14. Powder (salt) flow on vibratory conveyor	83
Figure 2-15. A view from a side of tumbler mixer after powder coating.....	83
Figure 2-16. Diagram of experimental procedure	85
Figure 2-17. QTS Texture Analyser (Brookfield).....	86
Figure 2-18. Schematic drawing of experimental design of crack strength test. a) before and b) after deformation of substrate.....	87
Figure 2-19. AccuPyc 1330 pycnometer.....	88
Figure 2-20. Sieves with agitator.....	88
Figure 2-21. Particle size distribution of a powder sample.....	89
Figure 2-22. Placing of veneer substrate into a centrifuge tube specially designed for substrate housing	90
Figure 2-23. A view of a centrifuge head and an illustration of substrate placing.....	91
Figure 2-24. Ohaus Explorer 4 digit balance	92
Figure 2-25. Backscattered electron SEM images of representative portions of crisp samples.....	95
Figure 2-26. Backscattered electron SEM images of representative portions of prawn cocktail flavoured crisp samples:.....	96
Figure 2-27. Backscattered electron SEM images of representative portions of Salt and Vinegar flavoured crisp samples:.....	97
Figure 2-28. Backscattered electron SEM images of representative portions of Cheese and Onion flavoured crisp sample:.....	98
Figure 2-29. SEM images of flavouring powders a, cheese and onion; b, prawn cocktail; c, salt and vinegar	99
Figure 2-30. Glass particles under microscope	100
Figure 3-1. Log chart of adhesion forces acting on particles	105
Figure 3-2. Calculated total adhesion forces versus particle size.....	106
Figure 3-3. Experimental forces acting on particles for different powder material from experimental data.....	108
Figure 3-4. Comparison of theoretical total adhesion force to total forces acting on single particle (at 10 and 100 g decelerations) versus particle size.....	110
Figure 4-1. Force-deformation curve of crisp substrate.....	112
Figure 4-2. Normal distribution of fracture strength of different crisp substrates	113
Figure 4-3. Impact force generation over drop heights.....	114
Figure 4-4. A snapshot from oscilloscope.....	115

Figure 4-5. Deceleration peaks obtained by using Hobo wireless accelerometer from 1 mm drop distance.....	116
Figure 4-6. Cumulative size distribution of different flavour powders	116
Figure 4-7. Salt particles under an optical microscope:.....	119
Figure 4-8. Distribution of mean value of % detached particles versus number in sample for different size fractions	120
Figure 4-9. Distribution of mass of coated and detached particles versus number in sample for different size fractions	121
Figure 4-10. Percentage of salt particles detached as a function of particle size and force acting on particles (by using IAT).....	122
Figure 4-11. Percentage of glass particles detached as a function of particle size, particle shape and force acting on particles (by using IAT).....	123
Figure 4-12. Effect of surface oil content on particle loss of salt	124
Figure 4-13. Effect of different process parameters on particle adhesion	125
Figure 4-14. Percent particle loss of different flavour powders over deceleration forces.....	126
Figure 4-15. Repeatability results of % particle loss at 48 g	127
Figure 4-16. Repeatability results of % particle loss at 105 g.....	128
Figure 4-17. Percentage of salt particles detached as a function of particle size and force acting on particles (by using centrifuge).....	129
Figure 4-18. Comparison of adhesion forces reported in this PhD thesis to other researcher's findings.	132

LIST OF TABLES

Table 1-1. Typical formula for baked snacks (Second generation snacks)	8
Table 1-2. Typical third generation snack formulations	9
Table 1-3. Particle densities of some powdered material used by Otsuka et al. (1988). ..	24
Table 1-4. The solid densities of the major components	35
Table 1-5. Some characteristics and factors affecting powder flowability.....	37
Table 1-6. Hausner ratios of powder flow behaviour	38
Table 1-7. Description of some techniques for adhesion force measurement	49
Table 1-8. Summary of results obtained from different research work on adhesion.	61
Table 2-1 Basic specifications of chosen accelerometer	74
Table 2-2 Basic specifications of data logger	75

Table 2-3. Classification of particle size ranges.....	93
Table 3-1. Numerical values used in calculation of adhesion forces	104
Table 3-2. Calculated adhesion forces acting on particles.....	105
Table 3-3. Mean mass of a single particle of powder materials used.....	107
Table 4-1. Particle densities of powder material.....	117
Table 4-2. Calculated average force (N) acting on salt particles at different rotational speeds	128

CHAPTER 1

INTRODUCTION AND LITERATURE REVIEW

1.1 Introduction

The history of snack production is relatively old. The pretzel is known to be produced after 610 AD in southern France and tortilla chips have origins in Mesoamerica where corn masa has been used in snack making for centuries.

Snack foods, which are flavoured with savoury and salty flavourings such as cheesy crisps (the term – crisps - refer to many different types of snack products in the UK and Ireland, some made from potato, but may also be made from maize and tapioca), potato chip and corn chip are relatively new in the food market (being developed into the form that they currently exhibit within the last four decades (Kunzt, 1996; Guy, 2001).

Snack foods constitute an important activity within the food and drinks industrial sector and account for annual sales of more than \$25 billion world-wide (Enggalhardjo, and Narsimhan, 2005; Kunzt, 1996). They are packaged in a variety of forms (plastic bags, cardboard tubes, etc.). The customer perception of the quality of these products is mainly influenced by features such as texture, shape, colour, flavour, and nutritional content. The snack industry is constantly striving to obtain a competitive advantage by either optimising their product quality or reducing waste (Yu and MacGregor, 2003). Another form of competitive advantage lies in the development of new flavourings and snack types. The development of new flavours and the prediction of their adhesion performance at full scale production are becoming important.

There is increasing demand on delivering ‘healthy’ foods, by reducing salt, sugar and fat loadings (Wong et al, 2005). This should be achieved without reducing flavour performance and perceived texture by understanding the adhesion behaviour of flavour

powders by using a test procedure while decreasing the amount of salt or sugar and oil content of the product.

Seasoning is applied to many snack products, after they are either fried or baked, in order to provide a specific flavour before they are sent to packaging. Seasoning can serve to bring out and compliment the flavour of the snack to which it is applied and therefore can play an important role in the flavour and appearance of a coated snack and greatly influence its acceptability to customers (Kunzt, 1996; Wong et al, 2005; Buck and Barringer, 2007; Gould, 1999). One of the most important problems experience by snack industry is the lack of control over the quantity of seasoning applied to the food substrate and the consistency of its distribution of the coating over the surface (Buck and Barringer, 2007). Most manufacturers intentionally over-apply coating powders in order compensate for unequal flavour distribution on the surface and particle detachments during inter-plant transportation due to vibration, shock and impact resulting from production and handling machinery (Sumawi and Barringer, 2005). No data was found in literature review about the magnitude of forces acting on snacks during production.

Problems caused by deposition of detached powder can be seen in Fig. 1-1.



Figure 1-1. Flavour particle built-up on the top of the packing unit (Photo courtesy of United Biscuits Plc).

The detachment of applied flavouring powders from food substrates during handling and packaging stages can lead to substantial financial losses (current coating technologies often operate with an accepted particle loss rate) for the industry in terms of variable flavour performance and extended cleaning down time of fugitive particle build-up (Fig. 1-1) on process equipment and production machinery/measuring devices (Salazar-Banda et al, 2007; Buck and Barringer, 2007).

This PhD project aims to establish and further expand the knowledge base relating to the application of flavour and other value enhancing powder coatings onto food products. A test equipment, designed to evaluate particle adhesion on a macro level, has been constructed to be relevant to industrial need (particle drop-off in handling before packing). The particulate adhesion performance is studied as a function of process history, particulate formation and environmental influences. Understanding the adhesion strength of applied bulk particulates used for flavouring will help analysts to evaluate the efficiency of coating processes and potentially enable them to assess the adhesion strength of newly formulated flavouring powder prior to commitment to full scale plant trials.

1.1.1 Motivation and objectives

This PhD project is concerned with developing a bench scale adhesion tester (Fig. 1-2) capable of delivering a level of data of use to industrialists and which would enable an evaluation of potential issues associated with particle adhesion. A primary consideration has been to incorporate design features or operational practices that would best serve to overcome some of the limitations of promising tests (such as associated single particle detachment). The most important design/technical variables that must be quantified or controlled in order to conduct the proposed new test technique are the deceleration value of the plate and the controlled coating consistency of the test substrates. The deceleration values of the tester should be kept constant for different experiments (since this is directly related to the proportion of particle detachment following impact) at the same drop heights and the consistency of coating should be uniform and equal throughout the batch of surfaces being tested.

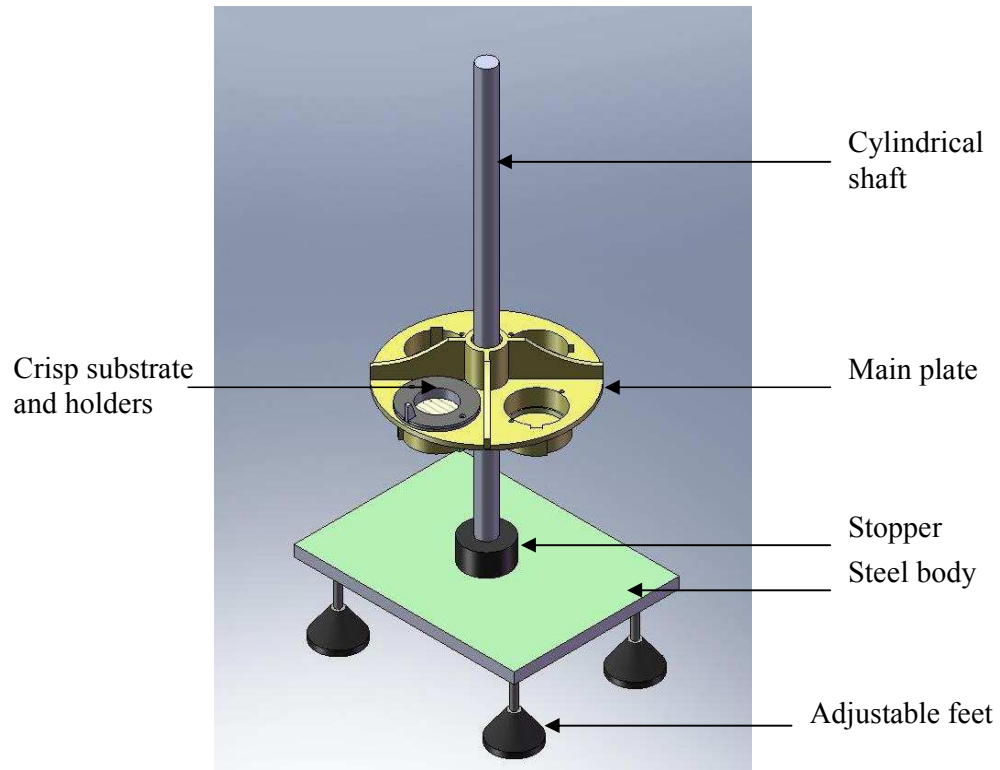


Figure 1-2. A novel adhesion tester: Impact Adhesion Tester (IAT)

In addition to the functional aspects of the tester, a secondary requirement exists in the need for the equipment to be portable and require a relatively small bench “foot print” so that the tester could potentially be used to conduct the test procedure adjacent to production lines in the factory.

This project involved designing/constructing a prototype adhesion tester together with development of its experimental procedure (performing preliminary laboratory tests and conducting a feasibility study of measuring the adhesion strength of different powders onto crisp surface in the laboratories of The University of Greenwich, UK and Technical University of Munich, Germany).

The premise of the new tester is that a measure of the adhesion strength of particles onto surfaces is detachment force, which is measured as nN (nano Newton) and that this force can be correlated to the mass loss of particles resulting from controlled impact forces induced by the operation of the test apparatus. The results were statistically treated to obtain the mean adhesion force of the particles. The technique which has been

developed can be used to measure the adhesion force among particles of organic and inorganic nature, and particles with irregular shapes and rough surfaces. Additionally, it has the advantage of determining the adhesion force of poly-dispersed powdery materials. The results relate to particle size and therefore mean value of particle size for a given bulk material need to be calculated.

Determination of the influence of factors such as particle size, particle shape, surface oil content, coating retention time etc. dominate adhesion onto crisp substrate and can be evaluated using the new tester.

1.2 Literature review

This opening chapter describes the rationale behind the study of this research project on understanding the adhesion characteristics of particulate ingredients to food products. The work is centred on characterisation of the adhesion of powder material onto food surfaces and establishing a test procedure to measure the adhesion strength at different processing conditions (tumbling speed in coating process, amount of surface oil on food substrate, physical characteristics of flavour powder used etc.). There is a fundamental need to determine what causes certain powders to offer superior adhesion during coating process. The impetus of this research has been driven by the potential benefits that could be derived through the optimisation of particle size distributions or controlled surface morphology of flavouring particles in terms of reduced fugitive particle generation through handling and packing processes.

1.2.1 Snack foods

According to Hui (2006), snack manufacturers use three main terms to identify the snacks: (i) first generation snack, (ii) second generation snack, and (iii) third generation snack (Fig. 1-3). For the first category, the natural products used for snacking, nuts, potato chips and popped popcorn can be considered. Single ingredient snacks, simple shaped products such as tortilla chips and all directly expanded snacks fall into the second category. The third category includes multi ingredients formed snacks and pellets made by extrusion cooking.



Figure 1-3. Examples to first, second and third generation snacks from left to right: potato chips, tortilla chips and fry type extruded snack.

Hay (2001) classifies the snack food as:

- Raw cut vegetable snacks: based on frying of thinly cut fresh potato
- Formed dough products from potato derivatives: dried potato derivatives are used to make dough and dough is formed by extrusion or sheeting and cut into small pieces such as chips.
- Formed dough products from maize derivatives: pre-cooked grains are milled to make dough and extruded to cut them into small pieces.
- Half-product or pellet snacks: the dough may be mixed with pre-gelatinised starch-based raw materials. This category is very similar to formed dough products.
- Directly expanded extruded snacks: raw maize grits are fed into an extruder at low moisture to create a very hot melt within the barrel at temperatures of 140 to 180 degree. As the pressure is released the melt stream generates water vapour and expands in microseconds to form foam, which is cut into small pieces by a rotating knife.
- Popcorn and buffet wheat: popping and puffing is formed by heating the cereals such as corn, wheat and rice on pans or in chambers.
- Related processes, such as snack biscuits and breadsticks: one or more of the processing techniques such as heating and dehydration described above can be used to produce this group of products.

1.2.1.1 Common ingredients used for extruded snacks

The most common sources of base ingredient are corn, wheat, rice, potato, tapioca, and oats (Hui, 2006). A major ingredient in snack food formulation is starch although there are several other sources of ingredients for snack food all around the world (Hui, 2006). The starch is insoluble, tasteless, and not digestible or useful for human use without cooking (Hui, 2006). The most common cereals used in snack food production are corn, wheat, rice, and oats as given examples of typical snack composition in Table 1-1 and Table 1-2.

Table 1-1. Typical formula for baked snacks (Second generation snacks)

Ingredients	Amount (%)
High protein snack	
Rice flour	35
Wheat flour	35
Soy concentrate	20
Sugar	6
Corn starch	2
Vegetable oil	2
Potato stick snack	
Potato granules	64
Degermed corn meal	35
Vegetable oil	1
Corn curls	
Degermed corn meal or grits	100

Reference: Hui, 2006.

Corn

Corn which is also called as maize is a primary ingredient for many pellet products (Hui, 2006). Cornmeal, corn grits, corn flour and corn cones are different forms of dry-milled dent corn and generally vary in particle size distribution (Hui, 2006).

Wheat

Wheat flour is used in formulations to make baked or fried snacks, flavoured crackers, snack cakes, pretzels, bread and the like (Hui, 2006). Semolina which is produced from hard wheat milling is also used in snack production (Hui, 2006). Snack foods with all semolina will have a very crispy texture (Hui, 2006). Wheat is rich in protein (%8-15) when it is compared to other cereals and gluten provides nutritional value, crispness and desired texture (Hui, 2006). Reduced gluten wheat flour will give more tender expanded product than semolina, or hard varieties (Hui, 2006). The use of wheat in snack formulations is limited due to cost (Hui, 2006).

Rice

One major reason of using rice in snack food formulations is the cost of it as compared to other snack food ingredients (Hui, 2006). Flavours from different rice varieties have

some differences in physical and chemical properties, which can affect the snack cell structure and expansion (Hui, 2006).

Table 1-2. Typical third generation snack formulations

Ingredients	Amount (%)
Corn based	
Hard, crunchy texture	
Ground corn	94.5
Corn starch	5
Monoglyceride	0.5
Soft, frothy texture	
Corn starch	55.2
Wheat starch	27.5
Tapioca starch	14
Liquid shortening	2.5
Monoglyceride	0.8
Potato based	
Hard and crunchy	
Potato flakes	49
Durum flour	30
Wheat starch	20
Monoglyceride	1
Crispy	
Potato flakes	47
Durum flour	30
Wheat starch	20
Vegetable oil	3
Soft	
Potato flakes	47
Corn flour	30
Wheat starch	20
Monoglyceride	1
Speciality snacks	
Fresh shrimp recipe	
Tapioca starch	64
Fresh shrimp	20
Rice flour	10
Vegetable oil	3
Salt	3
Pepper seasoning	1

Reference: Hui, 2006.

Oats

Oats were found to reduce serum cholesterol level in human body and that increased the market value of oat brans in snack food industry (Hui, 2006). Oats have high oil content (%7-9) and lipase enzyme (Hui, 2006). Lipase can catalyze the hydrolysis of oil and hence increasing the level of bitter testing free fatty acids (Hui, 2006). For this reason, lipase enzyme should be inactivated before using in snack production (Hui, 2006).

Potato

Potato is one of the main raw materials to produce snack food. Either it is cut into thin pieces before frying in vegetable oil or potato starch is isolated and used in snack dough before forming into different shapes and baking or frying (Guy, 2001). In a standard recipe the bulk of the raw materials might be potato granules with 20-30% of flakes and 0-5% of starch. The materials will form dough with 30-40% water w/w by mixing in mixers (Guy, 2001).

1.2.1.2 Snack food production

There are three stages in the formation of all snacks (Guy, 2001):

1. The formation of a dough by hydration of starch polymers so that they form a mass that can be shaped into pieces.
2. Water in dough is superheated and released rapidly as vapour within the dough mass by heat treatment.
3. The snack is stabilised by being dried to low moisture levels to form a hard brittle structure.

Since it is not possible to discuss all snack production techniques in detail, only two of the major production methods which are extrusion and dough formation techniques will be discussed in this part.

Common steps of snack food production are outlined in Appendix 8.

1.2.1.2.1 Extrusion and dough formation techniques

Food extrusion is defined as the process in which a mixture of material forced to flow, under certain mixing, heating and shear conditions through a designed die to give the mixture desired shape and form (Hui, 2006; Guy, 2001; Brennan, 2006). The food extruders can transform a variety of raw ingredients into intermediate and finished products (Hui, 2006; Brennan, 2006). During extrusion the temperature could be as high as 180-190 °C and the residence time could be up to 30 seconds (Hui, 2006). Several different shapes, texture, color, and appearances can be processed by little changes in the design of the extruder and processing conditions (Hui, 2006). Extrusion process is low cost production technique compared to other processes and result in better quality of the products (Hui, 2006). It is suitable for heat sensitive material due short retention time at high cooking temperatures (Hui, 2006).

Snack extruders can be divided into two main categories: (i) single-screw and (ii) twin-screw extruders (Brennan, 2006). Single screw extruders can be further be divided into different categories such as low shear forming, low shear cooking, medium shear cooking, and high shear cooking extruders (Brennan, 2006; Hui, 2006). Twin screw extruders can also be divided into four different categories such as co-rotating intermeshing, co-rotating non-intermeshing, counter-rotating intermeshing, and counter-rotating non-intermeshing (Brennan, 2006; Hui, 2006).

Many common snack foods such as fried or baked are produced by single-screw extruders (Hui, 2006). However, the twin-screw extruders have been used widely for the new generation snack foods which have new and complex ingredients, different shapes and color (Hui, 2006).

The alternative to extrusion forming is sheeting and cutting. This process needs cohesive and elastic dough (Guy, 2001). The idea of forming the potato dough is that every crisp should have the same shape and can be stacked together easily (Guy, 2001). However, frying these formed chips does not match the appearance or texture of cut potato chips (Guy, 2001).

1.2.1.2.2 Frying and Baking

The cutted potato chips (20-22% solid content) or formed snack dough pieces should be fried at a high temperature of 185 to 190 °C in vegetable oil or baked in an oven (Guy, 2001). At this temperature they change from dough to dried crispy pieces in 12-15 s and the colour changes into brownish which is a result of Maillard, non-enzymatic browning reaction as they dry out (Guy, 2001; Brennan, 2006). Frying can be divided into two groups: (i) batch frying, (ii) continuous frying (Brennan, 2006).

1.2.1.3 Particulate ingredients in the snack industry

In snack industry, most snack foods are typically enhanced by seasoning the product with flavoured coatings, which are generally in powder form (Fitzpatrick and Ahrne, 2005; Yu and MacGregor, 2003; Wong et al, 2005). According to Shrankel (2004), flavourings are a unique class of food ingredients and excluded from the legislative definition of a food additive because they are regulated by flavour legislation and not food additive legislation. Schrankel (2004) defined flavour as the sum total of the sensory responses of taste and aroma combined with the general tactile and temperature responses to substances placed in the mouth, and further stated that flavour can also mean any individual substance or combination of substances used for the principal purpose of eliciting these responses.

The major reason for production of flavouring in powder form is simply to prolong the shelf-life of the ingredient by reducing water content and to prevent the ingredient from degradation. The major functionalities of food ingredients were classified in three categories by Fitzpatrick and Ahrne (2005); (i) Nutritional such as vitamins, nutraceuticals (ii) Physical/Chemical such as gelation, emulsification, foaming, pH control (iii) Organoleptic such as colour, smell, taste and texture.

Most snack food may be seasoned with a wide variety of seasoning agents and flavours, including sweet, salty, and savoury flavours. Kuntz (1996) has observed that the most important flavours tend to fall into two categories: (i) Dairy, such as cheese or sour cream and (ii) Tomato-based, such as barbecue and salsa. According to Lusas and Rooney (2001) (Kunzt, 1996), seasonings for salty snacks are blends of salt, dairy

powders, vegetable powders, flavour enhancers, spices, compounded flavours, colours and processing aids.

Salt is a key ingredient in salty snack seasoning. Its main purpose is to potentiate the overall flavour of the seasoning (Kunzt, 1996). Salty snacks contain app. 1.5 % to 2 % salt as a target and when applied topically, from about 6 % to 12 % total seasoning (Enggalhardjo, and Narsimhan, 2005). The level depends on several factors such as the flavour impact required, size of the crystals, type, amount of surface oil, the method of application, and the adhesion characteristics (Kunzt, 1996). It should also be determined through consumer testing (Kunzt, 1996).

1.2.1.3.1 Application of snack seasoning

Powder coating is a common way to apply a variety of flavours to snack foods (Ratanatriwong and Barringer, 2007). Flavour coating on crisp is an effective way of improving the taste and appearance (Yousuf and Barringer, 2007). The common objective of flavouring snacks is to apply the seasoning uniformly and consistently to reduce costs and to increase consumer acceptability (Kunzt, 1996; Yousuf and Barringer, 2007). Hence, all sides of the product should have the same appearance (Kunzt, 1996). However, this is almost impossible to achieve in practice (Sandadi et al, 2004). The size, density and charge of particles and air velocity have a significant effect on coating transfer efficiency and evenness in flavour applications onto food surfaces (Yousuf and Barringer, 2007). Flavour powders are mixture of powders with different physical properties and these properties need to be investigated to determine their effect on mixture transfer efficiency, evenness and separation during coating (Yousuf and Barringer, 2007). Some researchers report that the increase in particle size increases transfer efficiency onto food surface (Yousuf and Barringer, 2007).

In the snack producing industry, two main technologies have been used for coating the products. (i) Conventional liquid (wet) coating has been used for more than two centuries whereas, in the last thirty years, (ii) powder (dry) coating technology has become of interest. (Burns and Fast, 1990; Sandadi et al, 2004).

The feed rate may be controlled either volumetrically or gravimetrically. With volumetric control, the product bed depth on a vibratory tray or conveyor belt are the

variables to be adjusted, but variations in the feed rate can occur as a result of changes in the product base bulk density. A gravimetric feeder eliminates the first of these sources of variation in the feed rate (Fig. 1-4).

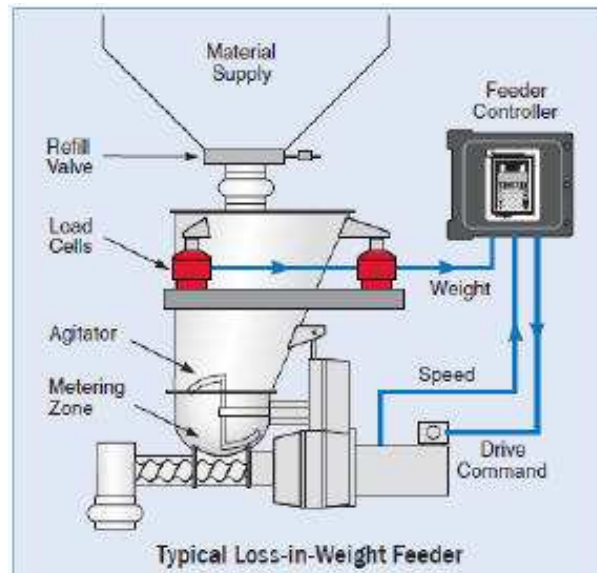


Figure 1-4. Schematic cross section view of a typical loss-in-weight gravimetric feeder (courtesy of: <http://www.ktron.com>)

Most of the seasonings which applied typically require a carrier which will carry the smaller particles to ensure proper distribution and adhesion (Kuntz, 1996). Most commonly salt is used for seasoning blends, but other carriers are also often used in industry, including corn syrup solids, malto-dextrins, crystalline acids and monosodium glutamate (Kuntz, 1996). The selection of a specific type of carrier depends on a number of factors, particularly the type and characteristics of flavour.

1.2.1.3.2 Methods of application

The most common methods of depositing a flavour particles onto a snack food surface are by gravity feed or spraying of particles into a rotating drum that contains product. The adhesion of a particle to a particle or food material is governed by the mechanisms such as interlocking or mechanical resistance (hooking and twisting together of the packed material and hence formation of stable arches), wetting, electrostatic and chemical forces and diffusion (Wong et al, 2005). Michalski et al (1997) reviewed the

theories describing these mechanisms and state that the food industry in general is still in need of understanding fundamental mechanisms of food and contact surfaces interactions.

Lusas and Rooney (2001) and Kunzt (1996) describe the types of seasoning applications: (i) single-stage seasoning, (ii) two-stage seasoning and (iii) electrostatic seasoning. In single-stage seasoning type, the material is a single phase, not slurry. Usually it is a dry seasoning or seasoning blend.

Dry single-stage coating is applied to products that have received a certain amount of surface liquid (such as vegetable oil) - freshly oil-fried potato chips fall in this category.

Dry two-stage seasoning is used for the products that have insufficient liquid on the surface to adhere seasonings. Thus, it is necessary to apply a liquid first, then applying dry seasoning. Tortilla chips, snack crackers, oven-baked crisps are coated by using this technique. A solution of a polymer like gum arabic or starch dextrin dissolved in water (or most commonly oil) can be used. The use of oil also provides a kind of mouth feel. The two application phases can be controlled independently of each other (Kunzt, 1996).

Biehl et al. (2003), Hui, (2006), and Burns and Fast (1990) report two common methods used to coat food products: (i) drum coating and (ii) conveyor based coating. Many challenges exist with these traditional coating methods. Metered powder-dispensing systems used in these, simply convey the powder to a set location. The result is often unevenly coated products with poor flavour distribution and high levels of particle build-up in process equipment. To compensate for the lack of uniformity in the powder distribution, additional powder must be added into the coating system. This results in an adverse impact on homogeneity, an overuse of expensive seasonings and an increase in waste.

1.2.1.3.2.1 Blending drum application

A tumble drum is the most common and efficient way to apply coatings, if the product can be tumbled (Burns and Fast, 1990; Kunzt, 1996). Tumble drums (Fig. 1-5) are horizontal cylinders with one end raised so that product flows from one end to the other end (Hui, 2006). The main disadvantage is having insufficient retention time within the drum to achieve the proper degree of blending and uniform coating. In many cases, a liquid media such as oil is sprayed onto the product in the tumbler to help the seasoning adhere to the surfaces (Kunzt, 1996).

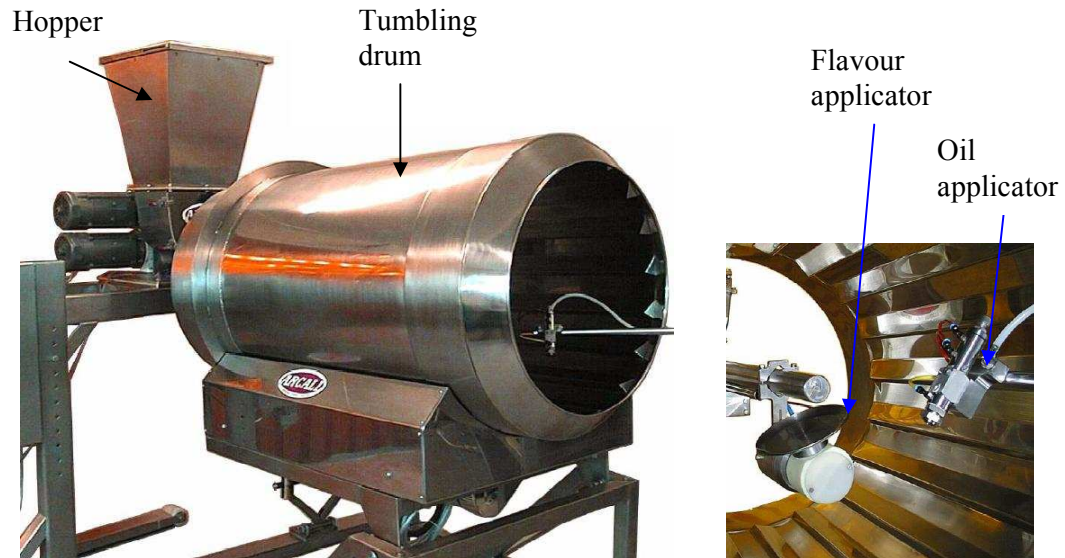


Figure 1-5. Tumbler for flavour coating on snack products (Photo Courtesy of Arcall plc).

Uniformity is achieved by matching the large coating zone with a drum capable of exposing the entire base product to the spray within the coating zone while mixing the food product with flavour powders in a tumble drum (Elayedath and Barringer, 2002). The flux of particles impacting the surface of food product depends on density, concentration of particles in the air and the volume swept out by the food product, which will in turn depend on surface area and rotational speed of the drum (Wong et al, 2005). The drum must be designed to create a “folding-in” action (Fig. 1-6) that carries

the bottom layer of the product bed from the six o'clock to the nine o'clock, from which it cascades down the surface of the bed. The flavouring particles near the wall are carried in a direction opposite the cascading layer, and there is no relative motion between them (Denis et al, 2003).

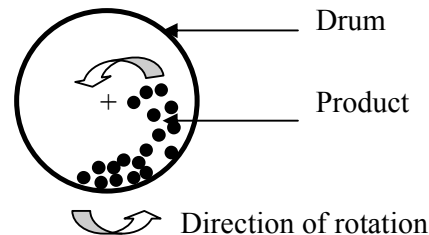


Figure 1-6. Schematic side view of fold-in action in drum

According to Burns and Fast (1990), there are two main problems if the coating is added in a localised area, and the drum is relied upon to distribute the coating through the remainder of the product.

Firstly, as the product blend tumbles over, the mass of coating hits the internal surfaces of the drum, creating an accelerated build-up problem on the inner wall surface of drum. Once the powder dries out, powder agglomerates can become extremely hard and may be similar in size to the finished product, therefore complicating their removal by screening.

The second problem relates to the poor distribution of the coating throughout the product stream. As the product travels through the drum, the rub-off effect coupled with the coating material on the drum itself may cause the coating to spread around, but the variation can still be significant.

Burns and Fast (1990) report that, a non-clogging spray system can be used in conjunction with a coating drum to practically eliminate both problems. This approach may decrease the amount needed for over-application.

Wong et al. (2005) have studied a model of flavour deposition onto food surfaces in a rotating drum. They have reported that percentage transfer efficiency can be calculated using the following relationship:

$$\% TE = n_{FA} / N_T \quad (1)$$

where n_{FA} is the number of adsorbed flavour particles and N_T the total number of sites which adhesion may take place.

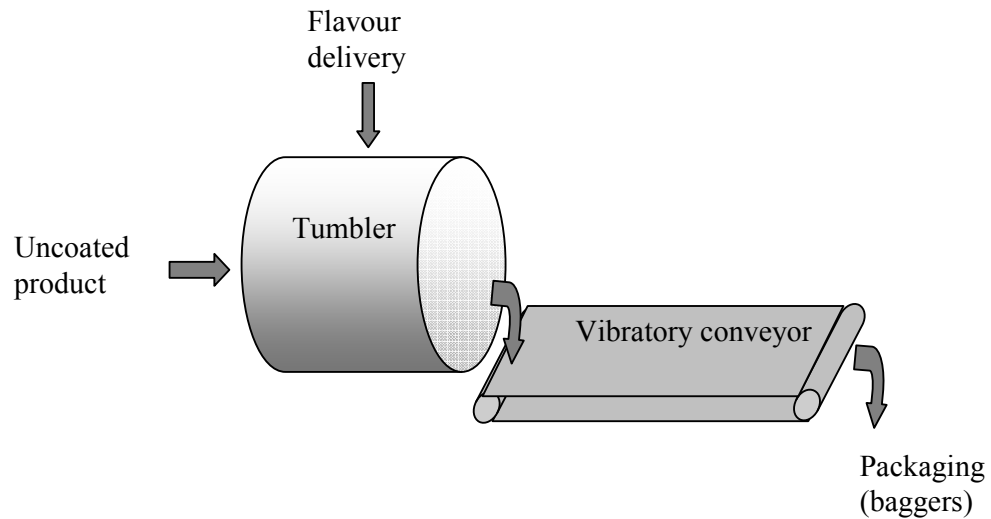


Figure 1-7. Schematic diagram of typical flavour coating in tumbler mixer.

1.2.1.3.2.2 Conveyor belt-type systems

These systems have traditionally been employed to coat products like salted crisps, crackers or pretzels and generally facilitate single-side coating of products (Dreier, 1991). Burns and Fast (1990) report that, in some cases, the conveyor is the only means suitable for a product coated in a single pass whether because of the cost of adding a drum to the process, space restrictions, or the fragility of a product incapable of accepting additional handling. The foundation of any conveyor-belt application is that a given amount of coating is applied for every square inch of the conveyor entering the coating zone, whether the product is there or not. Vibratory conveyors for product handling are another method of coating application. The ease of accessibility for cleaning and changing the product of these systems leads to generally faster changeover times than drum systems (Burns and Fast, 1990).

The conveyor can be vibratory, open wire belt, closed fabric belt, or other selected types. The first and very important criteria which should be considered is that, without some device for turning the product over, only the top surface of the snack will be coated (Kunzt, 1996) (Fig 1-8). Thus, a conveyor system may not produce snacks that are as evenly coated as other methods, but requires much less space and shorter changeover times (Hui, 2006). The amount of waste produced is high because the food does not cover the entire surface of the belt in case there is not a waste recovery system.

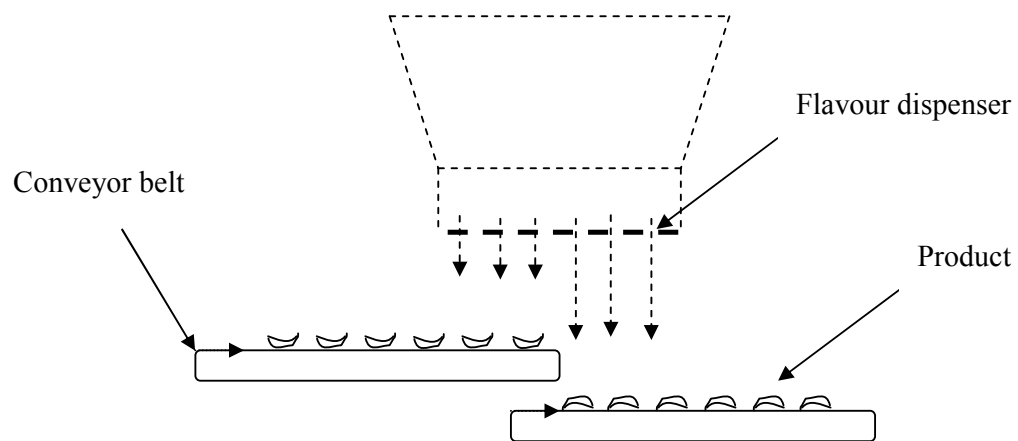


Figure 1-8. Schematic view of conveyor belt coating system.

1.2.1.3.2.3 Electrostatic powder coating

Electrostatic coating is a subset of dry single-stage seasoning described above and can be considered as an alternative to traditional coating methods. Although this technology is well-established in many different processes in industry, it is relatively new in the coating process in food industry (Kunzt, 1996; Elayedath and Barringer, 2002). This type of coating can improve the adhesion of food powders onto various food types and surfaces - resulting in a more uniform coating with less waste, less dust and less clean up time (Elayedath and Barringer, 2002; Sumawi and Barringer, 2005; Mayr and Barringer, 2006; Halim and Barringer, 2007; Ratanatriwong and Barringer, 2007). Barringer et al. (2005) report that by using this method, powder waste is reduced and a decrease in dust emissions from the process of 65% over non-electrostatic coating is attainable. According to Yousef and Barringer (2007), small particles show greater electrostatic coating improvement than large particles. They also report that as particle

density increases nanoelectrostatic coating transfer efficiency increases. Increase in charge to mass ratio of the particles increases the improvement in coating transfer efficiency (TE) (Ricks et al, 2002; Mazumder et al, 1997). Biehl and Barringer (2003) report that free flowing powders increase nonelectrostatic and electrostatic TE. However, some limitations due to physical and chemical characteristics of powders can be predicted.

The coating material is charged by passing it through an electric field or by releasing it from a charged spray gun (Fig 1-9). This latter one is relatively new technique in seasoning applications (Dreier, 1991). Powder surface charge (negative) is one of the most significant factors in electrostatic coating. It accelerates the transfer of the powder to the substrate, determines the strength of adhesion, and limits the thickness of the powder coating (Bieth and Barringer, 2003). The varying size distribution of coating material makes this application less efficient if pressurised air is used as the intervening medium (Kunzt, 1996).

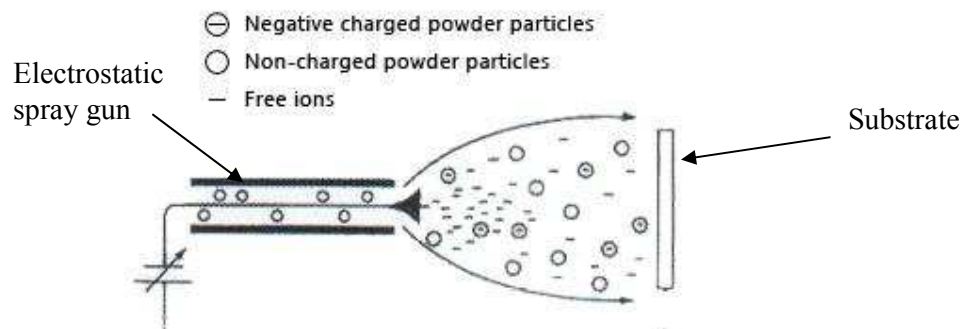
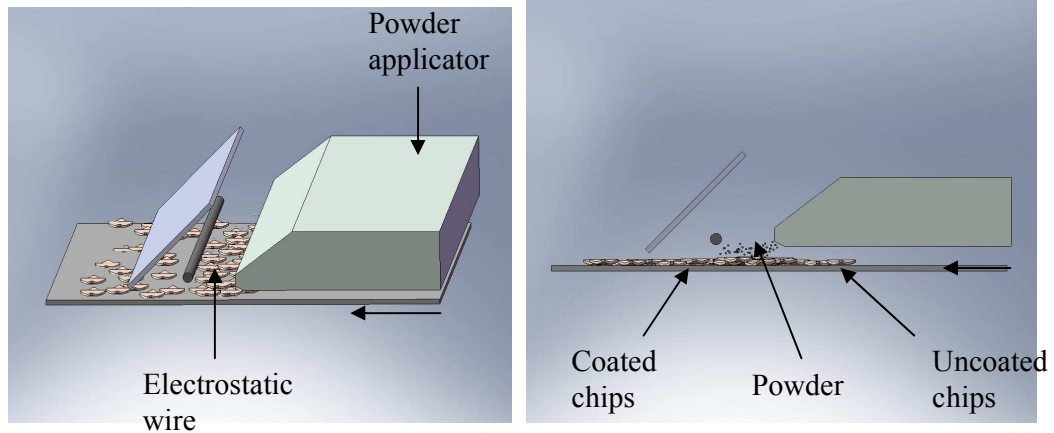


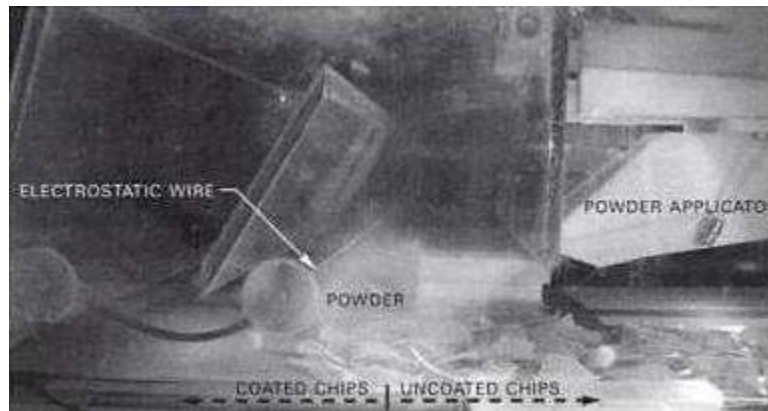
Figure 1-9. Schematic view of a charged spray gun (from www.corrocoat.com.ph/powdercoating101.htm)

Three forces direct the charged particles to the substrate: aerodynamic (by the flow of a gas), gravitational (by gravity) and coulombic (Bieth and Barringer, 2003). Coulombic forces become predominant as the powder particles move closer to the substrate. When the charged particle lands on the substrate (the nearest grounding surface) an image charge is created on the substrate that is equal and opposite in polarity to the particle charge (Bieth and Barringer, 2003; Buck and Barringer, 2007). This mirror image charge is responsible for the formation of an attraction force between the particle and

the particle surface, which in turn creates an electric field between them that holds the powder to the substrate (Fig. 1-10). The adhesion force caused by the image charge reduces the loss of coating from shaking and dropping off the product (Bieth and Barringer, 2003). According to Buck and Barringer (2007), small particles have a higher charge to mass ratio compared to large particles and thus show greater improvement in adhesion and transfer efficiency.



a



b

Figure 1-10. Electrostatic coating of tortilla chips, a) schematic view, b) a photo form production line (Photo courtesy of Hui, 2006)

1.2.1.3.3 Factors influencing the coating efficiency

Adhesion, which can be described as the interactions between the seasoning particle and the food surface, is one of the main factors controlling coating quality of the finished product (Berard et al, 2002). For dry application methods three important factors influence the consistency of the seasoning in the finished product: (i) the consistency of the flow of the seasoning, (ii) well dispersion of the particles to prevent clumping them together and (iii) the degree of adhesion. Bailey (1998) reports that the particle properties and the aerodynamic (i.e. lift and drag), gravitational (gravitational force of one particle with mass on another particle or body with mass) and electrostatic forces acting on the particles should be considered to model the coating process accurately.

1.2.1.3.3.1 Flow of seasoning

Many ingredients are hygroscopic and subject to moisture pick-up and caking, so adding flow agents can help reduce the problem. These include compounds such as sodium silicoaluminate, silica dioxide and magnesium carbonate (Kunzt, 1996). The use of flow agents is limited by the legal limit requiring less than 2% in the finished product as well as adding low levels of propylene glycol or other wetting agents that can reduce dusting problems (Kunzt, 1996). If humidity is too high, the powder tends to clump and uniformity in application suffers as well as having negative effect on the applicator system (Dreier, 1991); hygroscopic seasonings, such as cheese and other fine powders, lead to most problems on agglomeration.

The more free flowing the powder, the greater the coating efficiency (Bieth and Barringer, 2003). This is because the less cohesiveness enables free-flowing powders to deposit more effectively onto the substrate. Instead, cohesive powders have a propensity to form aggregates that hinder their ability to flow through the system, and as a result cause variations in mass flow rate and transfer efficiency (Bieth and Barringer, 2003).

1.2.1.3.3.2 Processing conditions

A number of parameters have been reported by Jiang et al (2008) affecting the interaction force between a particle and a solid surface and hence the degree of

adhesion. These are temperature, surface roughness, particle shape, material properties, environmental conditions and surface oil.

Temperature

To obtain the best adhesion, the base product should be as warm as possible, yet cool enough so not to suffer from fragility problems (Dreier, 1991). The length of the (post-coated) finished product conveyor should be sufficient to cool down the product to a safe packaging temperature. On the other hand, excessively long conveyors can result in product breakage and flavour loss from the product.

Surface Roughness

Roughness is scale-sensitive; hence a surface that looks smooth to the naked eye maybe quite rough at higher magnifications. Surface roughness can have such a large effect on the adhesion forces, mainly on vdW and electrostatic adhesion forces (Eichanlaub et al, 2004). According to Katainen et al (2006), increase in surface roughness reduces the contact area between the bodies leading to reduced interaction. On the other hand, Quevedo and Aguilera (2004) report that particle adhesion is believed to be firmer on rougher surfaces for two main reasons: (i) a higher surface area available for attachment, and (ii) protection from shear forces. The contact between two solid surfaces occurs where the microscopic asperities connect (Li et al, 2006).

Studies on effect of roughness on adhesion forces have been reviewed by Walz (1998). Traditional adhesion models work well with smooth surfaces. However, using rough particles and surfaces is likely result in substantial deviations and hence may require some simplifications in the description of surface topology (Kappl and Butt, 2002). Greenwood and Tripp (1967) improved the Hertz contact model by taking into account the effect of roughness.

Particle charge, size and shape

Irregularly shaped particles have higher adhesion values than spherical particles at a similar q/m (charge per mass) level (Takeuchi, 2006). This may be attributable to non-uniformity of surface charge on the particle. Similarly, adhesion force distribution shifts

in a larger direction with increasing charge-to-diameter ratio, q/d . This agrees with the findings of Bieth et al. (2003) and Miller and Barringer (2002) who state that for both electrostatic and non-electrostatic coating, as particle size decreases, the percent transfer efficiency, or extent of coating, is increased.

Niman (2000) and Halim and Barringer (2007) report that small particle size enhances adherence. According to Buck and Barringer (2007), van der Waals and capillary forces per unit mass area are stronger for smaller salt crystals than mass due to higher surface area.

Many of the particles that are found in industrial applications are generally irregular in shape (Ahmadi and Guo, 2007). Miller and Barringer (2002) found that flake like particles coated more efficiently than cubic and dendritic shapes. Niman (2000) reports similar adhesion for flake and dendritic crystals, but for crystals larger than 300 μm , higher adherence for flake than for cubic salt particles. Shimada et al (2003) studied the influence of particle shape on the adhesive force of glass beads and report that the adhesion forces of irregular glass beads are about five times higher than that of more spherical beads.

Particle density

Table 1-3. Particle densities of some powdered material used by Otsuka et al. (1988)

Name of the material	Particle density (g/cm ³)	Average particle diameter (μm)
Glass beads	2.4	40
Crushed glass	2.4	35
Silica sand	2.61	44
Potato starch	1.48	41
Corn starch	1.52	29
Caffeine	1.37	41

Studies by Biehl et al. (2003) have concluded that as particle density increases, transfer efficiency is increased for non-electrostatic coating. No effects of particle charge on electrostatic coating have been reported which has been attributed to electrostatic forces dominating over gravitational forces making density insignificant (Bieth and Barringer,

2003). Particle densities of some powdered material are given in Table 1-3 (Otsuka et al, 1988).

Surface oil

Potato chips contain 20 to 35 % oil wet basis (Pedreschi and Moyano, 2005; Caixeta et al., 2002). The film of oil that remains on the surface after frying or after oil application causes the seasoning to adhere. The condition of the oil has been shown to influence adhesion as well as the temperature on the surface (Kunzt, 1996; Enggalhardjo and Narsimhan, 2005). Increasing oil content leads to more efficient coating, regardless of the size and shape of salt crystals (Miller and Barringer, 2002). If the liquid such as oil (warm or cold) is spread over the product, it is critically important that all product surfaces should be coated in a uniform and consistent manner (Kunzt, 1996). If the liquid application is sporadic, seasoning application will be correspondingly inconsistent.

Due to presence of an oil film on food bases, the deposition of flavour particles onto wet surfaces often forms liquid bridges (Wong et al, 2005). Rennie et al (1998) reports that surface roughness may reduce or even eliminate liquid bridging effects and hence reduce the coating efficiency.

Surface oil content decrease as oil is absorbed inside the chip after they are removed from the fryer (Moreira et al., 1997). Strong adhesion of the seasoning can be obtained by coating immediately after frying (Buck and Barringer, 2007). If the chips are allowed to cool after frying it has been found that this results in oil absorption inside the chip - weakening the capillary forces and decreasing adhesion (Moreira et al., 1997).

Oil composition plays an important role in oil absorption and quality of chips (Melton et al., 1993). Some researchers examined the effect of different frying oils on flavour adhesion (Buck and Barringer, 2007). According to Enggalhardjo and Narsimhan (2005), the tortilla chips sprayed with olive oil have higher adhesive force holding the seasoning than chips sprayed with soy bean oil. They have added monooleate in soybean oil to decrease the surface tension and they observed increase in seasoning loss when surface tension is lower.

1.2.1.3.3.3 Adhesion mechanisms

Adhesion can be defined as interactions between molecules when two or more solid bodies are in contact (Endevco, 2007). According to Enggalhardjo and Narsimhan (2005), adhesion has been quantified as the work done in separating two surfaces that are in contact with each other (Mittal, 1977; Michalski et al, 1997).

In process engineering applications such as flotation, conductive surface coating, powder inhalation systems for drugs, paper making, printing, stainless steel polishing, surface filtration, bulk storage and transportation, agglomeration etc, adhesion forces determine the macroscopic behaviour of particle systems (Sonnenberg and Schmidt, 2005; Kappl and Butt, 2002).

Deformation of the bodies which depends on the acting forces may affect adhesion strength between surfaces significantly (Kappl and Butt, 2002).

Three different interaction forces are considered to be responsible for adhesion of the flavouring powders onto a crisp surface as illustrated in Fig. 1-11 (Sonnenberg and Schmidt, 2005). These are van der Waals, electrostatic and capillary forces (Enggalhardjo and Narsimhan, 2005; Endevko, 2007).

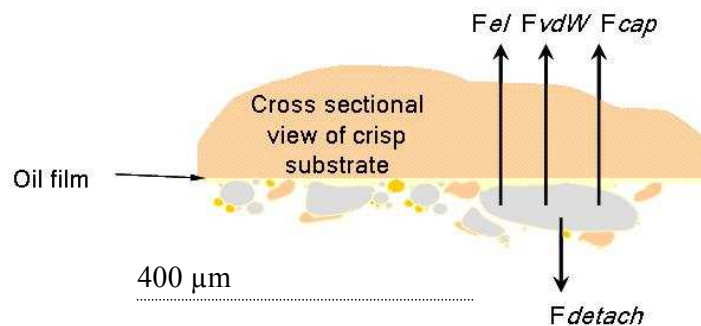


Figure 1-11. Interaction forces acting on flavour powder (from 20 to 600 μm) particles on crisp surface

These forces become increasingly significant for fine particles due to the increase of the magnitude of particle adhesion force per unit mass as the particle size decreases (Ahmadi et al, 2007).

Van der Waals forces (F_{vdW}):

Van der Waals forces are intermolecular forces that arise from a fluctuating electromagnetic field within a given media (i.e. air) resulting in instantaneous (electrical and magnetic) polarisations between atoms and molecules (Israelachvili, 1992; Hamaker, 1937; Feddema et al, 2001; Cardot et al. 2001). Van der Waals forces are the most common adhesion forces because it occurs in all situations, often plays a large part in determining the bulk behaviour of fine particles (Li et al, 2006). Sonnenberg and Schmidt (2005) and Ahmadi et al (2007) report that in dry and uncharged particle systems with particle sizes less than 10 μm van der Waals forces are dominant. These forces are dependent on the geometry and on the physical and chemical properties of the interacting bodies (Oliviera, 1997).

The van der Waals force of interaction between a spherical particle of radius R_p and a crisp surface at a surface-to-surface distance of separation of h is given by (Vasquez et al, 2005)

$$F_{vdW} = \frac{A_{eff} R_p}{12h^2} \quad (2)$$

and between a cylinder and a flat plane is given by

$$\frac{F_{vdW}}{\text{lenght}} = \frac{A_{eff} R_p^{1/2}}{16h^2} \quad (3)$$

where A_{eff} is the effective Hamaker constant defined as

$$A_{eff} = A_{123} = (A_{11}^{1/2} - A_{33}^{1/2})(A_{22}^{1/2} - A_{33}^{1/2}) \quad (4)$$

where subscripts 1 refers to the flavour particle, 2 refers to the crisp, and 3 refers to the intervening medium. The intervening medium can be considered to be oil due to oil

application onto the crisp surface after baking or during frying. The Hamaker constant is about ten times lower in water than in air (Israelachvili, 1992). This may reduce the Van der Waals effect in the presence of oil on the surfaces.

Electrostatic forces (F_{el}):

Flavour particles are usually charged (Enggalhardjo, and Narsimhan, 2005). Because of the presence of oil layer on the surface, crisp can be considered to be an uncharged semiconductor or an insulator. For that reason, flavour particles would induce an equal and opposite charge on the crisp surface. Hence, the electrostatic interaction between the flavour particle and crisp can be considered as coulombic interaction between two oppositely charged particles situated on both sides of the surface and is given by Enggalhardjo and Narsimhan, (2005)

$$F_{el} = \frac{q^2}{48\pi\epsilon_0\epsilon_r(R_p + h)^2} \quad (5)$$

where, q is the net charge of the flavour particle, ϵ_0 is the permittivity of vacuum (a measure of the degree to which molecules of some material polarize or align under the influence of an electric field), and ϵ_r is the dielectric constant of the intervening medium.

Capillary forces (F_{cap}):

Because of the curvature of the oil layer between the particle and the crisp surface, the pressure inside the oil will be less than outside due to negative Laplace pressure as a result of surface energy and intermolecular forces. The pressure difference varies with the surface tension of the oil and the principle radii of curvature of the oil interface. Consequently, the excess outside pressure will exert an adhesive (attractive) force on the flavour particle and is given by Enggalhardjo and Narsimhan, (2005); Ranade, (1987); and Zimon, (1982):

$$F_{cap} = 4\pi\sigma R_p \cos \theta \quad (6)$$

where σ is the surface tension and θ is the contact angle of oil to crisp surface. The contact angle is the angle of the tangent drawn to a resting droplet on the surface with the horizontal surface and can be obtained by analyzing the picture of an oil droplet resting on crisp surface (Fig. 1-12).

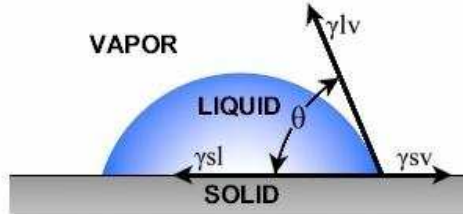


Figure 1-12. Schematic view of a droplet resting on a solid surface. θ is the contact angle, γ^{lv} is the liquid surface free energy, γ^{sv} is the solid surface free energy, and γ^{sl} is the solid/liquid interfacial free energy.

For dry uncharged particles on a dry and uncharged surface, only van der Waals forces become dominant. Capillary forces are present in wet systems. The presence of liquid is found to shield van der Waals and electrostatic interactions, thus weakening these adhesion forces (Enggalhardjo and Narsimhan, 2005). Therefore, the force needed to detach a particle is given by (Salazar-Banda et al, 2007)

$$F_{po} \geq F_{vdW} + F_{el} + F_{cap} \quad (7)$$

where F_{po} is pull of force to detach the particle from the surface.

1.2.2 Characterisation of food powders

One of the main reasons for supplying products in powdered form is simply to prolong the shelf life of the ingredients by reducing the water content (Fitzpatrick and Ahrne, 2005). Another reason is that dry powders are lighter to transport compared to liquids, take less storage space and can be varied in formulations. However, powder material

may show some difficulties in industrial applications such as poor flowability, dust generation, segregation etc.

Powders are commonly mixtures of particles by size, shape, density, porosity, specific surface area, chemical composition and flow properties. The composition and bulk properties of many food powders may change to different degrees with the time depending on environmental conditions such as humidity, temperature, oxygen concentrations etc.

According to Peleg (1983), food powders can be characterised in a large number of ways, these are:

- By usage: e.g. flours, beverages, spices, sweeteners;
- By major component: e.g. starchy, proteinaceous, fatty;
- By process: e.g. ground powders, freeze-dried, agglomerated;
- By size: e.g. fine, coarse;
- By moisture sorption characteristics: e.g. hygroscopic;
- By flowability: free flowing, sticky, very cohesive.

Hayes (1987) summarises a detailed system used for characterising a wide range of food powders based on size, shape, density, flowability, porosity, abrasiveness, flammability, explosiveness and corrosive nature. Further classification could be by hardness and by microbial hazards (Grandison and Lewis, 1996; Krokida and Maroulis, 1997).

1.2.2.1 Particle size

Food powders come in a wide range of sizes (from nanometers up to millimetres) and shapes (Grandison and Lewis, 1996). The particle size of a food powder can be in a range of several orders of magnitude, that is, between microns to several hundreds or even thousands of microns. Brown and Richards (1970) and Nedderman (1992) classify powders as a function of the particle size as shown in Fig. 1-13.

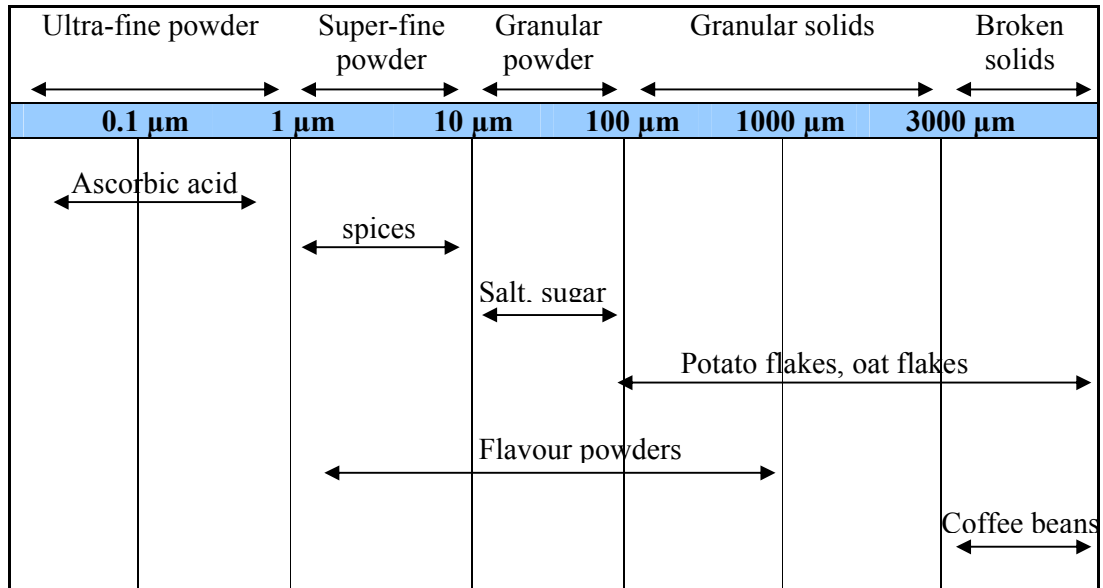


Figure 1-13. Classification of powder as a function of the particle size (source: Brown and Richards ,1970; Nedderman, 1992)

For most of the complex shapes, two or more measurements are required while one dimension, i.e. the diameter, can be enough to characterise uniform shapes such as spheres (Grandison and Lewis, 1996). There are numerous methods available to characterise the size and particle size distribution. Size distribution affects the bulk properties of the powder material which is very important in the powder production and handling stages (Grandison and Lewis, 1996). Shubert (1987) reports that criteria used to characterise particles are (i) geometric characteristics, such as area, volume, dimensions, (ii) mass, (iii) settling rate and (iv) light or laser scattering or diffraction. The methods have been used for food materials based on these attributes are microscopy and image scanning techniques, wet and dry sieving, sedimentation and enumeration by using Coulter counter, electrical impedance and laser diffraction. Due to irregularities in the shapes and sizes and different physical characteristics of powder material, these methods may not give comparable results (Grandison and Lewis, 1996).

1.2.2.1.1 Dry Sieving

Sieving is the most popular method for size analysis and separation of the fractions of the powders. It is commonly used for different materials especially powders, varying from metal powders to food and pharmaceutical powders.

A sieve is an open container, which has usually square or cylindrical, definitely spaced and uniform openings in the base (Tillman, 2000; Grandison and Lewis, 1996) (Fig. 1-14). A whole range of standard sieves are available up to 25 mm in size. Sieves for powder systems may be from a few millimetres down to about 20 μm . A number of standards such as BS 410, 1969, ISO R 565 and ASTM E11 81 are used to produce such sieves (Grandison and Lewis, 1996).



Figure 1-14. An example view of a laboratory test sieve (source: www.retsch.com/sieves)

By stacking the sieves in order of ascending aperture size and placing the powder on the top sieve and agitating by mechanical means, the material is classified into fractions. A closed pan is placed at the bottom of the stack to collect fines among the sample and a lid is placed on top to prevent loss of material. Results are usually expressed in cumulative percentage distribution. Fractionation by sieving is a function of two dimensions only, maximum breadth and maximum thickness, for unless the particles are excessively elongated; the length does not hinder the passage of particles through the sieve apertures (Tillman, 2000). This statement is valid when the longest dimension is

called length, the smallest dimension called thickness and the intermediate dimension is called breadth.

A single sieve separates the powder material into two fractions. The particles having the close size to that of the nominal aperture of the test sieve may pass through if the particle has a non-spherical nature (Grandison and Lewis, 1996). These particles are called near-aperture particles and may block or blind the sieve aperture and reduce the effective area. Therefore the particles having less size than the nominal size of the aperture may be retained by the sieve. The effectiveness of the sieving process depends upon (i) the amount of material placed on the sieve, (ii) the type of agitation applied to the sieve and (iii) the duration of the sieving process. Taking a uniform and representative sample for analysis is important in order to obtain objective results. The sampling criteria may be different for separation and analysis (Grandison and Lewis, 1996). According to British Standards Institute 1796 (1989), the sieving time required can be affected by several factors:

- The material characteristics, e.g. fineness, particle shape, size distribution, density;
- Intensity of sieving;
- Nominal aperture size of the test sieve;
- Characteristics of sieving medium;
- Humidity of the air.

Normally a number of sieves are clamped together, with the largest on the top and the smallest is located on the pan at the bottom. The powder material is placed in the top sieve and the vibrational excitation is applied to the sieve stack. By the effect of vibration, the powder is separated into its fractions and particle size distribution can be determined. The sieve method is recommended for the particles ranging from 100 to 1000 μm for better performance (Grandison and Lewis, 1996).

Some problems occur with sieving results due to sample stickiness, sieve blockage and agglomeration. As the sieve size decreases, these problems are more likely to occur (Strumpf, 1986).

1.2.2.1.2 Laser diffraction (lasersizer)

The laser diffraction method relies on the fact that particles passing through a laser beam will scatter light at an angle that is directly related to their size. As particle size decreases, the detected scattering angle increases logarithmically. Scattering intensity is also dependent on particle size, diminishing with particle volume. Large particles therefore scatter light at narrow angles with high intensity whereas small particles scatter at wider angles but with low intensity (see Fig 1-15).

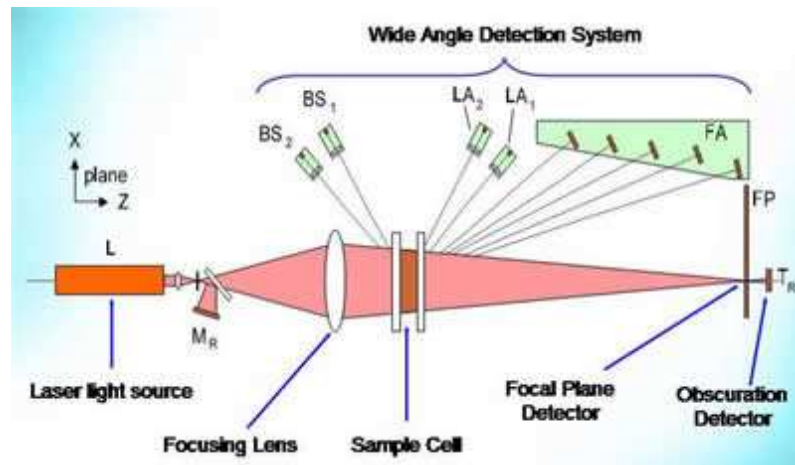


Figure 1-15. Typical laser diffraction instrument layout. (courtesy of www.chemie.de)

The instrument is based on the technique of laser diffraction-exploited in order to determine particle size. A typical system consists of a laser (to provide a source of coherent, intense light of fixed wavelength) a series of detectors (to measure the light pattern produced over a wide range of angles) and a sample presentation system to ensure that material under test passes past the laser beam as a homogeneous stream of particles in a known, reproducible state of dispersion. The international standard for laser diffraction measurements is ISO13320-1-1999.

1.2.2.2 Powder density and porosity

Bulk density is one of the parameters to classify the powder material and can be defined as the mass divided by the total volume occupied by the material (Grandison and Lewis, 1996):

$$\text{Bulk density} = \frac{\text{Weight of powder}}{\text{Volume of powder bed}} \quad (8)$$

Bulk density strongly depends on the treatment or handling of the powder. Hence, the bulk density of powders is usually reported as ‘freely settled’ or ‘loose’ bulk density (i.e. after the powder has only been poured), ‘tapped’ density (i.e. after vibration), or compact density (i.e. after compression) (Peleg, 1983).

According to Grandison and Lewis (1996), all solid components except fat are substantially denser than water. However, most food particles have a similar solid density depending on the moisture content (Peleg, 1983). This is due to the similar density of the main ingredients, except for salt-based and fat-rich powders (Table 1-4).

Table 1-4. The solid densities of the major components

Material	Solid density (g/cm ³)
Fat	0.90-0.95
Water	1.00
Protein	1.4
Starch	1.5
Citric Acid	1.54
Glucose	1.56
Sucrose	1.59
Cellulose	1.27-1.61
Salt	2.16

Source: (Peleg, 1983)

$$\text{Particle density} = \frac{\text{Particle actual mass}}{\text{Particle actual volume}} \quad (9)$$

Barbosa-Canovas et al (2005) have given different explanations of particle density depending on how the total volume is measured: (i) the true particle density, (ii) the apparent particle density or (iii) the effective (or aerodynamic) particle density.

True particle density represents the mass of the particle divided by its own volume excluding open and closed pores and regardless of their position in the particle structure (Barbosa-Canovas et al, 2005; Peleg, 1983).

Apparent particle density is the mass of a particle divided by its volume, excluding only the open pores. It is measured by gas or liquid displacement methods such as liquid or gas pycnometry (Barbosa-Canovas et al, 2005; Grandison and Lewis, 1996).

Effective particle density is the mass of a particle divided by its volume, including both open and closed pores (Barbosa-Canovas et al, 2005). The volume of particle is within an aerodynamic envelope as seen by a gas flowing past the particle (Barbosa-Canovas et al, 2005).

The total volume includes air trapped between the particles. The volume fraction trapped between the particles is known as the porosity (Grandison and Lewis, 1996):

$$\text{Porosity} = 1 - \frac{\text{Bulk density}}{\text{Solid density}} \quad (10)$$

Food powders vary in porosity depending on water content and geometric structure from about 40% to 80% (Peleg, 1983). According to Peleg (1983), most food powders are known to be cohesive, which means that their interparticle attractive forces are significantly high relative to the individual particle's weight. The variation in the shape of food powder particles is enormous. Fine particles fill the spaces between larger ones resulting in higher bulk density and lower porosity unless the bulk is a mono-size material (Peleg, 1983).

1.2.2.3 Flowability

Peleg (1978) defines the powder flow as the relative movement of a bulk of particulates among neighbouring particles or along the container wall surface. Flowability depends on the powder's bulk properties (moisture content, density, composition, shape, and particle size distribution), some of which can change as a result of impact during handling, air relative humidity, temperature, and storage time conditions (Juliano and Barbosa-Canovas, 2009; Otsuka et al, 1988). Powder flowability increases with increasing particle size and decreasing moisture content (Grandison and Lewis, 1996). High relative humidity and temperature may cause poor powder flowability which is important in operations, such as storage in hoppers and silos, transportation, formulation and mixing, compression and packaging (Knowlton et al, 1994; Teunou and Fitzpatrick, 1999; Juliano and Barbosa-Canovas, 2009). Some of the factors that can significantly change the flowing behaviour of powder are summarised in Table 1-5.

Table 1-5. Some characteristics and factors affecting powder flowability

Particle properties	Intrinsic Factors
Composition (type of material)	Temperature
Density (voidage)	Air relative humidity
Particle size	Compaction level
Particle shape	Coating, agglomeration
Particle roughness	Segregation
Surface friction (coating)	Anticaking agents
Particle compressibility (hardness, elasticity, ductility)	
Moisture	
Electrical properties (conductivity, capacitance, propensity to electrostatic charge)	
Powder properties	External factors
Size distribution	Feeding rate
Bulk density	Vibration
Homogeneity (mixture type)	Hopper dimensions and design
Attrition level	Discharge aids
Powder compressibility	
Cohesiveness (powder stickiness)	
Coefficient of internal friction	
Coefficient of wall friction	

(Source: Juliano and Barbosa-Canovas, 2009)

Food powders with poor flowability often, but not always, tend to cake readily and caking usually occurs with amorphous materials such as tars, gels, lipids, waxes, or some soft crystalline substances that stick together when subjected to either pressure or higher temperature (Juliano and Barbosa-Canovas, 2009).

Hausner ratio, Carr index, compressibility, angle of repose, and friction are common criteria used to characterise powder flowability (Juliano and Barbosa-Canovas, 2009).

1.2.2.3.1 The Hausner ratio

The *Hausner ratio* is defined as the ratio of tapped bulk density to the loose bulk density (Hausner, 1967). Peleg (1983) reports that the Hausner ratio may be used for flowability index in powders, where friction is the major factor preventing the flow. Hayes (1987) reports some figures and values for some food powders (Table 1-6). An equation (Eq. 11) widely used to evaluate flow properties follows that calculates powder volume changes in a cylinder after a certain period of time or number of taps (Hayes, 1987; Grandison and Lewis, 1996).

$$H_R = \frac{\rho_n}{\rho_0} = \frac{V_0}{V_n} \quad (11)$$

where n is the number of taps to the sample, ρ_n and ρ_0 are the tapped and initial bulk densities, and V_0 and V_n are the initial and tapped volumes, respectively.

Table 1-6. Hausner ratios of powder flow behaviour

Hausner ratio	Flow behaviour
1.0-1.1	free flowing
1.1-1.25	medium flowing
1.25-1.4	difficult
>1.4	very difficult

Source: (Grandison and Lewis, 1996)

1.2.2.3.2 Carr's compressibility index

Powder flow properties can be evaluated by measuring the Carr's compressibility index. The Carr's compressibility index is calculated from the loose and tapped bulk densities (ρ_i and ρ_t) of the granules using the following equation (Carr, 1965);

$$\text{Carr's compressibility index (\%)} = (\rho_t - \rho_i) \times 100 / \rho_t \quad (12)$$

Carr's compressibility indices of less than 20% are generally associated with good flow properties.

1.2.2.3.3 Compressibility

Confining a bed of powder in a cylindrical cell and measuring the force applied to a flat punch suspended between locking screws, when in contact with the top surface of the bed, as a function of the displacement of the punch gives the compressibility of the powder. By compressing a powder bed and following the force-displacement curve, the change in bulk density can be attained and powder contact volume versus compressive force or stress can be represented (Juliano and Barbosa-Canovas 2009).

1.2.2.3.4 Angle of repose

Angle of repose is defined as the angle at which a material will rest on a stationary heap or the angle θ formed by the heap slope and the horizontal when the powder is dropped on a platform (Fig. 1-16). Depending on the environmental conditions as well as measuring methods, different values of the angle can be obtained for the same powder, not being an intrinsic characteristic of the powder material. Geldart et al (2006) report that there are at least eight methods of measuring angle of repose, and each method will give different values and therefore they are seldom comparable.

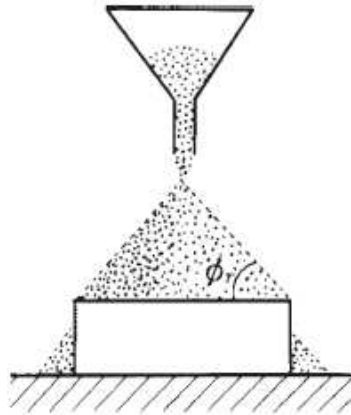


Figure 1-16. Angle of repose method (from Juliano and Barbosa-Canovas, 2009)

The most commonly used methods are the drained (Fig 1-17a) and the poured (Fig 1-17b) angles of repose.

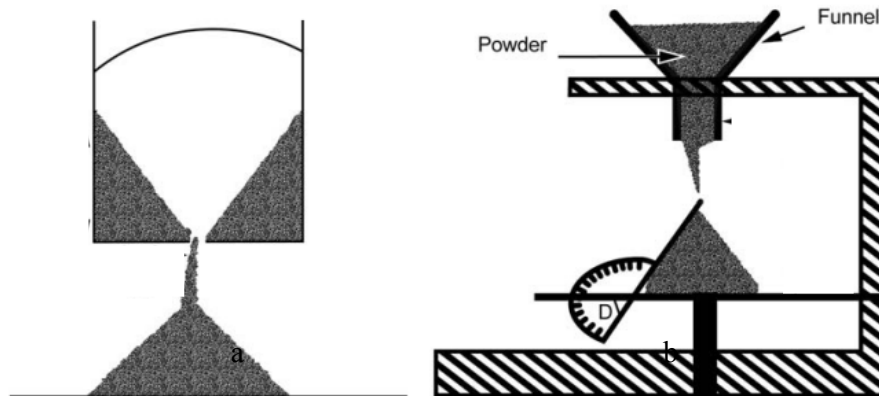


Figure 1-17. Examples to methods to measure angle of repose (from Barbosa-Canovas et al. (2005))

Carr (1965) suggested that angles of repose below 30 indicate good flowability, 30-45 some cohesiveness, 45-55 true cohesiveness, and >55 sluggish or very high cohesiveness and very limited flowability.

This measurement is widely used in characterising flow properties of powders in different applications although it is a rough flowability indicator. In fact, it is the actual measurement applied by different industries such as food industry quality control or

research in order to evaluate flowability. There are some other sophisticated tests that measure flowability such as Geldart and Hosokawa but they are rarely used because the results are not yet useful in design of equipment such as hoppers (Juliano and Barbosa-Canovas, 2009).

1.2.2.3.5 Friction

Flowability of powder material can be characterised by using different testers such as annular shear cells and uniaxial testers. Jenike Shear Tester and Wolfson Annular Shear Tester can be given as example to these testers.

Jenike's Shear Cell

The most common shear cell used for flowability evaluation and determination of failure properties is Jenike's Shear Cell (Leniger and Beverloo, 1975; Peleg, 1978; Schubert, 1987). Jenike's Shear Cell consists of the upper ring, and lower ring resting on top of the stationary base as shown in Fig. 1-18. The main principle of operation of the tester for carrying out a test consist three stages which are pre-shear, consolidation and shear. The powder material is filled inside the rings and normal load is applied to the lid. A horizontal shear rate is applied to the side of the lid to the projecting bracket attached to the upper ring. For different normal rates, different shear loads are obtained. Division of normal and shear forces by the cross sectional area will give normal stress and shear stress. According to Jenike's method (two stage process), material is consolidated and sheared under a normal load until the shear force reaches steady state. The steady state flow of powder material occurs with no change in stresses and bulk density. After steady state shear, the sample is subjected to a smaller normal stress and sheared to failure. New samples are pre-sheared identical normal stresses and sheared to failure at different levels of normal stresses to establish yield locus. This procedure is repeated for several different values of consolidating stress producing different yield locus (Fig. 1-19). Therefore this yield locus data describes the flow behaviour of powder (Grandison and Lewis, 1996). Plotting unconfined yield strength which is represented by Mohr's semicircle through the origin tangential to the yield locus and passing through zero versus the major principle stress at steady state flow on a graph gives the flow function (Grandison and Lewis, 1996). Flow function is used to

characterise the flow of powders and is very useful for designing hoppers, bins, conveying systems, dispensers, etc. (Grandison and Lewis, 1996). Juliano and Barbosa-Canovas (2009) explain these parameters and methods in detail. Berry and Bradley (2007)'s investigation is a good example to analysis of failure functions obtained from annular shear cells.

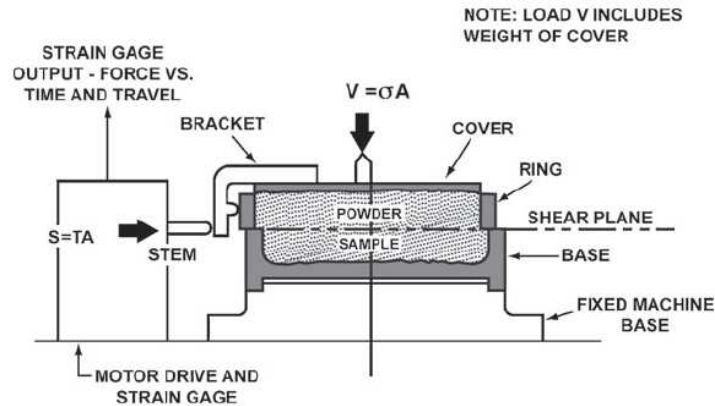


Figure 1-18. Schematic drawing of Jenike's Shear Tester (from Juliano and Barbosa-Canovas, 2009)

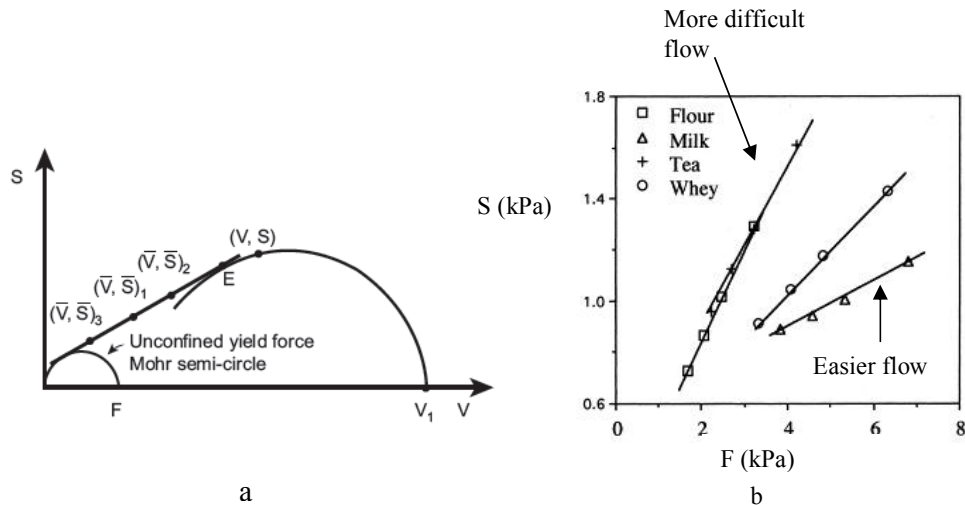


Figure 1-19 a) Construction of a yield locus. S, shearing force reached during consolidation (N); F, unconfined yield strength (N); V, normal force applied to a shear cell during consolidation(N); b) flow functions (unconfined yield strength against maximum consolidation stress) of 4 different food powders (temperature of 20°C and 25% RH) (from Barbosa-Canovas et al (2005) and Teunou et al. (1999))

Wolfson Annular Shear Tester

The Wolfson Annular Shear Tester (Fig. 1-20) uses an annular shear cell (lid and trough). The powder is contained in a shear trough, which rotates at angular speed (ω) (Juliano and Barbosa-Canovas, 2009). The trough is slowly rotated at a fixed speed by a motor and reduction gearbox. Two radial torque arms are connected between lid and two load cells to measure shear force. Weights are placed on the lid and on the counter balancing unit to apply desired load on powder material. This device was further developed by Wolfson Centre for Bulk Solids Handling Technology to be able to get an automatic operation named as Brookfield-Wolfson powder flow tester. It consists of an automated annular shear tester, with a trough of 150 mm outer diameter and 100 mm inner diameter. The tester is used to determine the flow properties over a varying consolidation normal stress range from 0.3 to 5 kPa (Kulkarni et al., 2010).

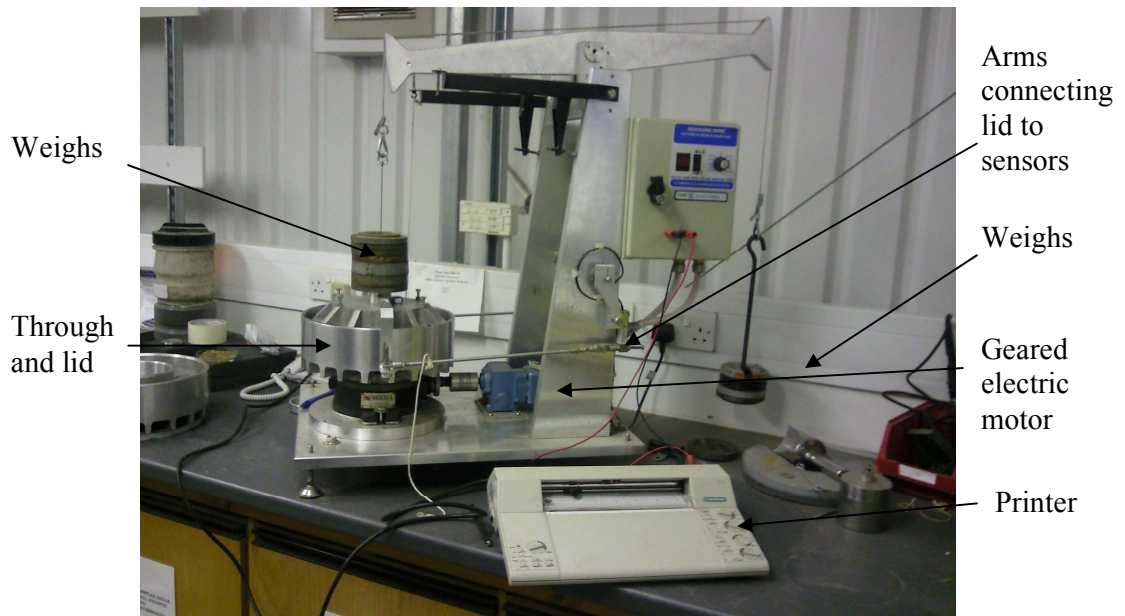


Figure 1-20. Wolfson Annular Shear Tester

1.2.2.4 Methods for measuring particle adhesion

Adhesion forces can be measured either during attraction between two surfaces, or during removal. Traditional techniques measure adhesion forces during detachment. Measuring adhesion during attraction requires advanced techniques.

1.2.2.4.1 Atomic force microscope (AFM)

Kappl and Butt (2002) report that the atomic force microscope (AFM), invented by Binnig, Quate and Gerber, could be the ideal tool for particle to particle and particle to surface studies because it provides information on surface forces (via force curves) and on particle geometry (via topographic images). Pull-off force measurements using AFM represent the most common method used attempting to characterize and quantify adhesion forces experimentally (Li et al., 2006). It is possible to measure the adhesion force of the same particle under different conditions such as in liquid or air (Gotzinger and Peukert, 2003; Bowen et al., 1998). A single particle is attached by using epoxy resin to the cantilever of the AFM and is brought into close proximity with the surface of interest. The cantilever is retracted from the test surfaces and the adhesion forces between the surfaces are measured as a deflection of the cantilever.

This technique requires a considerable effort to achieve a representative value for the adhesion force acting on a single particle per experiment (Salazar-Banda et al., 2007). This technique also cannot do a representative number of particles, orientations and contact points. Because of this reason, the atomic force microscopy shows limitations when the adhesion strength of particles with poly-dispersed sizes on a surface is studied. Reviews on AFM force measurements can be found at Butt et al (1995) and Capella and Dietler (1999).

Kappl and Butt (2002) gives information about the principle of colloidal probe technique and they report that it is identical to that of a standard AFM as described above. According to this technique, the cantilever deflection is measured by optical lever technique. The sample is moved up and down by applying a voltage to the piezoelectric translator, onto which the sample is mounted (Kappl and Butt, 2002). A beam from a laser diode is focused onto the end of the cantilever and the position of the reflected beam is monitored by a position sensitive detector. While the tip apex of AFM

has a radius of 5-50 nm, the radii of colloidal probes are in the range of 1-50 μm , resulting in much higher adhesion forces.

1.2.2.4.2 Centrifugal detachment

It has been quoted by Takeuchi (2006) as one of the most reliable techniques, by which quantitative results have been obtained. This technique (Fig 1-21) has been used for almost 50 years to measure adhesion forces between particles and planar surfaces (Larsen, 1958; Polke, 1969) and to characterise the behaviour of industrial powders in pharmaceutical or food applications (Newton and Lam, 1992; Podczeck, 1999; Rennie et al., 1998). Kappl and Butt (2002) reports that, statistical evaluation of more than one experiment might be necessary in the case of irregular shaped particles where the contact area and adhesion force will depend on the random orientation of the particles relative to the surface.

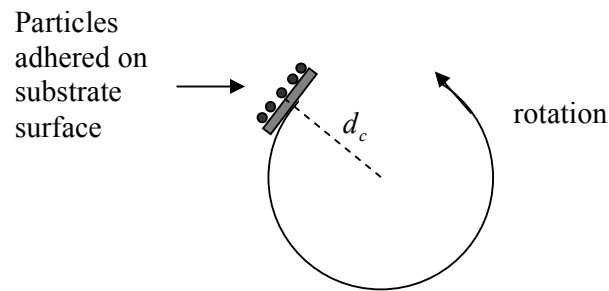


Figure 1-21. Schematic view of the rotation

The principle behind it is that the force resulting from the angular velocity of a particle of defined mass at a defined distance from the centre of rotation, will exceed the adhesion force between the particle and the surface above a critical centrifugal speed.

The centrifuge force F_{cen} , generated in the compression or detachment direction, can be calculated using Eq (2) (Lam and Newton, 1991)

$$F_{cen} = M\omega^2 d_c \quad (13)$$

where M is the mass of the particle; ω is the angular speed and d_c is the distance between the sample and the rotor centre (rotational axis). Salazar-Banda et al. (2007) and Podczeczek et al (1997) assume that the adhesion force is equal in magnitude, but with opposing signal to the applied centrifugal force at detachment, as seen in Eq. 14:

$$F_{ad} = -F_{cen} \quad (14)$$

and;

$$F_{cent} = M\omega_d^2 d_c \quad (15)$$

where ω_d is the angular speed necessary for detachment;

The force applied is used to detach the adhered particles (spin-off), where the sample is placed with the side of particles surface facing the opposite direction of centre in the centrifuge (Salazar-Banda et al, 2007). Centrifugation is repeated at a number of rotational velocities so that adhesion force distributions are obtained. Any angle other than 90 between the centrifugal force vector and the surface, results in friction taking part in the detachment process (Podczeczek, 1998). Friction force increase the amount of spin off force needed to detach the particle from surface and this is not desirable in adhesion strength measurements.

1.2.2.4.3 Detachment field method

A pair of parallel planar electrodes is used with a gap in between. Some particles fell onto the bottom electrode from a sieve 5 cm above. The occurrence of particle jump is observed by monitoring the current flow between the electrodes. The current is increased at a constant rate until a specific value is reached and the particles that have been deposited on the top electrode are wiped off. This step is repeated, increasing the preset voltage, a number of times such that adhesion force distributions are obtained.

1.2.2.4.4 Ultrasonic vibration

The measuring principle of vibration method is based on particle detachment from a vertical sinusoidally vibrating surface caused by its inertia at certain acceleration

(Ripperger and Hein, 2004; Deryaguin and Zimon, 1961). In the vibration method, the force acting upon particles is related to the frequency, amplitude and time of vibration. Sub-micron particles require frequencies in the range of several MHz which results in the possibility of causing cracks and breakages of the surface and particles adhered to them (Podczeck, 1998).

1.2.2.4.5 Aerodynamic technique

Particle separation is measured as a function of the gas velocity (Fig. 1-22) and direction of the gas jet. Detachment is usually forced in an angled direction, i.e. both adhesion and frictional forces participate (Podczeck, 1998). Measurements are undertaken at different detachment angles to calculate the static coefficient. Compressed air or nitrogen are used to produce the high velocity air current required (Podczeck, 1998).

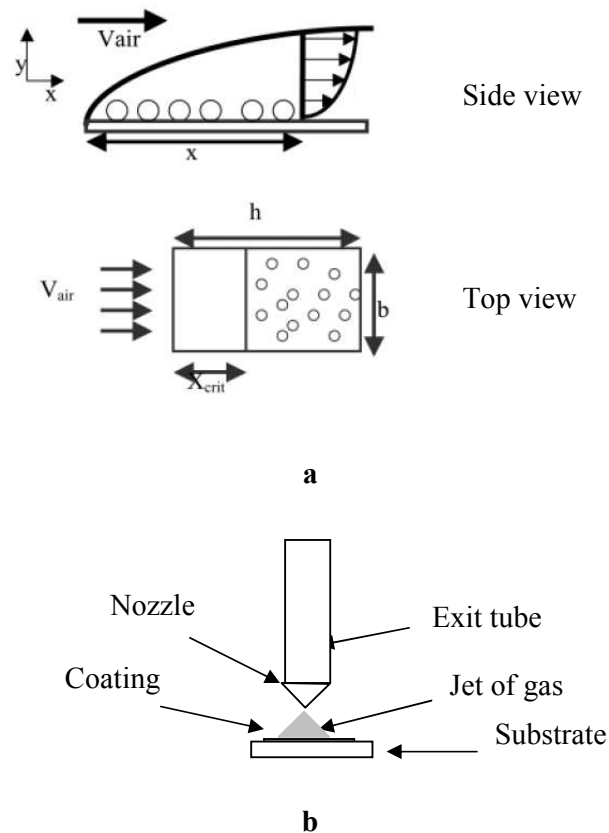


Figure 1-22. Adhesion testing by using air flow a) parallel (from Enggalhardjo and Narsimhan (2005)) and b) perpendicular to surface (from Russ and Talbot (1998)).

1.2.2.4.6 Impact separation

Adhered particles are caused to detach from a plane surface by an impact on the opposite side of the substrate plane. Otsuka et al (1988) investigated the adhesive properties of different organic and inorganic powdered materials of different shapes on a glass plate using the impact separation method. They have placed the particles on the glass plate in a measuring cell which was fixed to the motor driven impact hammer of a pendulum shock testing machine (Fig 1-23). The hammer was allowed to fall from different heights to impact a shock-absorbing mat. They have used an accelerometer to measure the impact acceleration generated and they have calculated the forces (from 1×10^{-8} to 1×10^{-5} N). Finally they have counted the number of particles by using an image analysis system before and after impact to calculate the percentage of particles adhering.

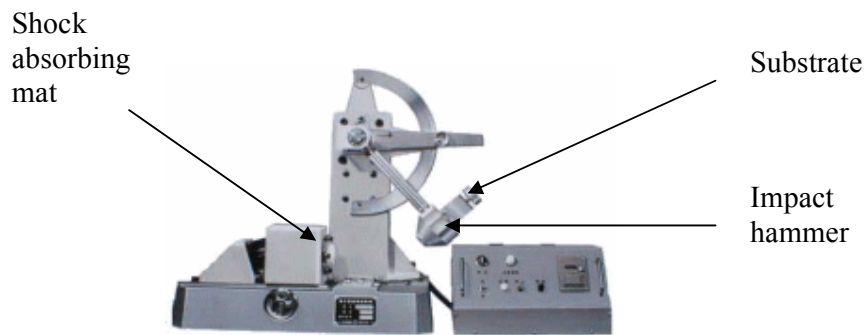


Figure 1-23. Pendulum shock testing machine (from www.yoshida-seiki.co.jp)

1.2.2.4.7 Comparison of the techniques

The techniques described above are quite different ways of measuring particle adhesion. A general comparison of the techniques is shown in Table 1-7. This table shows the advantages and disadvantages of these techniques.

Table 1-7. Description of some techniques for adhesion force measurement

Technique	Operation	Size (μm)	Advantages	Disadvantages
Centrifugation (Rennie et al , 1998; Salazar-Banda et al (2007); Tang and Busnaina (2000))	-Tangential detachment -Photographic images before and after Testing	R>20	-Accurate and repeatable -Simple and well established -Good statistics	-Particles of similar size -Highly cohesive powders can not be used -Time consuming
Aerodynamic detachment (Cardot et al (2001); Russ and Talbot (1998);Enggalhardjo and Narsimhan (2005))	-Detachment at angled positions by air jet -Photographic images before and after Testing	R> 10	- Flexible on substrate size-	-Further detachment by particle-particle collisions -High air current velocity
Hydrodynamic detachment (Freitas and Sharma.1999)	-Detachment caused by liquid stream	R> 0.5	-Flexible on substrate shape -Good statistics	-Insoluble particles only
Impact-Separation (Otsuka et al (1988))	-Detachment by impact on particles surface with adhered on opposite side	R>5		-Micronized particles require high g forces - existence of capillary forces requires more impact force
Vibration (Hein at al. (2002); Ripperger and Hein (2004))	-Detachment by acoustic transducer	R>0.3	-May be used with liquids	-Can damage surfaces and particles at high forces -Possible plastic deformation
Electrostatic detachment (Takeuchi (2006))	-Voltage is applied between Electrodes	R>5	-Fast -Good statistics -Detachment monitored	-charged particles only
Atomic Force Microscope (AFM) (Shaefer et al (1994); Bowen et al, 1998; Fuji et al(1998); Cooper et al(2000); Willing et al (2000))	-Optical beam deflection is proportional to deflection of Cantilever -Piezoelectric sensor measures	-	-High precision and control -Test at different conditions with same particle -Different tips distance -Short contact time -Measures attractive as well as removal force	-Uncharged particles only -Long sample preparation times -Difficulties with cohesive powders -High capital cost -Statistically validated experiments are time consuming -Poor statistics

The advantages and disadvantages of these techniques are summarised below:

Centrifugal detachment characterizes adhesion by using the centrifugal forces arising from rapidly rotating surface.

Centrifugal detachment can monitor the adhesion of both charged and uncharged particles and therefore may be the preferred technique when studying the mix of charged and uncharged particles.

Measuring adhesion with centrifugal detachment gives useful information about adhesion characteristics of particles, but it is more time consuming. At least 20 spins should be run for good statistics, and this operation may take hours. With these data, one has good measurements of how particle size, charge and neighbouring particles can affect adhesion.

Placing substrate-particle system into centrifuge tube which needs special design requires attention to prevent particle loss during this stage and it is not suitable for fragile substrate since the substrate need to be cut into appropriate shape to be able to place into the tube.

In conducting Aerodynamic method, inclination of the substrate, the applied gas pressure and gas velocity play important role. The force generated by flow of gas lead to detachment of particles from substrate surface. Particle-particle collisions may also cause detachment and this cannot be identified and differentiated.

Hydrodynamic technique can only be used for insoluble particles due to liquid flow over the surface. It is not suitable for soluble powder material and substrate.

When applying Impact separation technique, fine particles need more impact forces and existence of capillary force requires more impact forces which may deform the substrate.

Ultrasonic technique needs a special equipment and design. The substrate and particle structure may be damaged and deformed at high forces.

Electrostatic detachment characterizes adhesion by using electric fields to remove particles from a surface.

One limitation with this technique is that electric field detachment can measure the adhesion of only charged particles. The adhesion measurement of uncharged particles is not possible since the electric field cannot apply a force to them.

The advantage of electric field detachment is that it is one of the best techniques of characterizing the average adhesion properties of different classes of powders. Another advantage is that the data can be taken more quickly than the other techniques and therefore one can build up a database of many powder materials and identify how material aspects of the particles are influencing their adhesion and adhesion distribution.

Atomic force microscopy (AFM) measures the adhesion of single particles to a variety of surfaces. AFM is one of the best at measuring the adhesion of uncharged particles. One limitation is that it is difficult to measure the adhesion of charged particles. Another limitation of the AFM is that it can monitor the adhesion of only a single particle. Because most of the powders have irregularly shaped particles, there is a concern that the aspects of adhesion being monitored with AFM are not representative of the collection of powder which is studied as a whole.

Even though the AFM measures the adhesion of single particles, it can do this with quite high precision and control. The spacing between the cantilever and the surface can be accurately controlled and one can do specialized measurements such as monitoring the dependence of adhesion on contact time, loading force, and applied electric field.

Impact separation, Aerodynamic, ultrasonic, hydrodynamic, centrifugal detachment, and electric field detachment techniques all monitor the adhesion of many particles, and the outputs of these measurements are a distribution of adhesion forces for all the powder material. However, Aerodynamic and hydrodynamic techniques need special design and appropriate supply such as air or liquid flow over the surface. Centrifuges are generally heavy testers and captures big spaces and not easy to transport them. Electric field detachment technique also needs special equipment and design. Impact separation technique can be used with a simple design at low cost and it is easy to carry a bench size impact adhesion tester. In this project it was a necessity to carry the tester to

Germany and therefore impact adhesion technique was preferred as the most favourable technique for this study. Another reason to prefer this technique was its potential for representing the impacts acting on crisps substrates in real production environment. Other techniques were dismissed due their complexities, high cost and difficulties in transportation.

The critical discussion of these techniques and relevance of their findings to that of this study can be found in Chapter 4.

1.2.3 Recent works on particle adhesion

The flavour coating processes is affected by adhesion phenomena between powders and surfaces (Salazar-Banda et al, 2007). There have been numerous research works on adhesion of single particle to surfaces under different environmental conditions (Bowen et al., 1998; Katainen et al., 2006; Kappl and Butt, 2002; Willing et al., 2000; George and Goddard, 2006; Gotzinger et al., 2007; Cleaver and Tyrrell, 2004; Fuji et al (1998), however few research works have focused on bulk particle adhesion onto food surfaces. Different methods and techniques have been studied to better understand the adhesion behaviour of the powder material by various researchers – the most pertinent test techniques of which are detailed in the following sub sections.

1.2.3.1 Centrifuge technique

The centrifuge technique has been used to investigate the adhesion forces of whole milk powder (from 20 to 250 μm) to a stainless steel substrate followed by post-detachment evaluation using a microscope (Rennie et al , 1998). The powder was applied onto the polished surface of a steel disc (8 mm diameter) in a beaker by using compressed air (40 kPa gauge). Impact force generated by compressed air caused the particles to stick. The detachment experiments were conducted at 4000, 6000, 8000, 10000, 12000, 13000 and 14000 rev/min rotational speeds (researchers have not reported the g values). An aluminium holder and nylon sheath were used to hold the steel disc (8 mm diameter) and to collect the detached particles (Fig. 1-24). They have used a microscope along with a CCD and a PC equipped with a frame grabber board. According to the method they used, the reflected light by the particles was caught by the camera and showed up

as bright spots on a dark background. They used a software package to perform the feature analysis on the acquired images to get feature diameters and area equivalent diameters. It was reported that an increase in particle diameter increased the detachment rate while the centrifugal force kept constant and hence larger centrifugal force was needed for detachment of smaller particles. They have explained that a type of liquid bridge is formed between particles containing amorphous substances that are at a temperature higher than what is called the powder sticky point. To be able to better understand the effect of temperature on adhesion, the rotor of the centrifuge with substrate was heated up to 60 °C. It was reported that the d_{90} of the 40 °C distribution was 71.5 μm , and that for the 60 °C distribution was 93 μm , which mean the higher the temperature, the greater the adhesion.

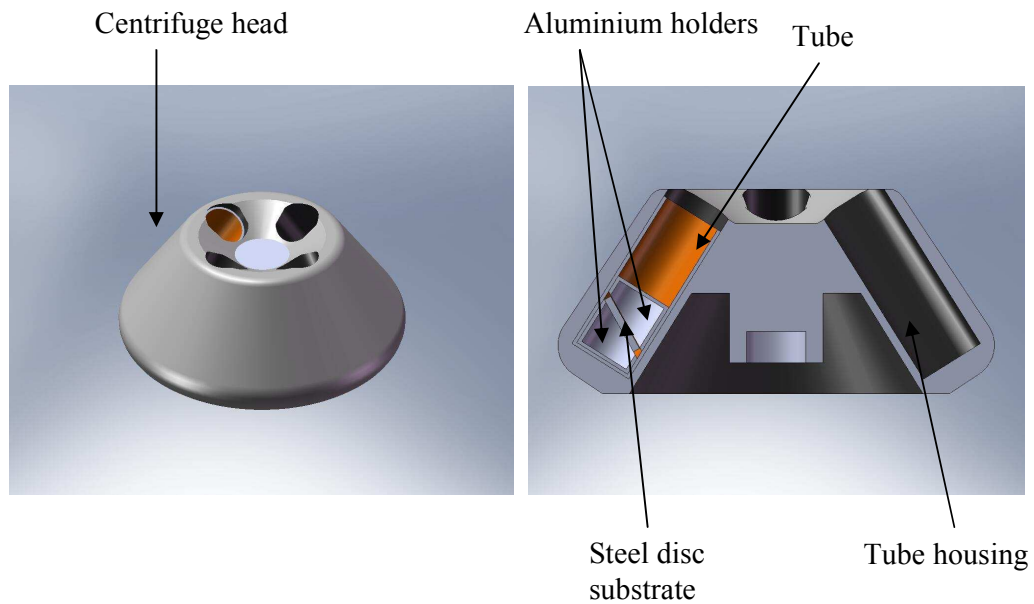


Figure 1-24. Schematic diagram of substrate housing in centrifuge rotor. (Tube dimensions: H:20 mm, D: 8 mm)

Salazar-Banda et al (2007) have used this technique to determine the influence of particle size on the surface adhesion force. Phosphatic rock and manioc starch particles on a steel surface were studied. They have polished the disc surface with silicon carbide sand papers in wet (water) and then in a low rotation polisher, using soft velvet impregnated with alumina suspension of 1 micron and 0.3 micron, in sequence. The workers used a micro-centrifuge that reached a maximum speed rotation of 14000 rpm

using purpose designed centrifuge tubes (Fig 1-25). Particle detachment was undertaken using a range of centrifugal speeds (3000, 6000, 9000, 12000 and 14000 rpm - calculated adhesion forces varied from 1×10^{-7} to 1×10^{-5} N) after dispersing the powder on the steel disks by using a powder dispersion system which uses vacuum. It has been reported that for smaller particles (13 μm mean diameter) a higher rotational speed was needed to detach the same percentage achieved by the larger particles (26 μm mean diameter).

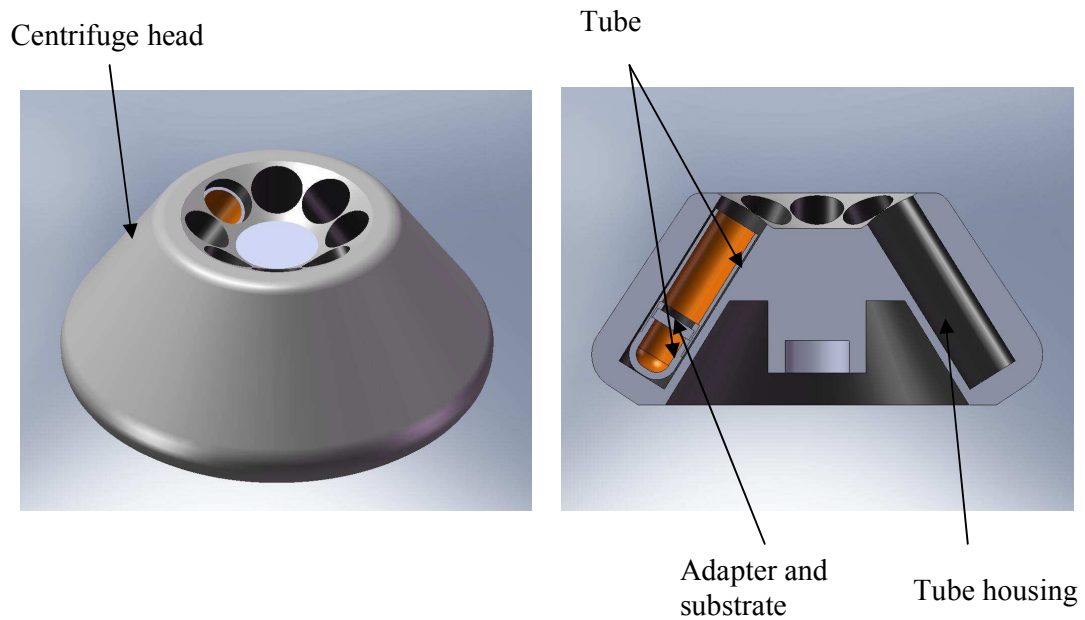


Figure 1-25. Schematic diagram of substrate housing in the head of centrifuge.

The combined effect of time and relative humidity on detachment of Polystyrene Latex particles (22 μm , mean diameter) from polished silicon substrates by using a spinner has been studied by Tang and Busnaina (2000). The particles were deposited on the silicon wafer and kept in a chamber at a controlled humidity (up to 100% Relative Humidity) for a controlled time (up to 8 days). A microscope was used to determine the number of particles deposited and still in situ after experimentation. The silicon substrate was spun at 3000 or 6000 rpm by a spinner for 120 seconds. They reported that the removal efficiency $[1 - (n_{after} / n_{before})]$ decreased with time, and an increase in capillary force (increasing relative humidity from 45% to 100%) decreased removal efficiency by 50% within 24 hours.

1.2.3.2 Liquid/gas flow

A review of a number of works on humidity controlled air flow on adhesion Cardot et al (2001) has indicated a significant variation in the experimental data generated from the use of gas flow technique. Spherical glass beads (21-37 micron) were used in an air shear flow cell. They have temperature and humidity controlled air stream in the flow cell mounted on the stage of an inverted microscope coupled to a CCD camera with a video image processing system for counting of particles. A gas impingement test procedure was developed by Russ and Talbot (1998) and used to measure adhesion forces in between phosphor particles (3 μm average diameter) and surfaces. The powder deposit is tested by placing the coated substrate (the procedure to deposit phosphors electrophoretically are described elsewhere (Russ, 1997)) target under a nitrogen gas jet and increasing the gas flow rate (and hence force) until particles are detached. It has been reported that the test developed can measure adhesion forces in the range of 100 to 450 Pa (Russ and Talbot, 1998).

A wind tunnel experiment has also been configured and the effect of air flow on flavour detachment from tortilla chip surface studied by Enggalhardjo and Narsimhan (2005) (Fig 1-26). They reported that the inferred force of adhesion increased with particle size, oil content of the chip, viscosity of oil, and surface tension of oil. The inferred force of adhesion has been reported to be in the range of 1.6×10^{-9} N to 3.3×10^{-7} N for the particles ranging from 32 to 300 μm .

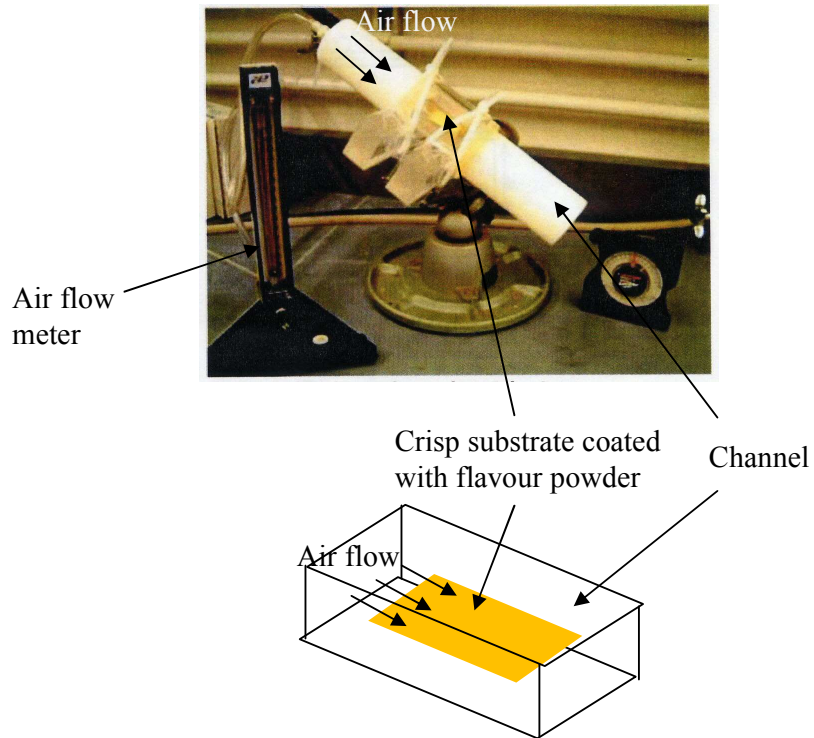


Figure 1-26. Wind tunnel experimental setup and schematic drawing of rectangular channel (from Enggalhardjo and Narsimhan, 2005)

1.2.3.3 Atomic force microscope (AFM)

A direct quantification of adhesion forces between a single particle (11 μm polystyrene spheres attached to cantilever) and a membrane surface by using an atomic force microscope (Fig. 1-27) has been reported (Bowen et al, 1998). The researchers attached the particles onto a cantilever (V-shaped Cantilever) known as colloidal probe with epoxy resin and measured the force of adhesive interaction between particle and two different membranes (polyethersulphone and a mixture of polymers) having different pore size distributions as 1.98 mN/m and 0.38 mN/m under the same experimental conditions. The reason for difference of force distribution between these two membranes was reported as due to their chemical and physical characteristics and hence molecular interactions between membrane and particle surfaces such as van der Waals interactions.

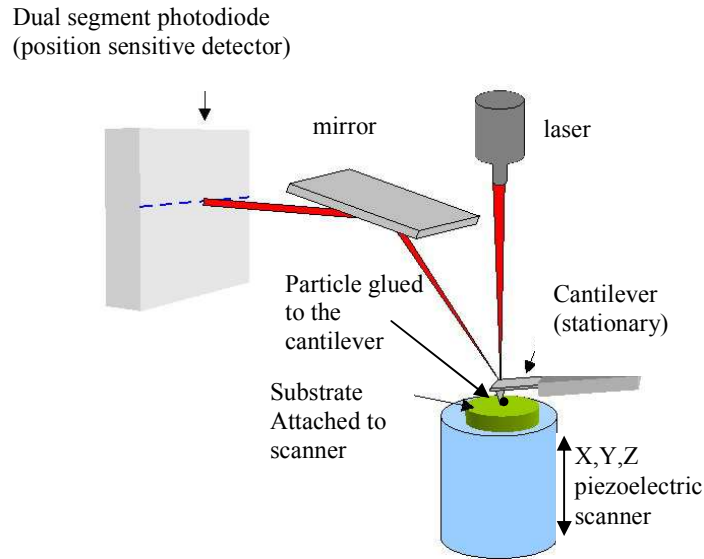


Figure 1-27. Colloidal probe technique in an atomic force microscope

1.2.3.4 Detachment field method

Takeuchi (2006) has used this method (as illustrated in Fig. 1-28) for adhesion force measurements of toner and polymer particles (9 to 11 μm) to aluminium substrates. The experimental system consists of a potential sweeper for the ramp voltage source, a high-voltage amplifier for applying voltage to the electrode, a power supply unit for the high-voltage amplifier, an electrometer and X-Y chart recorder. By increasing the voltage (10 V/s), toner particles jump from one electrode to another and thus adhesion force distributions were observed. It has been reported that the adhesion forces of toner particles (distributed over the range of 1×10^{-11} - 1×10^{-7} N) increased with an increase in either particle size or particle charge.

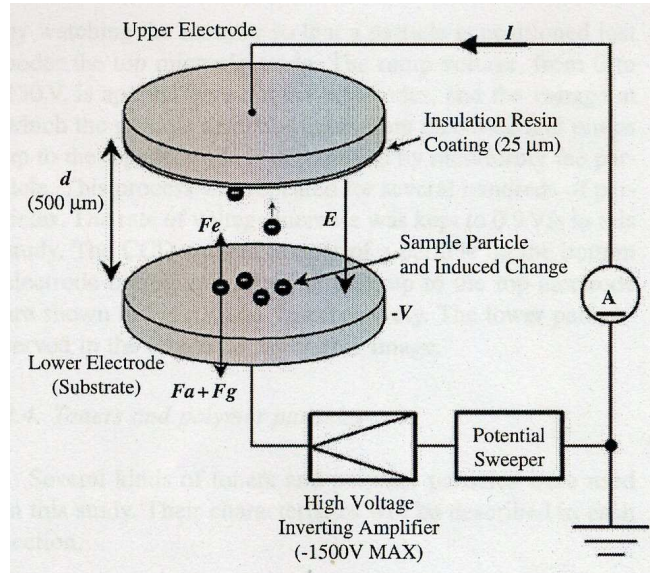


Figure 1-28. Experimental setup of detachment field method for adhesion force measurements of particles (Courtesy of Takeuchi, 2006)

1.2.3.5 Vibration method

The vibration is considered as an indirect method for the measurement of adhesion forces in between particles and surface (Hein et al., 2002). This method (illustrated in Fig. 1-29) which is used by Hein et al. (2002) is based on particle re-entrainment from a vertical-sinusoidal vibrating surface caused by its inertia at certain acceleration. They have measured the acceleration of the vibrating surface by using a laser-scanning-vibrometer. They have continuously recorded the particle re-entrainment by an image analysis method and correlated to acceleration to calculate the adhesion forces. They have used an air flow parallel to the surface to remove re-entrained particles. They have used glass spheres (40-50 μm and 60-70 μm) on silicon wafer. They have reported the adhesion force for smaller spheres as 200-400 nN and for bigger ones as 600-800 nN. Buck and Barringer (2007) have used a magnetic feeder which was closed off on the end using a piece of foam. They have divided the feeder tube into 8 slots using foam dividers and placed the chips coated side facing up inside the feeder. The vibration time has been set to 15 s. The chips have been weighed before and after addition of salt and after vibration and used Eq. 16 to measure adhesion. They report that the percent adhesion for 259 μm flake salt is 40-50% on crisp without surface oil; 70-80% with low surface oil (below 3 mg/cm^2) and 90-100% with high (above 3 mg/cm^2) surface oil.

They also report the percent adhesion as 70% for 24 μm salt crystals; 68% for 123 μm ; 48% for 259 μm ; 25% for 291 μm and 20% for 388 μm on the crisp without surface oil. With high surface oil, they report the percent adhesion as 95% for 24 μm salt crystals; 90% for 123 μm ; 90% for 259 μm ; 85% for 291 μm and 82% for 388 μm . They have not reported the measured vibration level.

$$Adhesion(\%) = \frac{Wt_{aftershakingsalt} - Wt_{beforecoating}}{Wt_{aftercoating} - Wt_{beforecoating}} \times 100 \quad (16)$$

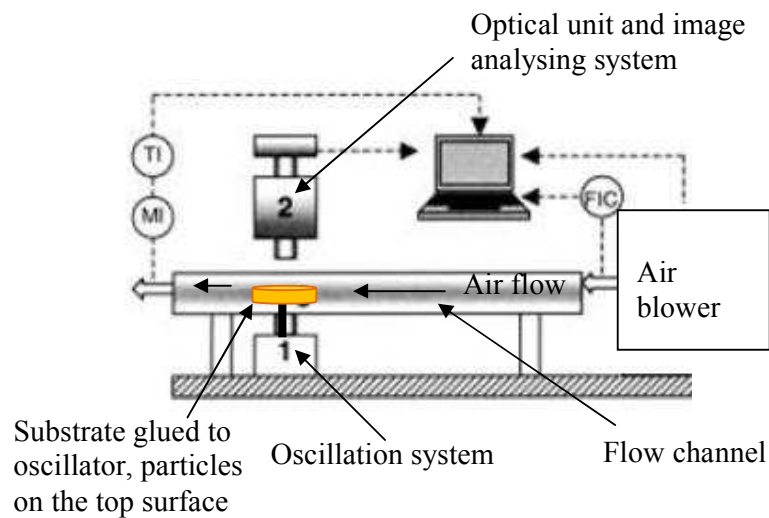


Figure 1-29. Schematic diagram of the vibration experimental apparatus (courtesy of Hein et al., 2002)

1.2.3.6 Summary of test procedures

Measuring the adhesion strength of a single particle and/or coating is a procedure commonly used by different Industries (Chemical, Food, and Pharmaceutical) to understand the quality of coating onto surfaces. The strength of adhesion that can be measured by different test techniques is usually correlated to several factors such as surface characteristics of the product, intervening media, and physical and chemical structure of the coating material.

The well-known adhesion test techniques for measurement of adhesion strength of a single particle attached onto a surface are AFM and Centrifugal (Salazar-Banda et al,

2007). These are standard procedures in which minimum force is determined to detach the particle from the surface. When performing the adhesion tests (AFM, Centrifugal), obtaining a result for a single particle has two difficulties. Firstly, the similarities of the surface used to the product and secondly the effect of a secondary-media such as oil. Due to the AFM, it is required that a single particle is attached to a cantilever. The vibration and the centrifugal rotational speed are the most crucial parameters for the accurate determination of the detachment force for a single particle and therefore they need to be measured carefully.

The vast majority of the research work has been undertaken to date on particle adhesion has been primarily for academic purposes and has largely focussed on single particle/cell adhesion. Table 1-8 summarises the results of selected research work previously discussed in this chapter. There is still lack of information about adhesion of food particles in bulk onto food surfaces at full production scale operations (i.e. crisp manufacturing).

Table 1-8. Summary of results obtained from different research work on adhesion.

Authors	Method	Materials-contact geometry	Data obtained
Rennie et al , 1998; Salazar-Banda et al (2007); Tang and Busnaina (2000)	centrifuge	milk powder (20-250 μm) on steel; phosphatic rock and manioc starch on steel; polystyrene latex particles on silicon wafer	d90 of the 40 °C distribution was 71.5 μm , d90 of 60 °C distribution was 93 μm ; for smaller particles (13 μm) a higher rotational speed was needed; the removal efficiency decreased with time, and an increase in capillary force (increasing relative humidity from 45% to 100%) decreased removal efficiency by 50% within 24 hours
Cardot et al (2001); Russ and Talbot (1998); Enggalhardjo and Narsimhan (2005)	gas flow	phosphor particles; flavour powder on tortilla chip	adhesion forces in the range of 1.6×10^{-9} to 3.3×10^{-7} N for the particles ranging from 32 to 300 μm
Takeuchi (2006)	detachment field	polymer particles (9 to 11 μm) to aluminium substrates	distributed over the range of 1×10^{-11} to 1×10^{-7} N
Hein at al. (2002); Ripperger and Hein (2004)	vibration method	glass spheres(20-30 and 60-70 μm) on silicon wafer substrate; glass particles (on silicon wafer substrate)	adhesion force for smaller spheres as 2×10^{-7} - 4×10^{-7} N and for bigger ones as 6×10^{-7} - 8×10^{-7} N; varied from 2×10^{-7} to 8×10^{-7} N according to particle size varied from 15 to 25 μm
Shimada et al (2003)	Direct separation by using a needle	Corn starch (30 μm), potato starch(60 μm), lactose (80), glass beads (68) (adhesion between particles)	$1,45(\pm 0,30) \times 10^{-7}$ N for corn starch, $2,71(\pm 0,50) \times 10^{-7}$ N for potato starch, $7,8(\pm 0,12) \times 10^{-8}$ N for lactose, $3,3(\pm 0,6) \times 10^{-8}$ N for glass beads
Shaefer et al (1994)	Atomic Force Microscope (AFM)	polystyrene particle(2.5-3.5 μm) on silicon substrate	applied loads between 2×10^{-8} – 3×10^{-7} N to particle on surface, adhesion force increased from 9×10^{-8} to $1,1 \times 10^{-7}$ N
Bowen et al, 1998	AFM	polystyrene spheres attached to cantilever	as 1.98 mN/m and 0.38 mN/m
Fuji et al(1998)	AFM	between single silica particles in nitrogen atmosphere	increase in RH from 70 to 80%, increase in adhesion force from 50 to 500 mN/m
Cooper et al(2000)	AFM	polystyrene spheres(5 μm) on silicon substrate in aqueous solution at 1.13 M ionic strength	at low pH (<4) $1,2 \times 10^{-7}$ N, at high pH $1,2 \times 10^{-8}$ N
Willing et al (2000)	AFM	lactose particles (2.5 μm) on gelatine capsules	$1,9 \times 10^{-7}$ and $2,9 \times 10^{-7}$ N for different capsules
Sonnenberg and Schmidt (2005)	numerical calculation	particle-slap interactions in dry uncharged conditions for separation distance from 10 to 30 nm	vdW forces varies from 2×10^{-10} , 1×10^{-9} , to 1×10^{-8} N based on shape

1.2.4 Theoretical adhesion models

Analytical models have been developed to predict the mechanical behaviour of ideal sphere-plane contacts by *Johnson, Kendall and Roberts (JKR)* (Johnson et al, 1971) and *Derjaguin, Muller and Toporov (DMT)* (Derjaguin et al, 1975) models. These models were used to analyse most experimental results on adhesion forces (Kappl and Butt, 2002). According to Kappl and Butt (2002), for both models, adhesion forces depend linearly on particle radius. On the other hand, the force between two surfaces also depends on both the material properties and the geometry of the surfaces (Salazar-Banda et al, 2007).

Most existing models either assume that the particle surface is perfectly smooth or there is no deformation at the contact area (Li et al, 2006). This is almost certainly the reason why there are differences between theoretical model calculation and experimental results.

The difference between these two models occurs in assuming the nature of forces acting between particle and substrate (Salazar-Banda et al, 2007). According to Johnson et al (1971), attractive forces act only inside the particle-substrate contact area, however, Derjaguin et al (1975) assume long-range surface forces acting outside the particle-substrate contact area.

Recent developments on adhesion models are presented by Tsai, Pui, and Liu (1991), Maugis (1992), and Rimai, Demejo, and Verrland (1992). Also some articles can be found in the books edited by Mittal (1991), and Quesnel, Rimai, and Sharpe (2001).

These models assume that substrate surface is smooth and there is no intervening media such as oil in between particles and surface. However, the substrate and particles used in this study have irregular surfaces and oil is used as intervening media. For these reasons these theoretical models were found to be inappropriate to use in this study.

1.2.5 Texture analysis

Texture is usually quantified by plotting the force required to deform or break substrate vs. their deformation (Segnini et al, 1999). Bourne et al. (1996) gave objective measurements of potato chip textures, in terms of resistance to bending. They conducted a punch test and measured the initial slope from the force-deformation curve. (see Fig. 1-30 and Fig. 1-31) The maximum force of break varied considerably. Katz and Labuza (1981) performed snap and punch tests and they have concluded that none of the mechanical analysis of texture produced useful quantitative information.

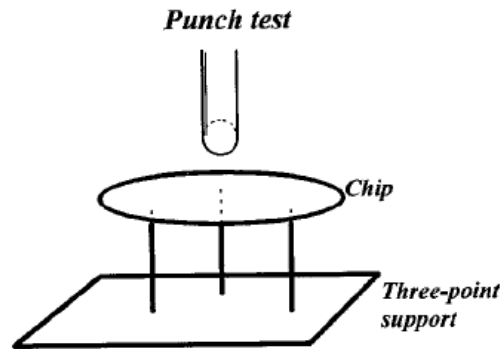


Figure 1-30. Support used to measure texture of potato chips. (source: Bourne et al, 1996)

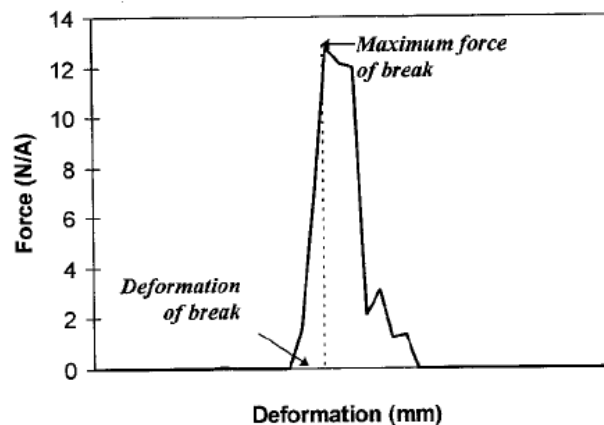


Figure 1-31. Typical force-deformation curve representing results by using Universal Testing Machine (source: Bourne et al, 1996).

1.2.6 Summary of the literature review

This chapter gave an insight to the production of crisps substrates, characterisation of powders, and some of the flavour coating techniques used in research and industry. Various research works on measuring particle detachment in the literature have also been reviewed. A number of important observations have been drawn:

- Flavour coating on the crisps in drum mixers have a distinct advantages over the electrostatic coating and conveyor type coating techniques that drum mixer operate at higher coating efficiency rate and easier to operate.
- Efficiency of coating is influenced by several factors such as powder flow rate into the mixer, size distribution, shape of the particles and adhesion mechanisms.
- It can be summarised from the literature review that flake shaped fine particles show better coating efficiency than other particles due to bigger surface area interacting with the surface of the substrate and lighter weight comparing to other shapes (cubic, irregular, spherical etc.) of bigger particles.
- Adhesion of powders is affected by the characteristics of powders (size, shape, and electrostatic charge to mass ratio), adhesion mechanisms (electrostatic, vdW, capillary) and process characteristics such as mixing technique used and application of oil on the surface.
- Some of the important parameters to characterize food powders are size distribution, powder density, porosity and flowability.
- There are different criteria to measure flowability. These are Hausner ratio, angle of repose, Carr's compressibility index, and shear/friction. There are different methods based on these criteria to measure flowability but most common technique used by researchers is Jenike shear cell and failure functions determined with the Jenike shear cell show close agreement with other complex testers.
- There are different methods reported in the literature used to measure adhesion of powders onto food surfaces. These are AFM, gas/liquid flow over the surface, centrifugation, electric field detachment, ultrasonic and impact detachment.

- Whilst Atomic Force Microscope (AFM) technique is difficult, expensive and time consuming to use, it can be derived from the literature that it measures the single particle adhesion to a reasonable accuracy, and has been widely used by previous researchers.
- Other techniques and testers developed such as centrifugation and impact detachment are easier and quicker to use, and comparable results obtained against the AFM. However, it can be drawn from the literature review that there is a degree of tester/technique dependence on the obtained results.
- From this literature review, it is evident that there is a significant deficiency of relevant work associated with this area of research. From the limited written works associated with measuring the particle adhesion, it can be stated that the many of the techniques and methods involved are exclusively of an academic nature and only consider single particle adhesion. Some other techniques such as centrifuge, aerodynamic, and impact separation use multiple particles at a time and the results are varying. An industrially appropriate approach for the assessment of particle adhesion behaviour is notable only by its complete absence in previous works.
- It is clear from the literature review that there is a need for a test procedure to investigate the particle adhesion in bulk to better understand the particle behaviour during production stages.

These observations were used to develop the structure of experimental investigation described in this thesis.

CHAPTER 2

MATERIAL AND METHODOLOGY

2.1 Introduction

As a consequence of the need to measure adhesion strength of particles on food surfaces, different design ideas have been explored to investigate the influence of particle characteristics and process conditions on adhesion strength and to develop a technique for quantifying the changes in adhesion behaviour of particles. The measuring techniques were considered were either build a dropping body on a vertical axis or a force applied type impact tester. As one of the consequences, the main goal for this research project was to aid industry by producing an economic and bench scale tester with which adhesion strength of flavour powders could be measured with a greater degree of understanding and confidence.

Various studies of adhesion strength of particles against food substrates have been conducted by many researchers by using a range of methods and test equipment. These are presented in Chapter 1 and the correlation of results is discussed in depth in Chapter 4.

A centrifuge tester was used for comparison with the designed and constructed tester. Both the centrifuge and the new tester were used to assess the effect of particle characteristics (size and shape) and coating process parameters (time, rotation speed etc) on the adhesion strength of particles to food substrates.

A texture analyser was used to investigate the strength of crisp substrates used in this project. The critical load on crisp substrate in terms of Newton was measured and recorded before crack of the substrate and repeated several times to get a mean value.

Different food powders were used to coat crisps substrate and wood veneer to investigate powder adhesion strength in different coating process conditions and results are discussed in Chapter 4.

2.2 Test Equipment

2.2.1 Evaluation of design of a novel adhesion tester

The novel tester that has been developed in this PhD project (referred to as the Impact Adhesion Tester - IAT), enables the estimation of particle adhesion strength to substrates. This apparatus has been designed such that it can accommodate a wide range of applied flavouring bulk particulates and substrates.

The pros and cons of other techniques have been discussed in Chapter 1. Other techniques were not taken into consideration to be used as primary tester in this study due to following reasons:

- Some of them are heavy testers to carry to another location (AFM, Centrifuge)
- It takes long time to prepare the substrate and to conduct the tests (AFM, Centrifuge)
- Some of them need gas or liquid supply which may not be available in production line where the tester may be located (aerodynamic, hydrodynamic techniques)
- Vibration and electrostatic detachment techniques were not considered due to their complex structures.

A key influence for the design of the IAT was that the apparatus should have equal application to laboratory based investigations and industrial quality assurance requirements.

The following design criteria were therefore applied:

1. The tester should be portable (it would be taken to Germany as part of the project in order to conduct tests at the Technical University of Munich).
2. The tester should be constructed with moderate expenditure.
3. The tester should have the facility to accommodate more than one test substrate at a time.

4. A range of test conditions comparable to industrial applications should be reproducible.

On the basis of the above criteria, the development of the IAT was based on the concept of a free-moving body to which multiple test samples are secured. The apparatus uses the principle of impact force generated by the vertical free motion of a plate (0.15 m diameter) along a steel cylinder shaft (0.5 m length, 0.016 m diameter) mounted on a base steel plate.

For measurement of adhesion forces by using IAT, particles were needed to be coated on the surface of substrates. For this purpose, a bench scale tumbler mixer along with a powder feeder unit was designed and constructed. The reason to choose this type of coater is that it the most efficient and easy to use coater as reported in Chapter 1.

The resulting testing system can be usefully divided into the following sub-systems, the design of which will be presented in detail:

- Impact Adhesion Tester (IAT)
- Sample holding sub units
- Tumbler mixer
- Vibratory feeding unit

2.2.1.1 Development of Impact Adhesion Tester (IAT)

The IAT was designed and constructed to measure the adhesion forces for different shapes of particles of flavour, salt and glass powders deposited on a food substrate under different processing conditions. The IAT was developed as a means of measuring the adhesion strength of particle coatings, and producing a quality control tool for the flavour experts and industrialists.

The tester is designed to hold 4 samples simultaneously and allowed the adhesion forces to be able to measure with the sensitivity of 1×10^{-8} N. This is achieved by detection of

deceleration forces measured by an accelerometer and by calculations based on single particles. It is capable of a height resolution of 1 mm (equal to 1 m/s²) by adjusting the height by using a ruler.

The main components of the IAT were manufactured by using computer aided design and rapid prototyping technology.

Sample platen

The platen was designed to accommodate four test samples simultaneously, in order to maximise the gathering of comparative data from a single test (Fig. 2-1). The platen features four apertures, each sized to accommodate a 3 cm diameter sample holder and collecting dish. The distance from the substrate surface to the collecting dish was 12 mm.

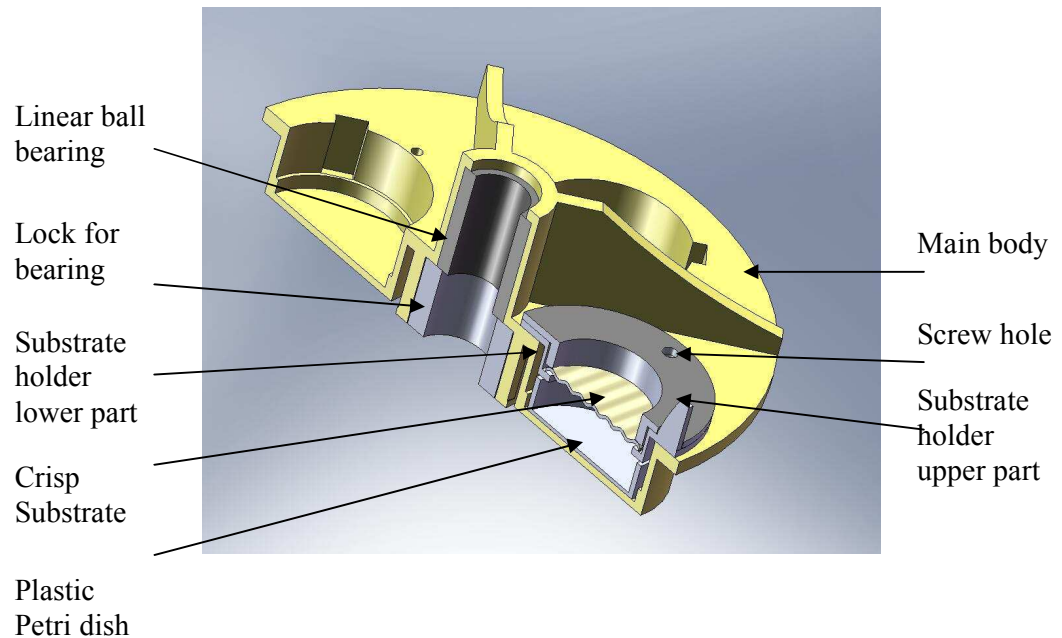


Figure 2-1. Cross sections of main parts of the Impact Adhesion Tester (IAT).

The dimensions of the plate can be seen in Appendix 1.

Crisp substrates were weighed before coating individually. Then the particles-substrate system after coating just before drop test and particles-substrate system after drop test were weighed by means of a digital balance in order to determine total mass of particle on the surface before and after drop of plate. From this information, the proportion of particles removed from the surface at each experimental setting was determined.

A linear ball bearing is placed into the centre of the plate to decrease the effect of friction forces in between surfaces to allow free motion to the platen. The ball bearing was placed in the centre of the plate and secured with a cylindrical lock by screwing it to the platen (Fig. 2-1).

The impact force is generated by the free fall movement and sudden deceleration of the platen. The linear ball bearing is mounted on the plate and assembled on a cylindrical shaft which is mounted on a steel plate to get impact force by deceleration of freely moving plate along the shaft (Fig. 2-2). It is secured in the middle of plate by using a hollow cylindrical part by screwing to plate. This design feature incorporated to decrease the effect of friction on movement of platen. A hollow stopper, which was glued on the base plate, was designed to act as a buffer between base plate and platen.

Appendix 2 summarizes the parts used in design of IAT and their dimensions.

Surface hardened (for wear resistance) stainless steel cylinder shaft was obtained from RS Components Ltd. UK and mounted into the drilled and tapped hole in the centre of base plate.

Four adjustable levelling feet were mounted on base plate into the drilled and tapped holes. They provided the option to adjust the height of base plate and to adjust the level with the help of a bubble spirit level.

The dimensions of the tester can be seen in Appendix 3.

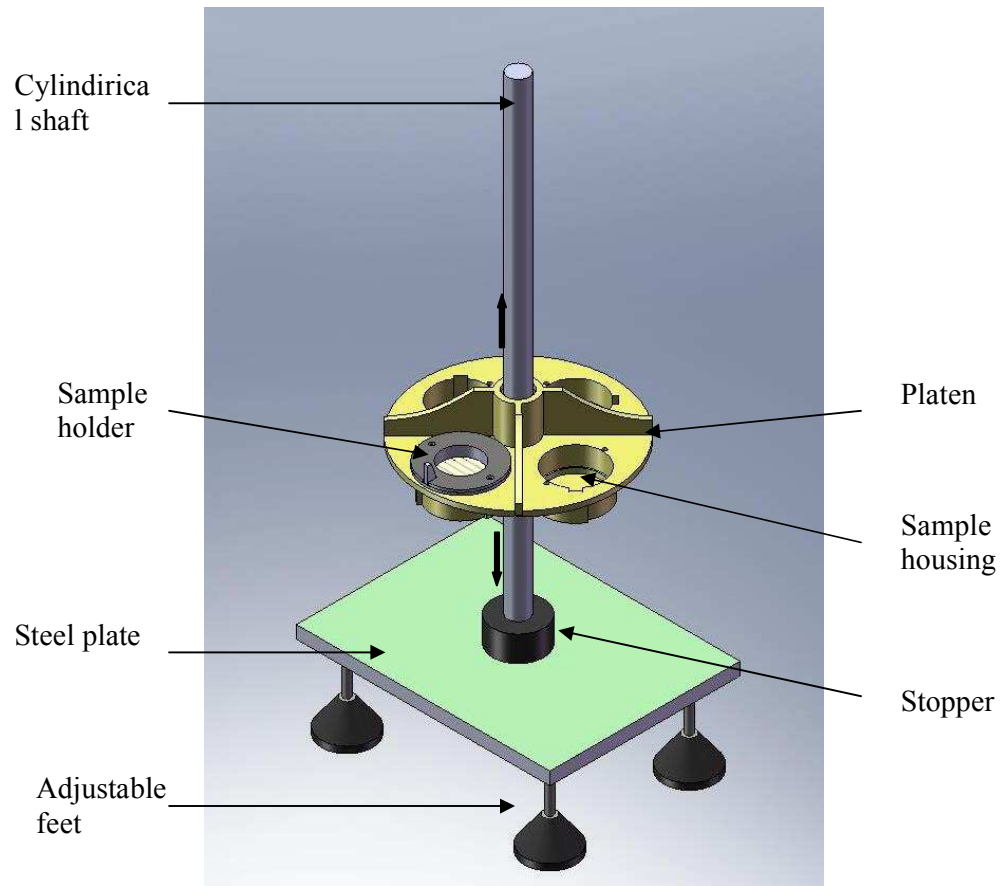


Figure 2-2. Main parts of Impact Adhesion Tester (IAT)

The sample holder consists of two parts (split horizontally) which serve to “sandwich” the test substrate securely in place (thus minimising the risk of substrate fracture during tests). Substrates up to 3mm thick can be accommodated with this design (Fig. 2-3). Placement of the test substrate is achieved using a specially designed tool (Fig. 2-4).

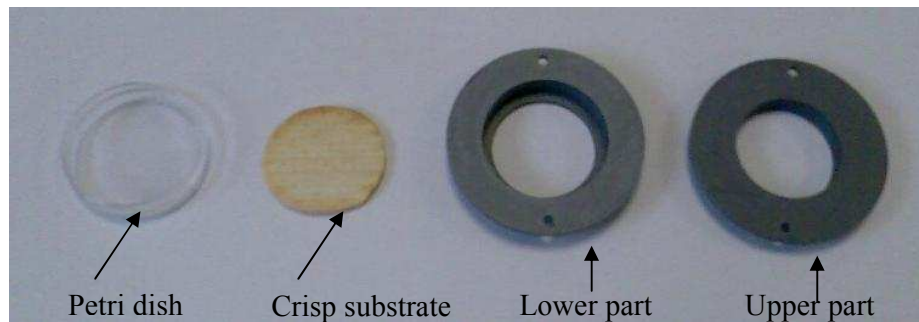


Figure 2-3. Sample holder

A specially designed sample placing tool was used to place the crisp substrates in between upper and lower parts of the sample holder. Sample placing tool and the drawings showing substrate placing is shown in Fig. 2-4.

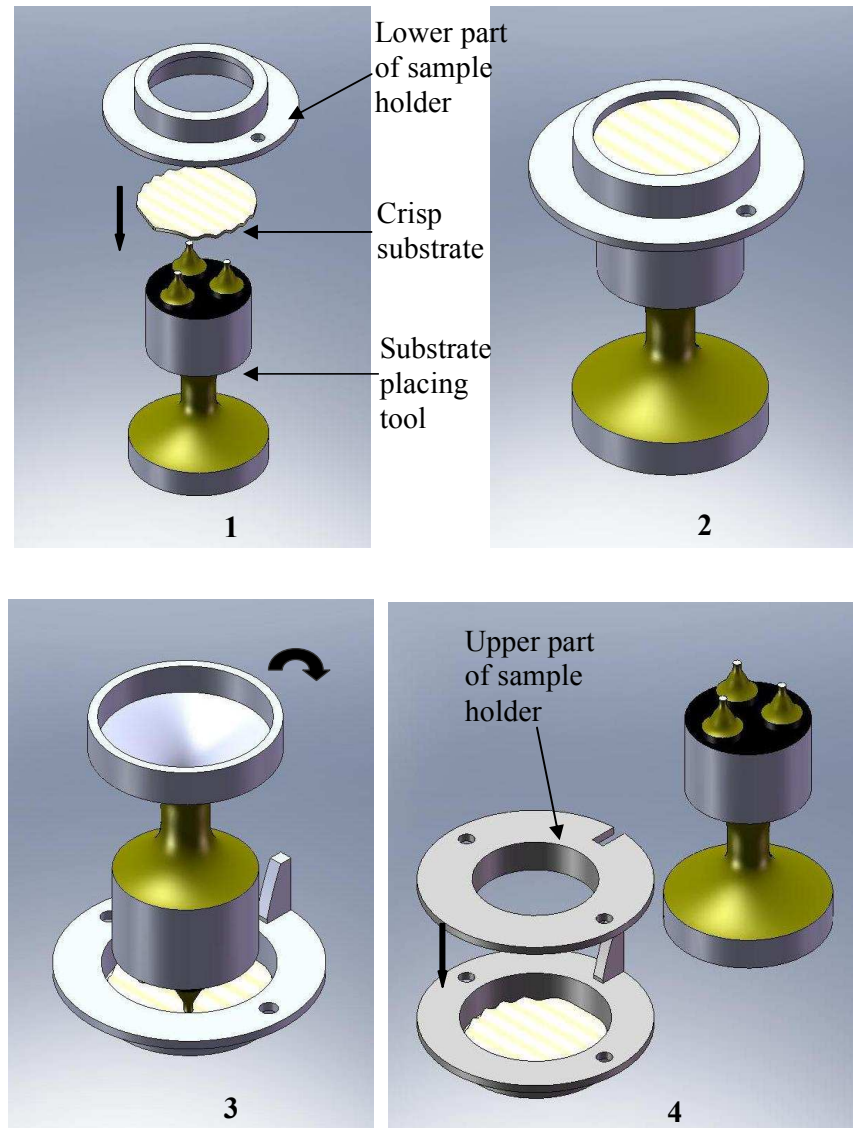


Figure 2-4. Specially designed placing tool and substrate placing

2.2.1.2 Deceleration measurement of the IAT

2.2.1.2.1 Choosing the right accelerometer

It can be stated that an object dropping from standing height can produce peak acceleration levels over 1000 g (see Appendix 6). The magnitude of deceleration generated by a dropping object is highly depending on the rebound impulse time as explained in Appendix 6. In high-g shock test where structural responses are often non-linear and difficult to characterize, choosing the right accelerometer can be critical to get the g peak values.

Some basic selection specifications were considered before making an investigation to find an appropriate accelerometer for the new tester to measure deceleration values of the plate being dropped from different heights. These were:

The accelerometer should

- be suitable to measure shock such as drop-testing
- be light weight to minimise mass loading since it may affect deceleration of platen.
- have a high resolution and wide bandwidth to catch short duration shock pulses
- have high range to be able to measure shock deceleration of drop
- be easy to mount on the test rig sample platen

In high-g testing, there is a potential for physical damage to the sensor to occur. It was considered to over-estimate the maximum shock level when selecting the specification of a suitable accelerometer. Survivability of accelerometers extends to cables and connections. The closer the accelerometer is to the impact area, the higher the input g level obtained.

Based on the information and criteria given above, an IEPE type (Integral electronics piezo-electric) accelerometer was chosen (Fig. 2-5). The basic specifications are outlined in Table 2-1.

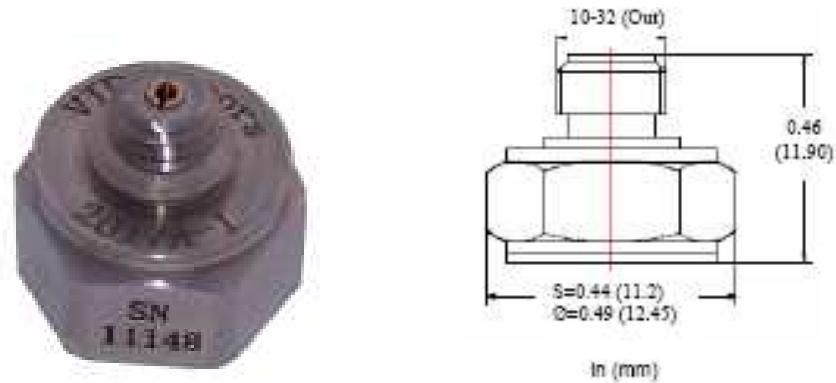


Figure 2-5. IEPE Accelerometer (VIP Sensors, USA)

The calibration certificate of IEPE accelerometer can be seen in Appendix 7.

Table 2-1 Basic specifications of chosen accelerometer

Characteristics	Units	Model 2017 AS-10
Weight	grams	5.3
Case material	-	Stainless steel
Range	g (m/s ²)	500 (4903.3)
Voltage sensitivity	mV/g	10
Resonance frequency	Hz	20000
Shock limit	g peak	2000

An acceleration data logger (Fig. 2-6) along with its software was also obtained to be used in laboratory based (and planned plant based) experiments for comparison of the data obtained from a given accelerometer. This accelerometer was aimed to be used in production line to understand the impact forces acting on crisp substrates while they are transported from coating unit to packing unit. The logger uses an internal three-axis accelerometer with a range of ± 3 g based on micro-machined silicon sensors consisting of beams that deflect with acceleration. The basic specifications are outlined in Table 2-2.

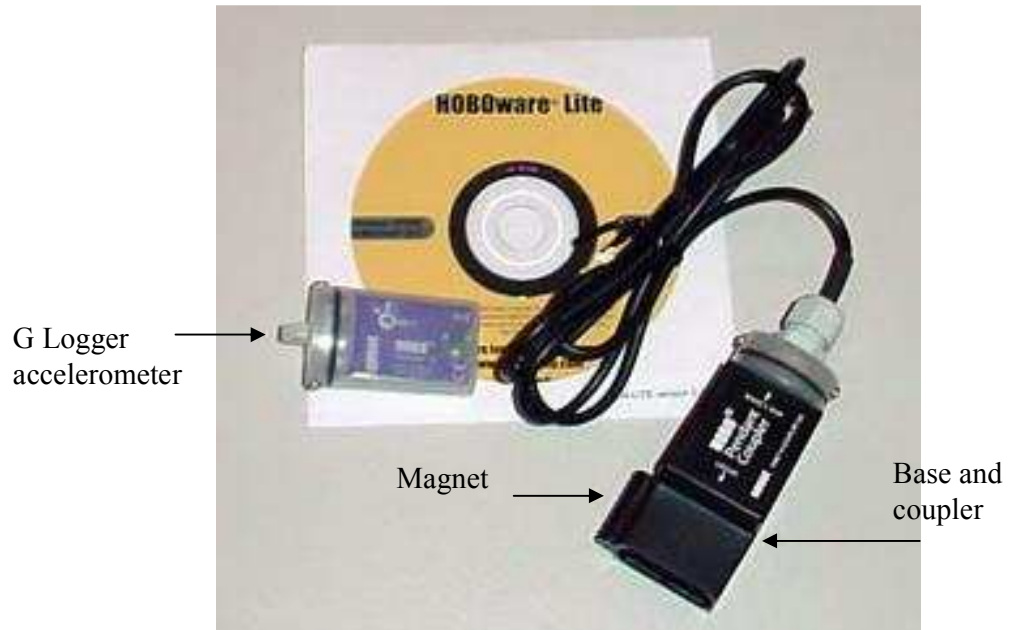


Figure 2-6. G logger set (Onset Computer Corporation, USA)

The G logger came with an optic USB base station and coupler to plug the USB connector on the base station into a USB port on any computer. Software which came also with the logger was used to process the data obtained from logger. There is a magnet on the side of coupler to activate/deactivate the logger. A schematic drawing of the logger and its coupler can be seen in Fig. 2-7.

Table 2-2 Basic specifications of data logger

Characteristics	Units	HOBO
Weigh	grams	18
Case material	-	Polypropylene
Range	$g (m/s^2)$	± 3
Resolution	g	0.025
Resonance frequency	Hz	Upto 100
Dimensions	Mm	58x33x23

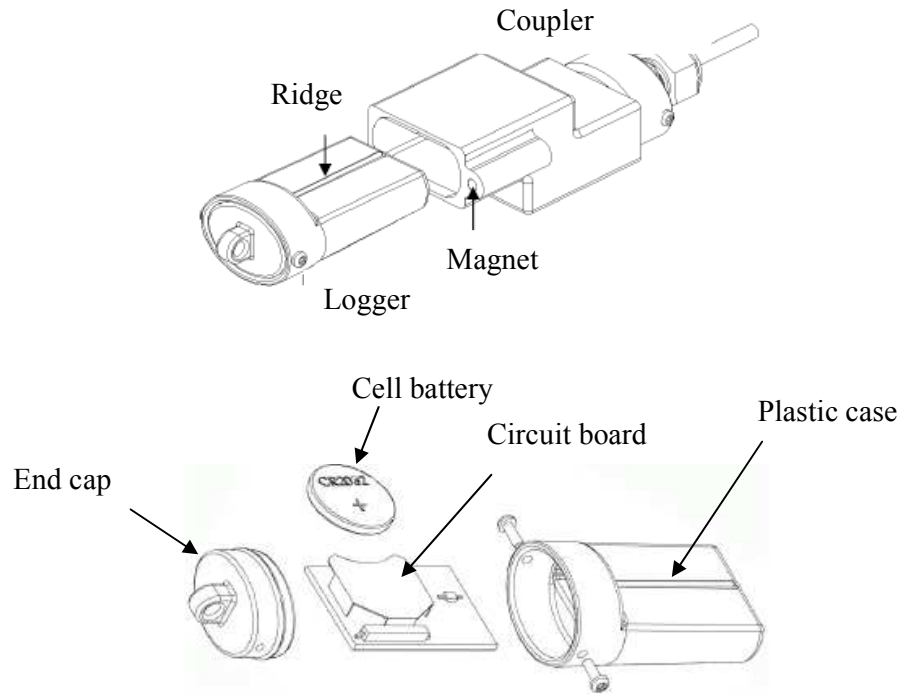


Figure 2-7. Acceleration data logger and coupler

2.2.1.2.2 Experimental set up for calibration

In order to determine the relationship between applied deceleration force on the platen (and its constrained test samples) and drop distance, the tester needed calibrating. This was accomplished by using an accelerometer in conjunction with an oscilloscope. The deceleration of the IAT plate dropped from different heights was measured using chosen IEPE type accelerometer which was attached to a signal conditioner (5100IEPE, VIP Sensors, USA) (Fig. 2-8). The signals from the conditioner were processed by an oscilloscope (GDS-8205, INSTEC, USA) and software (INSTEC Free Capture RS 232).

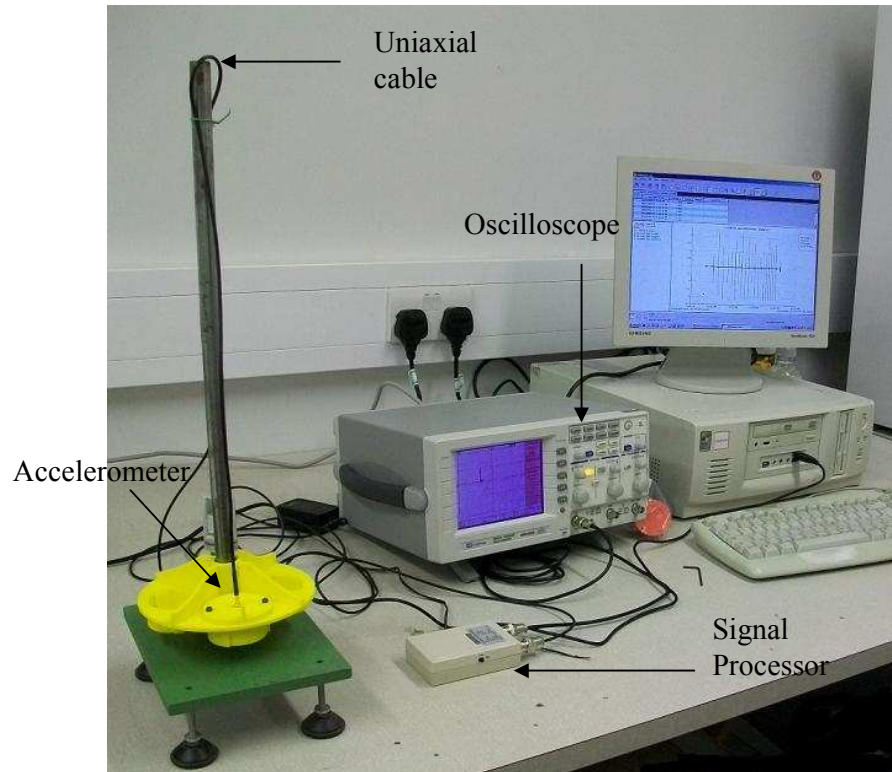


Figure 2-8. Deceleration experimental set-up

A special holder for the accelerometer was designed and constructed using CAD/CAM tool to secure the accelerometer on the plate. A uniaxial cable was attached to the accelerometer from one end and to the oscilloscope from another to get the signals to be processed. The oscilloscope was connected to the computer for using the software to get deceleration values.

2.2.1.3 Tumbler mixer for powder coating

A rotating drum (0.2 m length) with an internal diameter of 0.2 m, with 6 internal baffles, known as flights (Fig. 2-9), was designed and constructed for this study in conjunction with a vibratory flavour applicator. The rotation rate of the drum could be varied from 0 to a maximum value of 38 rpm and the vibration level of vibratory feeder could be controlled by a speed controller on electrical motor.

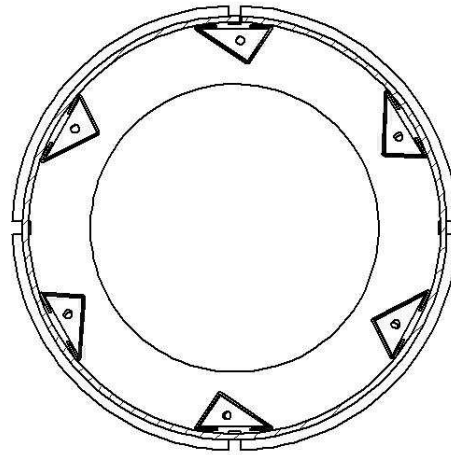


Figure 2-9. Cross section and side view of tumbler mixer.

The tumble unit and baffles (dimensions are shown in Appendix 4) are manufactured in stainless steel. The design, number and placement of baffles in the tumbler mixer were arranged based on the industrial scale mixers to get a uniform coating of the crisp substrate with the powders used in this study on both sides of the surface.

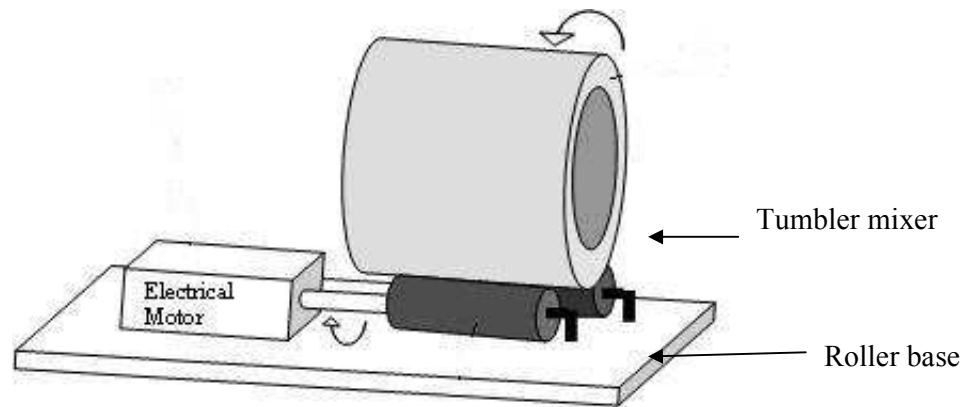


Figure 2-10. A sketch of the laboratory scale rotating drum.

In Fig. 2-10 and Fig. 2-11, the tumbler mixer along with a speed controlled electric motor is shown. As it can be seen in Fig. 2-11, driving motor is mounted to the gear unit and drives the rollers through a gear unit and let tumbler mixer rotates freely on the rollers.

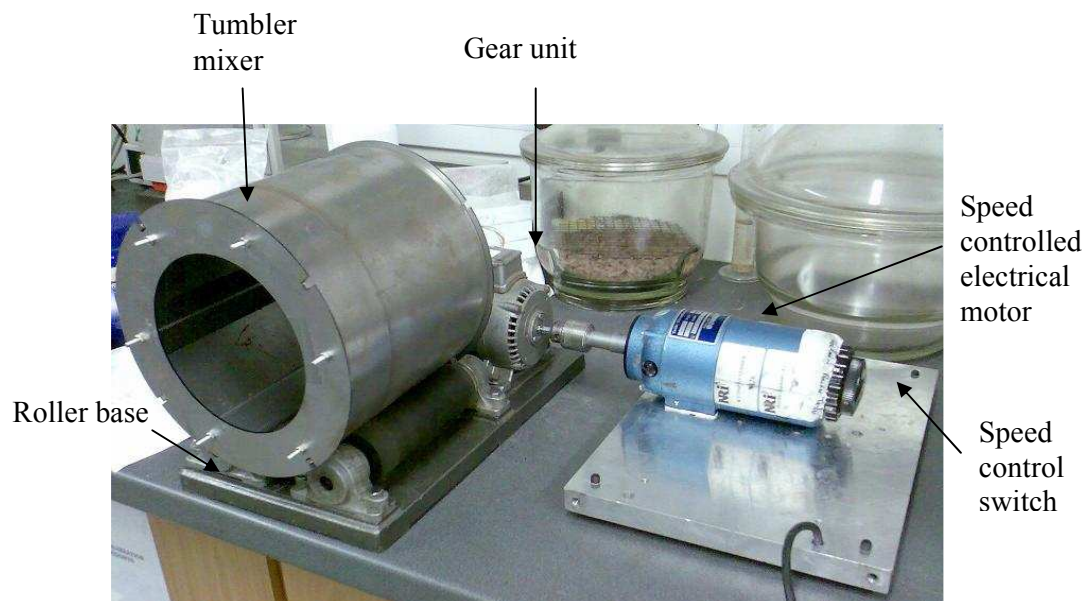


Figure 2-11. Speed controlled Electrical drive unit

The delivery of flavouring onto the crisps was achieved through the use of a vibratory feeder that deposited powder within the tumbler mixer in a dispersed form to coat the crisps. This will be explained in detail in the next heading.

2.2.1.4 Vibratory flavour applicator

A special flavour applicator was designed for the purpose of coating sample powders on crisp substrate in a tumbler mixer. The material used is circuit board pieces attached to each other by soldering. An inclined flat conveyor at a length of 300 mm provides a mono layer uniform flow of powder material feeding into the rotating tumbler mixer (Fig. 2-12). The vibratory electric exciter supports the conveyor to accelerate the particles on the flat surface by vibrating at different frequencies and amplitude which can be adjusted. Acceleration at the conveyor surface is proportional to the amplitude of vibration.

The powder feed unit consisted of a vibration tray unit on a height adjustable frame. An additional feeding conveyor and a rectangular feeder were designed and attached to feeder frame to make the delivery of powder onto the vibratory tray easier and in more dispersed way with screws to deliver powder into the tumbler mixer evenly and consistently (Fig. 2-13). Flow rate was evaluated by monitoring manually.

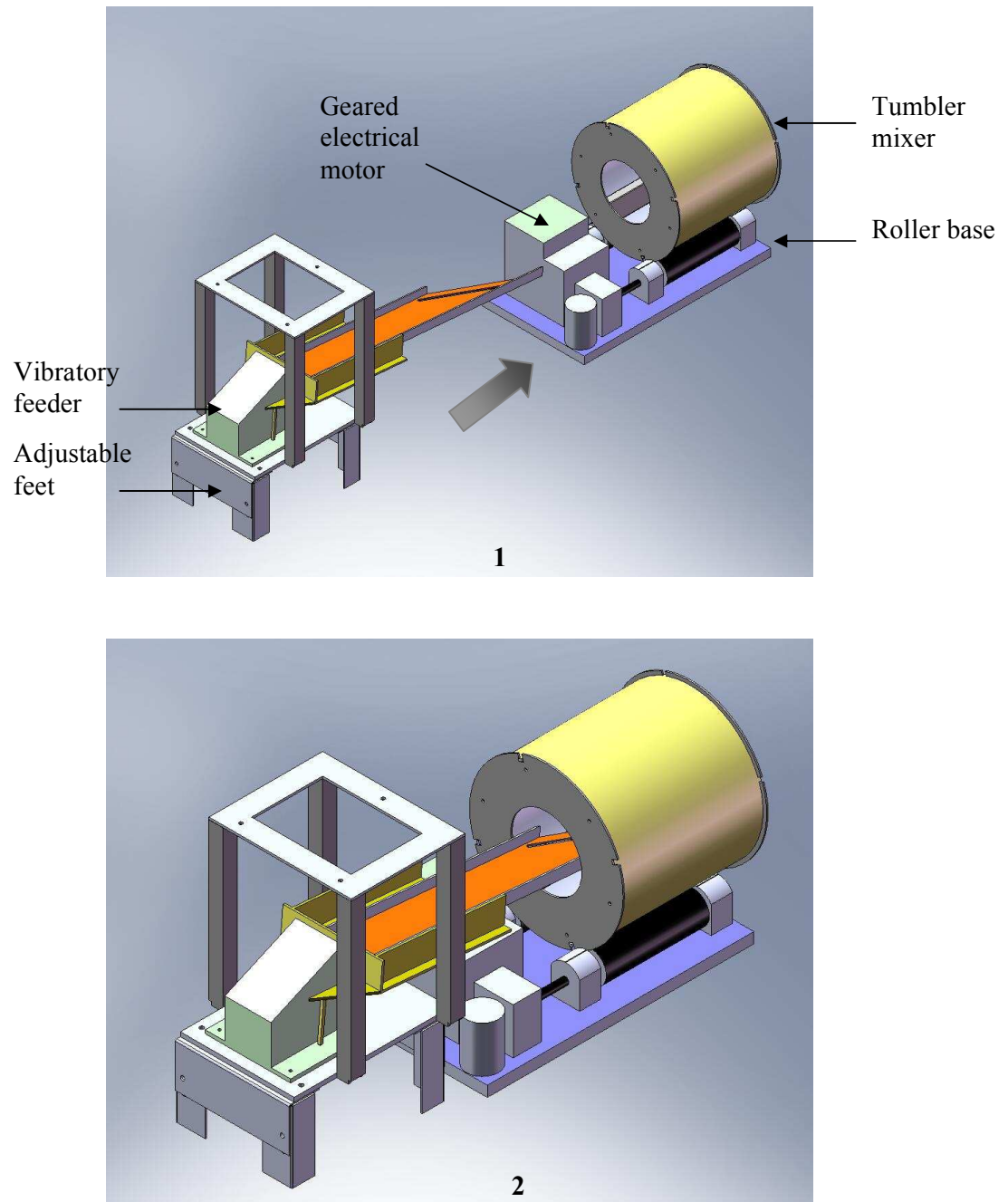


Figure 2-12. Vibratory feeder unit and placing in tumbler mixer

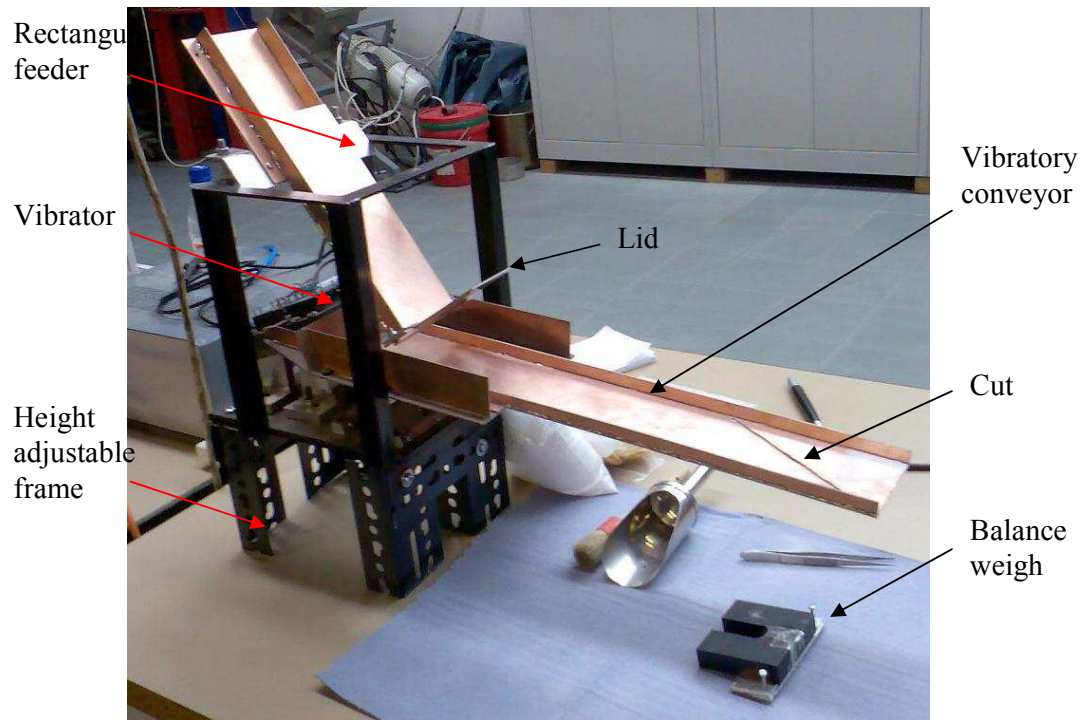


Figure 2-13. Vibratory feeding conveyor

Powder material was filled in the rectangular feeder (Fig. 2-13) on the top of the vibration unit and passed to the conveyor at a constant feed rate. Based on the length of tumble mixer, a 3 mm wide diagonal slot (approx. 30° to the axis of the tray) was cut in the conveyor for better delivery of powder as it can be seen in Fig. 2-14. This design feature allowed the powder delivery to be monolayer and in dispersed form (in other words, reducing uneven distribution of powder in tumble mixer). It was ensured that the weighed powder was uniformly spread on the crisp substrates by placing the conveyor along the axis of rotation of tumble mixer (Fig. 2-15). Powder was passed through the vibratory feeder and conveyor at a flow rate. The total weight of flavour powder was measured before applying on crisp substrates. This was repeated for different powder material and different amounts (3 and 6 grams) at different size ranges (63-125, 125-180 and 180-250 μm).



Figure 2-14. Powder (salt) flow on vibratory conveyor

The dimensions of feeding unit are shown in Appendix 5.

The crisp substrates move in the tumbler mixer at an adjusted rotational speed, the known amount of powder is applied to the surface of crisps. After a period of time, particle deposition on surfaces can be easily quantified. The particles shown in Fig. 2-15 are 180-250 μm sized salt particles.

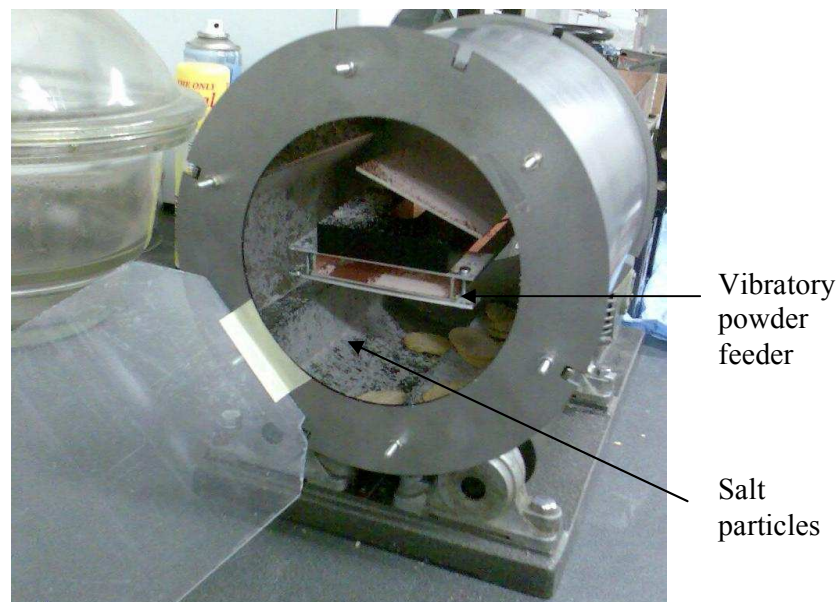


Figure 2-15. A view from a side of tumbler mixer after powder coating

The chosen powders were dispersed on the surface of the substrate in tumbler mixer. In conjunction with control of the powder delivery from the vibratory feeder, the rotational speed of the coating drum could also be adjusted for speed and duration. The substrate coated with powder was then weighed and placed on IAT sample holders using tweezers to minimise particle loss before and after conducting the experiments.

2.2.1.5 Experimental procedure of the IAT

The adhesion strength was tested by applying different deceleration forces on particles by using the IAT. An experimental procedure was implemented to investigate and assess the adhesion strength of powder material by using novel tester.

The basic experiment by which IAT is used to measure adhesion strength involves coating crisp substrate with flavour powders and observing the detachment force necessary to cause them to detach from the surface and relationship between the processing conditions of coating process and applied detachment force.

A schematic diagram of the implemented experimental procedure is shown in Fig. 2-16. In each experiment a total of 20 crisp substrate (each crisp substrate weighed app. ± 1 gram) and different quantities of salt and flavour powders were used. The dose of applied powders was varied from 3 to 6 grams per batch. Substrates were first coated with different amounts of oil before applying powder on the oiled surfaces and then the experiments were conducted with the IAT to get the detachment rate for different impact forces generated by the novel tester soon after the coating step to minimise time effect on oil migration from crisp surface into the crisp.

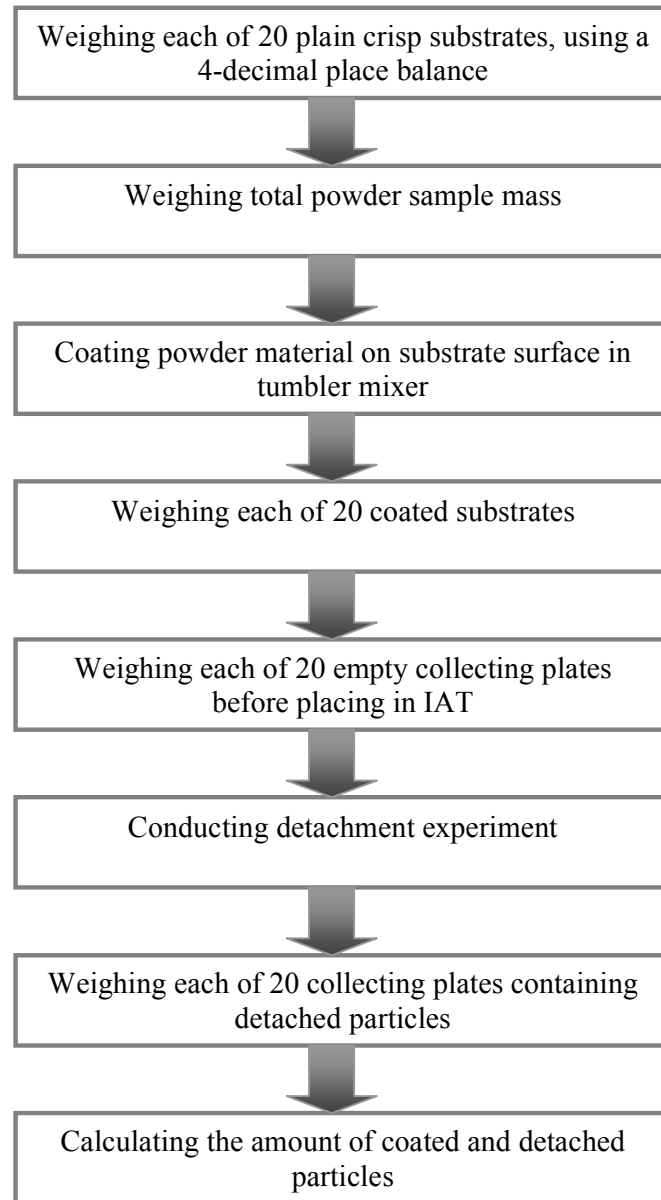


Figure 2-16. Diagram of experimental procedure

A four digit balance was used in this study to measure the weight of powder coated and detached. A crisp substrate, on which particles had been deposited, was placed in between sample holder parts. A collecting plate was placed in one of the sample housing on platen. Sample holder having crisp substrate was placed and secured on collecting plate. The platen was dropped from a height to obtain a level of deceleration upon impact with the bottom plate. This step was repeated, for a range of descent increasing heights and the quantities of particles detached for each test condition were obtained. Twenty different detachment levels were obtained from twenty different crisp

substrates for a single set of experiments and standard deviations were calculated in each case. The substrates were dropped only once to overcome the weakening effect of previous impacts on particle adhesion strength. The gravity force acting on a flavour particle is negligibly small compared with deceleration forces in this study.

A wide range of surface decelerations, up to around 100 g (m/s^2), obtained by varying the dropping height of platen. At a known deceleration, the magnitude of surface deceleration force required to remove a given fraction of adhering particles can be calculated according to the relationship:

$$F = ma \quad (17)$$

where m is the mass of particle and a is the deceleration in terms of g (m/s^2).

This formula can be applied to the average mass of particles of different sizes.

2.2.2 Texture analyser

In general, the texture analyser (Fig. 2-17) was used to assess the unconfined failure strength gained of the bulk solids. In this case it was used for measuring the maximum load strength of crisp substrate before getting cracked. Then this maximum load was used in design of Impact Adhesion Tester.

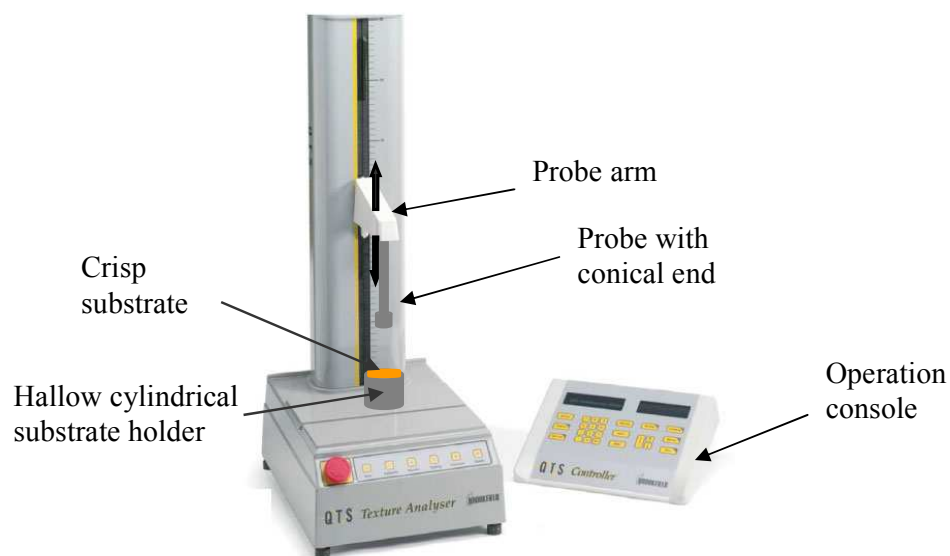


Figure 2-17. QTS Texture Analyser (Brookfield)

The uniaxial press of the texture analyser is utilised to apply a gradually increasing vertical load, via a probe (Fig. 2-18), to the crisp surface at the centre until failure occurs. The vertical load required to initiate failure of the substrate was used to calculate the value for Young's modulus.

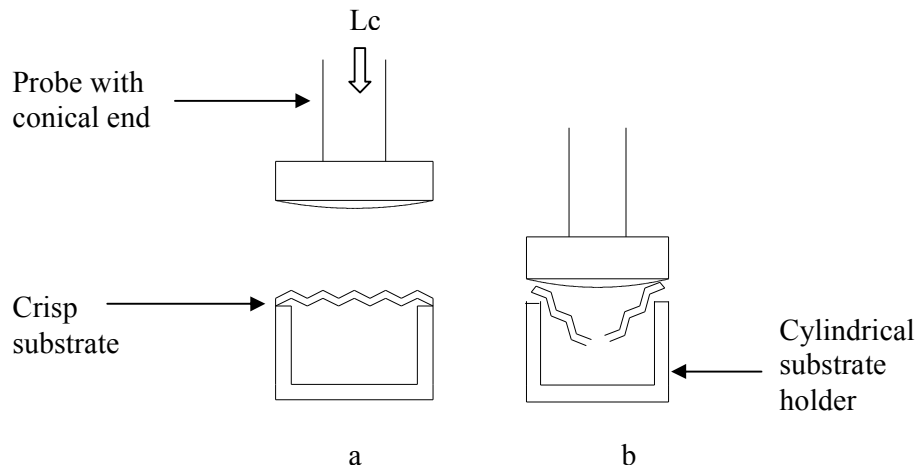


Figure 2-18. Schematic drawing of experimental design of crack strength test. a) before and b) after deformation of substrate.

The sample holder is a cylindrical cell which holds crisp substrate from edges. This design allows measuring the maximum load on the crisp before deformation occurs. Knowing maximum load before crack occurs would help to design the impact tester.

2.2.3 Pycnometer

The AccuPyc 1330 pycnometer (Micromeritics) (Fig. 2-19) was used in this study to get particle densities of the powders which were used to measure the mass of particles to calculate forces acting on them. The AccuPyc completed the analyses in 2 to 3 minutes with high accuracy by using a gas displacement technique for measurement.



Figure 2-19. AccuPyc 1330 pycnometer (courtesy of Micromeritics)

2.2.4 Sieves

In this project, sieves were used to determine the particle size distribution of flavour and separation of the size fractions of the salt powder.

The sieves used for the tests were 53, 63, 90, 125, 150, 180, 250, 300, 500, 850 μm and the pan (Fig. 2-20). The sieves were agitated for period of 5mins. The amount of powder was weighed on each sieve and pan to get a cumulative percentage distribution.



Figure 2-20. Sieves with agitator (courtesy of Wagtech International Ltd)

An example of size distribution graph is shown in Fig. 2-21.

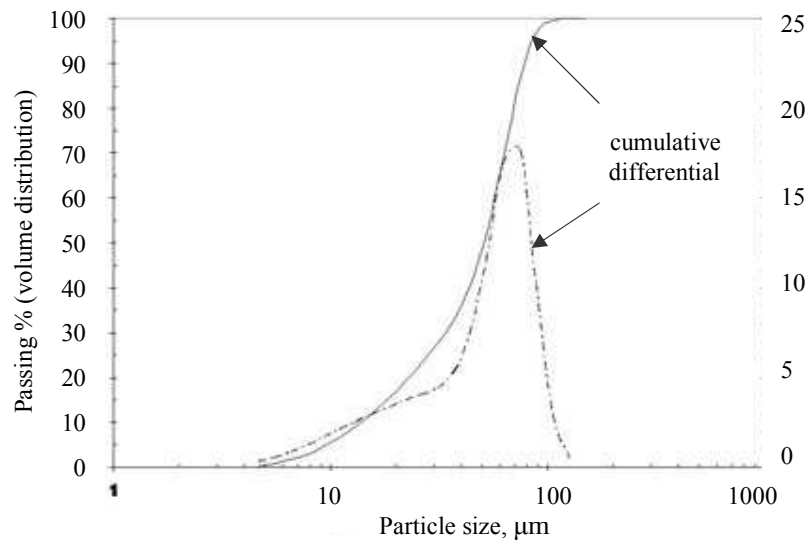


Figure 2-21. Particle size distribution of a powder sample

Laser diffraction and sieving can provide similar results when characterising spherical or semi-spherical particles. However, significant differences can be observed for non-spherical particles due to the different particle properties measured by each technique. Sieving has been used in this research project partly due to use of fractions corresponding to sieve sizes. Another reason not to use Laser diffraction technique is that pressurised air is used to carry the powder material through the channel where particles are exposed to laser beam. It was observed that the air pressure broke the big particle systems into small ones and changed the size distribution of flavour powders.

2.2.5 Centrifuge Tester

A second technique that was used to assess adhesion forces was the use of a centrifugal accelerator. The adhesion force in this part of experiment is defined as the force required detaching individual particles at room temperature by centrifugal spin-off force.

Wood veneer was chosen as test substrate to be used for centrifuge technique. One reason is its strength and another reason is that it is easy to cut into small pieces unlike crisp substrates.

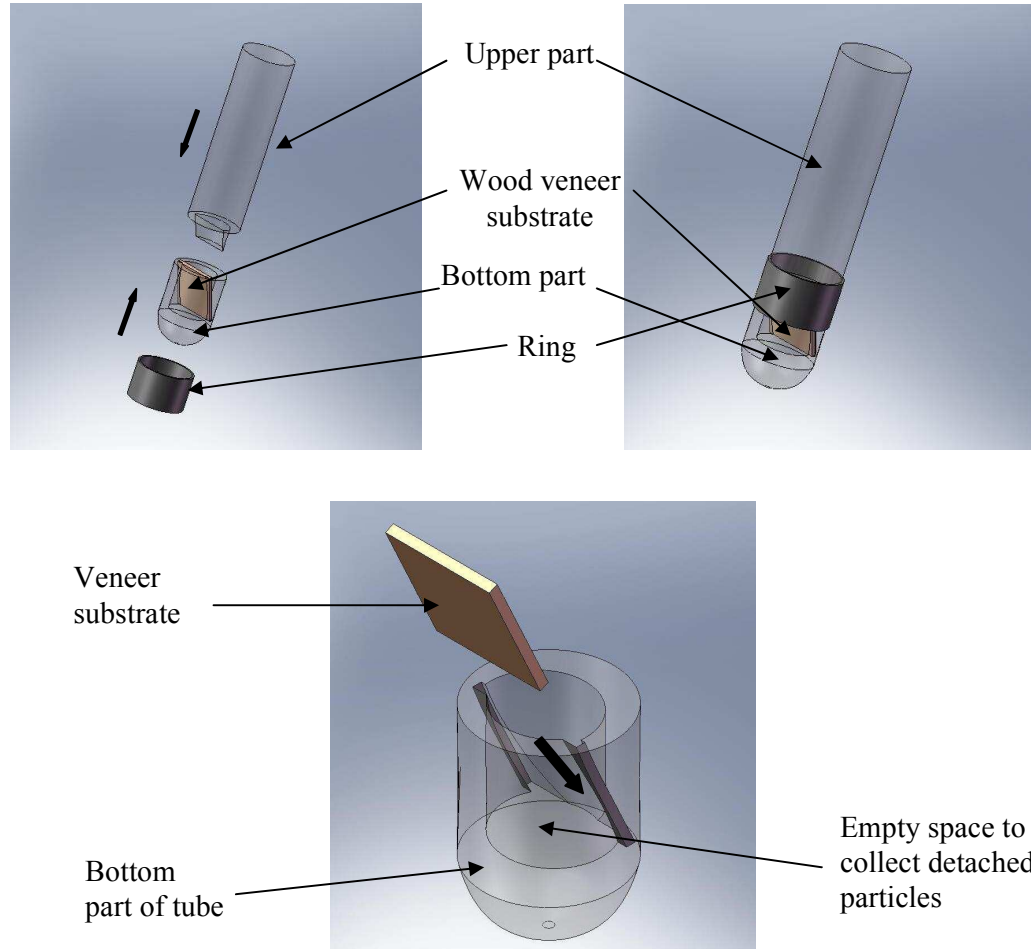


Figure 2-22. Placing of veneer substrate into a centrifuge tube specially designed for substrate housing

Onto the wood veneer substrate (dimensions 10 x 10 mm with 2 mm thickness), poly-disperse, flavour particles (Prawn Cocktail, Salt and vinegar, Cheese and Onion, particle diameter varies from 30 up to 600 μm) were deposited on pre-oiled veneer surface. Oil was applied on the surface by using an air brush with pressurised air ($5(\pm 1)$ atm). The amount of oil was calculated by measuring the substrate before and after coating with oil. In this way, a large number of individual particles could be positioned on the area studied (1 mm^2). Measurements were performed before and after the removal of

particles. Prior to centrifugation, the initial particle weight was measured by a four digit balance weight as well as after centrifugation to obtain the amount of particles detached. The particle-loaded substrate surfaces were placed in specially designed tubes (Fig. 2-22) and subjected to a centrifugal force that increased in steps, with each centrifugation step lasting 1 min. The particles-substrate systems were weighed before and after each centrifugation step. Correlation of centrifugal forces with the size of detached particles yields an estimation of adhesion strength of flavour particles. Sorvall Discovery 90SE floor type centrifuge was used in this study.

It is important to keep the surface of substrate perpendicular to axis of rotation facing the coated surface in the direction of spin-off force during centrifugation. This has been accomplished by using a centrifuge rotor (Fig. 2-23) and specially designed tubes illustrated in Fig. 2-22. The coated veneer substrate already covered with oil and flavour powder was placed carefully in the tube and then in rotor of centrifuge. To make sure that there is no particle detachment during placing substrate in the tube, a tweezers was used to place them carefully each time. Then different centrifugal speeds (from 300 to 4000 rpm) were applied to identify the effect on detachment of particles. The amount of oil was calculated by knowing the weight of substrate with and without the oil.

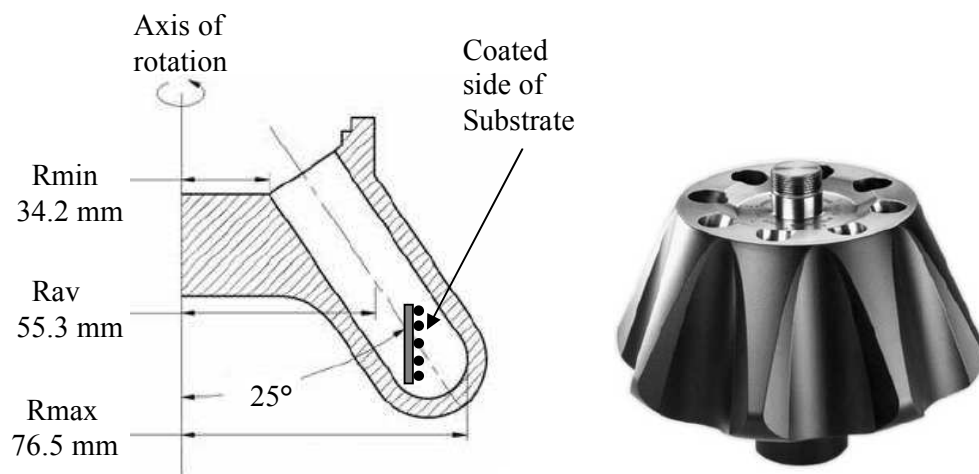


Figure 2-23. A view of a centrifuge head and an illustration of substrate placing

The comparison of the range of impact force acting on particles by using centrifuge to that of IAT is discussed in Chapter 4.

2.2.6 Balance

Ohaus Explorer 4 digit balance weight (Fig. 2-24) was used. Variations at 4th digit of the weighing values of repeated experiments were identified and these variations were used to calculate standard deviations.



Figure 2-24. Ohaus Explorer 4 digit balance

2.3 Test materials used for particle adhesion testing

Following criteria was considered on the selection of suitable substrate material to coat with flavour powder:

- The substrate material should be rigid and not degradable easily
- The material should have a uniform size and shape in order to conduct repeatable experiments
- The substrate should be strong enough to resist high level of impact force (up to 7 N)
- The substrates should have uniform surface textures to aid repeatability

A search was conducted into the applicability of substrate material that would fulfil the above mentioned criteria. This resulted in the selection of round shaped, crinkle cut and

lightweight crisps sold as “Crinkly’s” in the UK market. The post-coated plain and oiled crisp substrates were obtained from United Biscuits, UK. Crisp substrates were classified as oiled and non oiled and stored in small plastic bags.

Various powder materials were used for comparison in this study. They included three different kinds of flavour powders, salt powders and glass powders within different size fractions and shapes. The flavour powders and salt powder were obtained from Kerry Ingredients, UK. Salt powder was fractioned using laboratory scale sieves and stored in plastic bags. Sunflower oil was sprayed on the crisp substrate surface using an air brush with pressurised air at different amounts (This was controlled by adjusting the application time).

Three main physical factors were considered in this study; the irregular shape of particle, size of particle and the presence of neighbouring particles. Salt, glass and different flavour powders were used as coating material on crisp substrates.

Table salt was separated into appropriate fractions by using sieves. The size fractions of salt used in this study is classified in Table 2-3. The degree of classification of particle sizes was decided to have four main fractions which were thought as necessary to investigate the effect on adhesion strength.

Table 2-3. Classification of particle size ranges

Description	Size range(μm)
Ultra fine	<63
Fine	63-125
Medium	125-180
Coarse	180-250

2.3.1 SEM Image Analysis of Crisp Substrates

Selected crisp samples were analysed by scanning electron microscopy (SEM) in the SEM Laboratory at School of Science, University of Greenwich, Medway. The primary purpose of the SEM analysis was to provide visualisation of the surface of crisps and flavouring particles before and after oil coating and flavour application processes. Electron microscopy (JEOL Scanning Microscope, JSM-5310LV) with backscattered electron technique was used because its suitability for viewing extremely small particles of flavourings and detailed surface structure of the crisp. Random portions of samples were selected for this analysis. However, because of the corrugated surface of the Crinklys, it was not easy to obtain truly representative samples and therefore the images generated can only be taken to be indicative of the larger surface area of a single Crinkly. Samples of approximately 1 cm² from each crisp were prepared by hand for analysis under SEM. To be able to understand the particle sizes and to compare the images, samples were analysed at 100 and 500 magnification. A digital image capture system (Link ISIS 300, Oxford Instruments) was used to obtain images from SEM.

Eight different samples were prepared for analysis and 16 different images were obtained at different magnifications.

It was found that not all of the flavouring particles could be distinguished from each other. However, some of the surface characteristics and some particles covered by oil were successfully identified in several of the samples. Salt particles were easily identified. Other particles found in these samples include flavouring fine particles (e.g. cheese, onion and vinegar flavouring fine powders) have been attached to each other, to salt particles and onto surface of the crisp by capillary, electrostatic and van der Waals adhesion interactive forces (Enggalhardjo and Narsimhan, 2005).

Fig. 2-25 shows the SEM image of a representative portion of uncoated and coated crisp samples (with oil) with the magnifications of 100 and 500. Fig. 2-26 represents the images of crisp samples that were prawn cocktail flavoured. Fig. 2-27 and Fig. 2-28 show the images of representative samples of salt and vinegar flavoured and cheese and onion flavoured crisps.

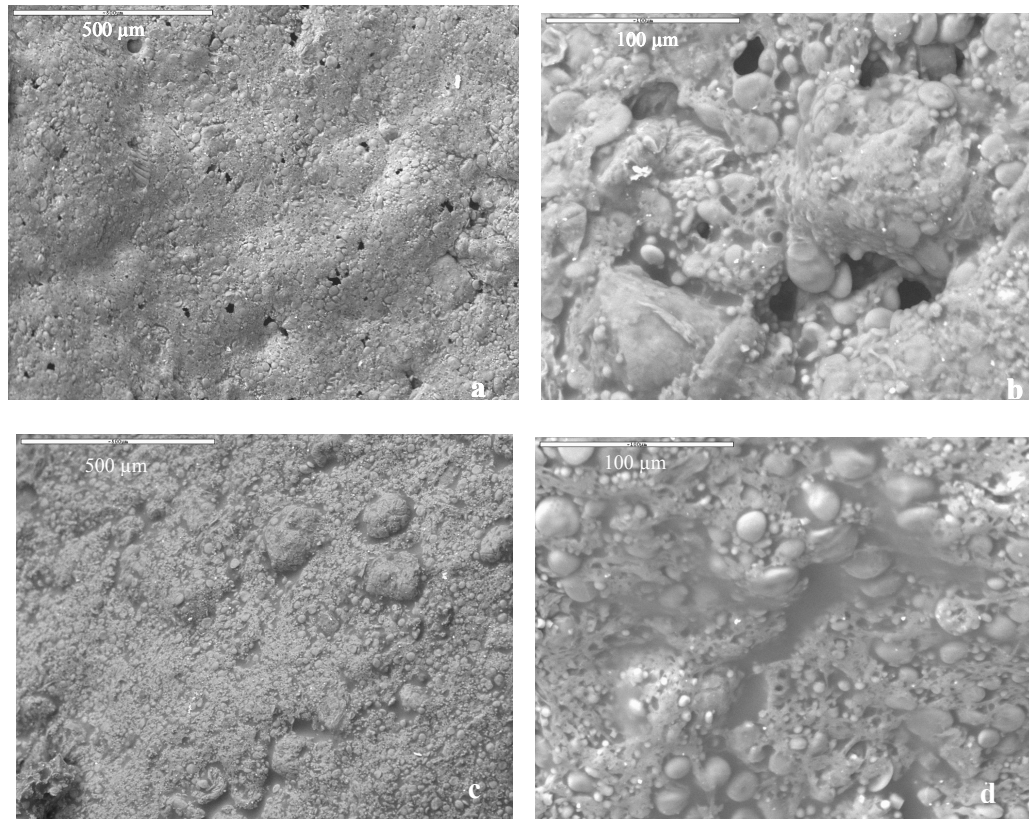


Figure 2-25. Backscattered electron SEM images of representative portions of crisp samples. (a) cooked, uncoated crisp surface with 100 magnification and (b) with 500 magnification, (c) coated crisp surface with 100 magnification and (d) with 500 magnification.

In Fig. 2-25, numbers of starch particles of different sizes can be observed on the surface of the crisp sample. SEM images after oil application onto the crisp surface can also be seen. Preliminary weight analysis of crisp samples indicated that oil is present at a level possibly as high as 18% by weight. The oil layer on the surface can be easily analysed from the images. While the surface of the crisp has porous structure, it can be clearly observed that oil has filled the openings and pores on the surface after coating process. The surfaces show considerably irregularity and do not exhibit even surface characteristics (due to porosity and the existence of organic particles in resulted in pre-processing steps). The irregular surface and porosity might help oil to diffuse into the crisp and to form a thin film layer on the surface - strengthening the particle-particle and particle-surface capillary adhesion forces. Surface irregularity and porosity also increase the surface area per unit mass which may result in adhesion of more particles per crisp.

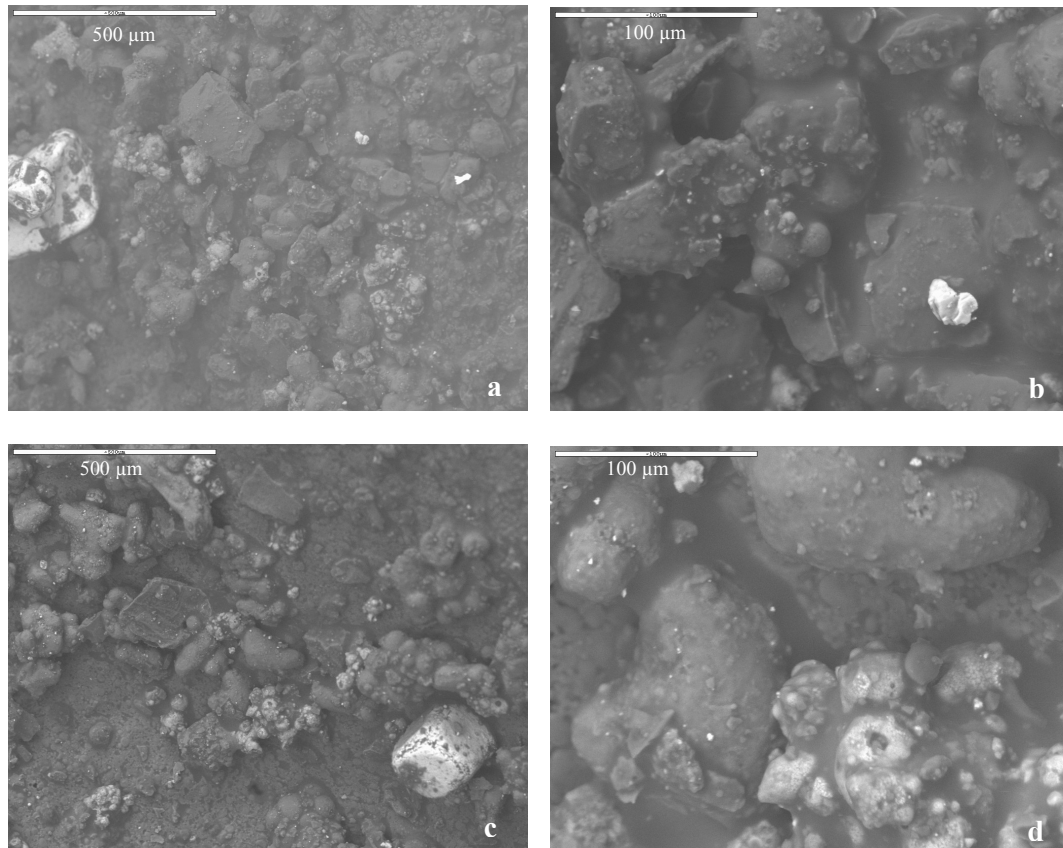


Figure 2-26. Backscattered electron SEM images of representative portions of prawn cocktail flavoured crisp samples: (a) post flavouring crisp surface with 100 magnification and (b) with 500 magnification, (c) packed crisp surface with 100 magnification and (d) with 500 magnification.

A number of salt and flavouring particles can be observed from Fig. 2-26. Although the salt particles can be readily identified on some parts of the surface (due to their size, shape and electron reflection capacity), flavouring particles are not that easy to differentiate and to identify (because of oil and adhering to each other as indicated by red arrows on the images). Because oil structure consist of triglycerides and poly-structured fatty acids, which are rich in carbon atoms, electrons are absorbed by the oil and observed as dark colour on the images. Light coloured regions represent mineral and crystal structures, such as salt.

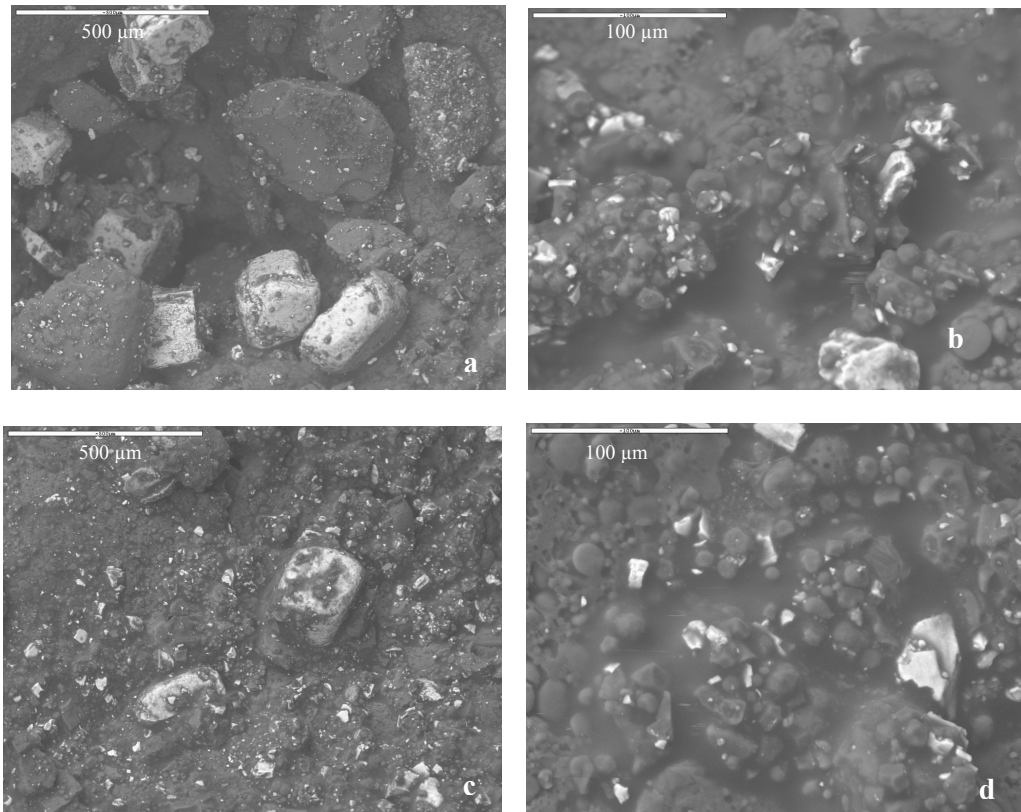


Figure 2-27. Backscattered electron SEM images of representative portions of Salt and Vinegar flavoured crisp samples: (a) post flavouring crisp surface with 100 magnification and (b) with 500 magnification, (c) packed crisp surface with 100 magnification and (d) with 500 magnification.

Fig. 2-27 shows the SEM images of salt and vinegar flavoured crisp samples before and after packaging. From these images it can be identified that there are higher numbers of salt particles from post flavoured than for packed crisp. This might be a result of either irregular distribution of particles on the surface or detachment of particles during operations between post flavouring and packaging processes.

Almost the same images have been identified from cheese and onion flavoured crisp surface with small differences in number and size of particles (Fig. 2-28). Again, the salt particles and agglomerated flavouring particles can be easily identified (the sizes of the salt particles are relatively bigger than that of flavourings).

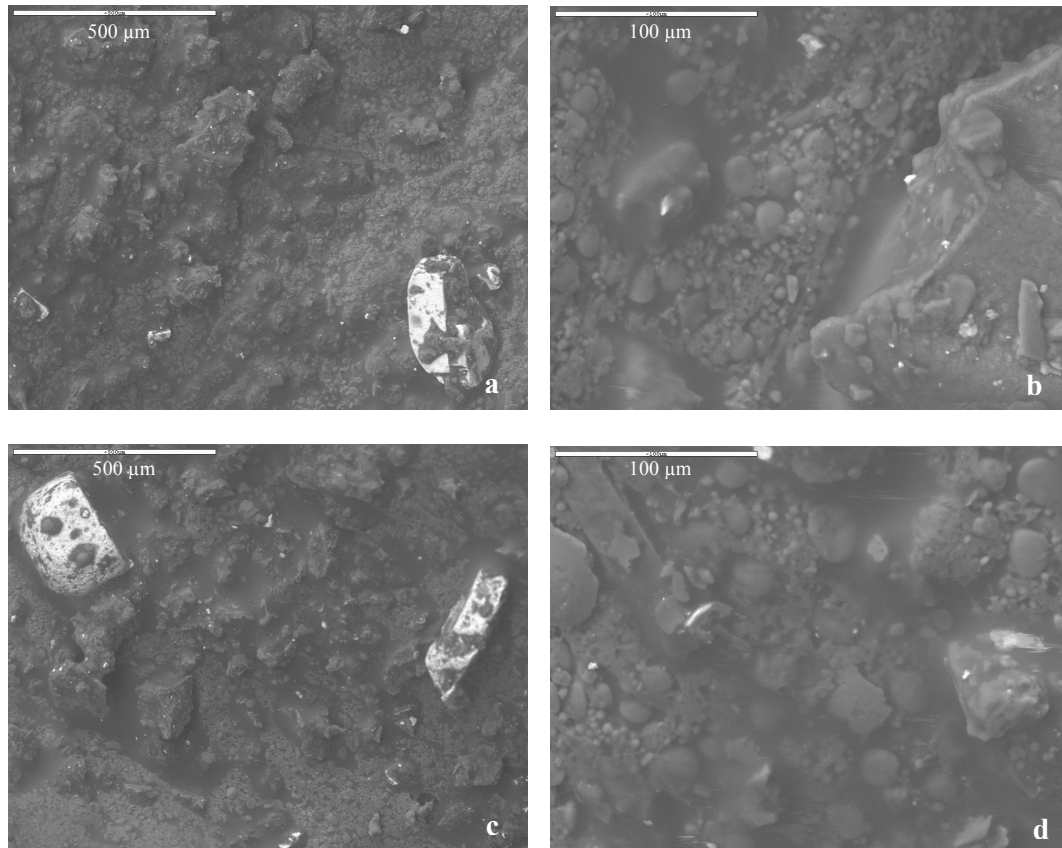


Figure 2-28. Backscattered electron SEM images of representative portions of Cheese and Onion flavoured crisp sample: (a) post flavouring crisp surface with 100 magnification and (b) with 500 magnification, (c) packed crisp surface with 100 magnification and (d) with 500 magnification.

It can be observed from the images that the size of the particles vary significantly and also that the shape of the flavouring particles is not uniform. However, salt particles have been observed as cubic shape - but still not uniform. Oil plays an important role in adhesion of particles to each other and onto the surface. Agglomeration of particles to each other makes bigger particles and this accumulated mass might facilitate the detachment of particles from the surface when subject to abrasion or acceleration.

2.3.2 SEM Image Analysis of Flavouring Powders

The powder samples used were flavourings (cheese and onion, prawn cocktail and salt & vinegar) provided by Kerry Ingredients, UK. These flavours are widely used as crisp or potato chips coating powders by snack industry in the UK. An electronic scanning microscope was used to obtain scanning electron microscopy (SEM) photographs of the samples (Fig. 2-29).

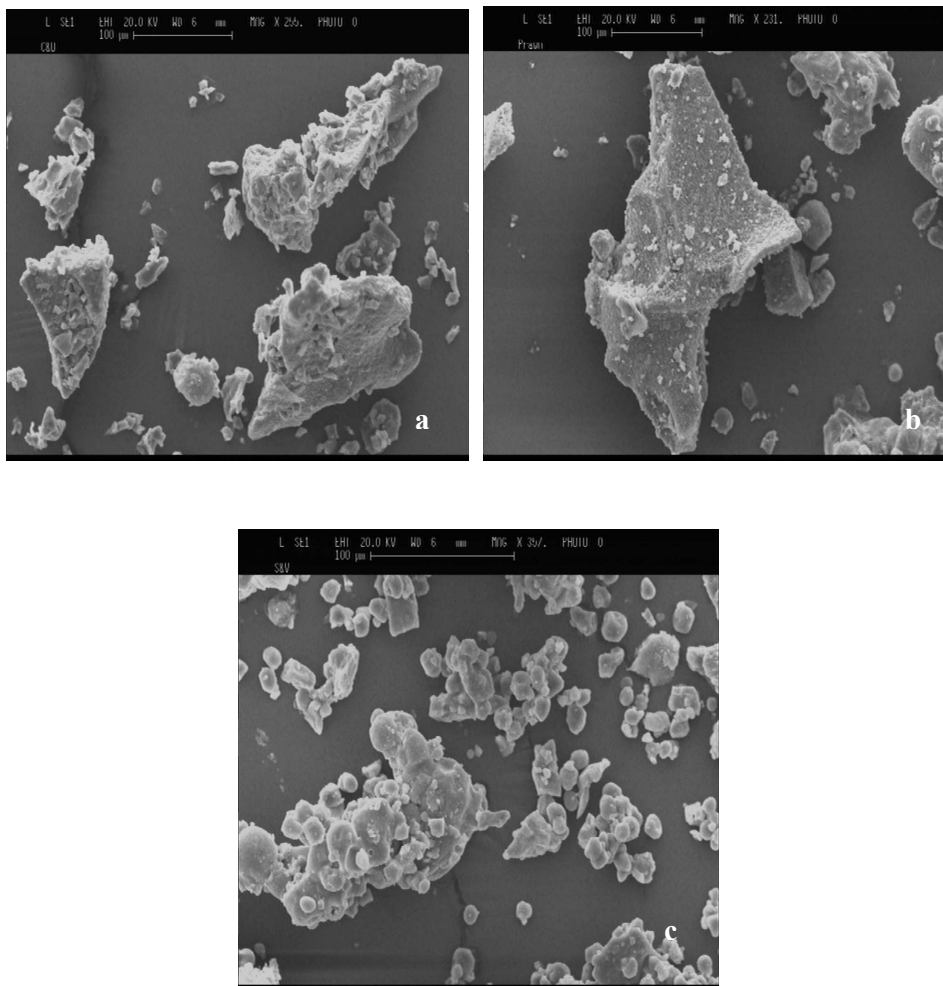


Figure 2-29. SEM images of flavouring powders. a, cheese and onion; b, prawn cocktail; c, salt and vinegar

If several particles are dispersed separately upon a substrate, the force required to remove each one will not be the same due to differences in their shape and size as can be seen in Fig. 2-29. There is higher number of particles remaining on the surface after

the application of force to the number initially. A value termed the ‘adhesion rate’ is expressed as the ratio of the weight of particles detached from the surface after the application of detachment force to the initial weight. In estimating the force, the existence of a value of this force under which a majority of particles are removed has been considered as important.

2.3.3 Microscope image analysis of salt and glass particles

Glass beads having a smooth surface were used as a spherical model particle for the experiments. Spherical glass beads were obtained from Whitehouse Scientific Ltd., UK. Crushed glass particles were also used to be able to compare results obtained from both model particle detachment experiments and discussed Chapter 4. The particles were fractionated by using laboratory scale sieves after crushing the glass to get different particle size fractions. Size and shape characteristics of glass particles were analysed by using light microscopy along with a digital camera with its software (Fig. 2-30).

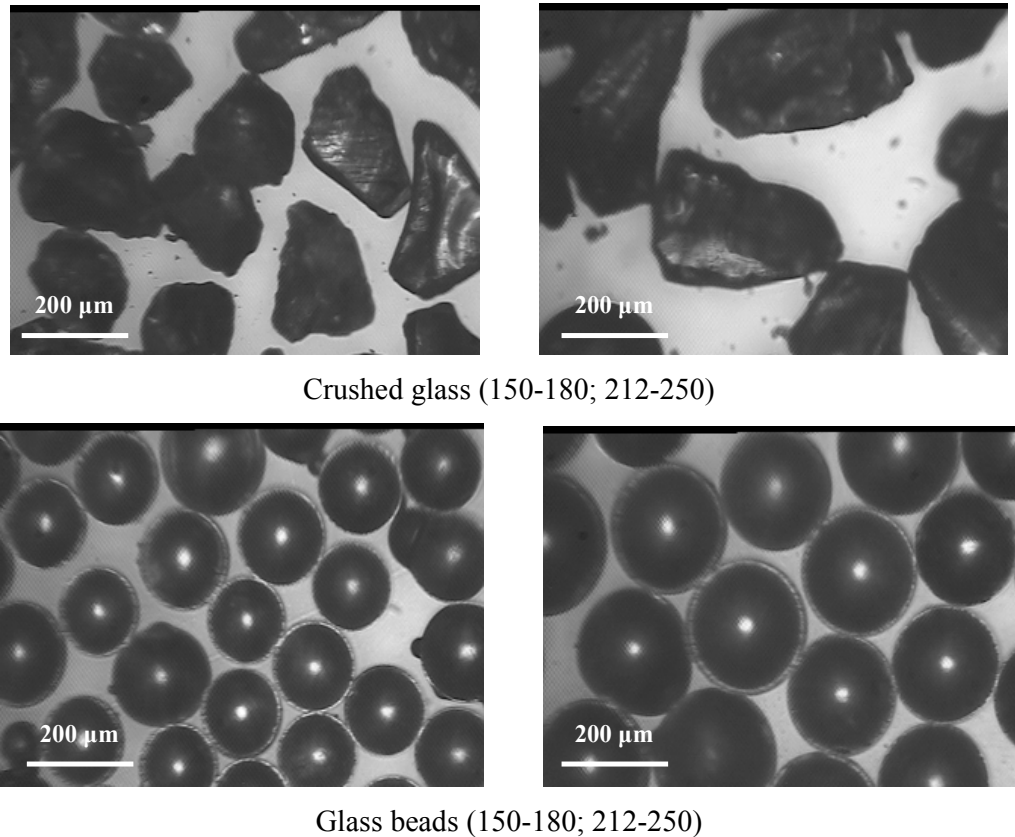


Figure 2-30. Glass particles under microscope

2.4 Problems and limitations

The problems with the experimental procedure are that it is time consuming; taking approximately 20 minutes for a single experiment and the operator need to be careful on variables such as weighing of material before and after experiment, adjusting drop distance of platen etc.

Regarding the limitations of the test procedure, the substrate used has to be in a certain shape and size, limited to 3 cm in diameter and up to 5 mm thickness, round shape. The size of tumbler mixer used in experiments is smaller than industrial applications and coating process parameters were set independently (random parameters) from industrial applications (tumbling speed and duration, amount of powder used etc). The measured deceleration of the substrate attached to tester is in the range of 1 to 200 g, these deceleration values may be different from those in production line, where crisp substrates are exposed to impact forces during transportation within production units, due to type and design of processing equipment which are for instance coating (i.e. tumbler mixer), transporting (i.e. conveyor belt and vibratory conveyor) and pre-packaging (i.e. dosage) units. There is also a limitation on the particle size so that the material tends to agglomerate while coating process and therefore fine particles may form bigger ones and adhesion behaviour changes significantly.

CHAPTER 3

THEORETICAL CALCULATIONS VERSUS EXPERIMENTAL RESULTS

3.1 Inferred total adhesion force from theoretical calculations

Current models for calculation of adhesive forces between a particle (sphere in general) and flat substrate have previously been tested in numerous experimental studies as explained in Chapter 1. However, little data exist for the adhesion forces between irregular shaped particles and substrates exhibiting irregular surface characteristics.

In order to understand the adhesion strength of particulates in processing conditions (i.e. factory production line), force balance acting on particles at different sizes is performed. The theory of adhesion models that apply to a single particle are used. The model for particle contact area is based on the adhesion forces acting between particle and surface. The contact area is represented by a disc of unknown radius and varies according to size/shape of particles and roughness of substrate surface. The three critical adhesion forces (van der Waals, electro-static and capillary) can be calculated by the mathematical models (Eq. 18, Eq. 19 and Eq. 20) and evaluated by performing a balance of forces. The models for the corresponding calculations are the following:

Calculation of van der Waals forces (F_{vW})

The van der Waals force of interaction between a spherical seasoning particle of equivalent radius R_p (= equivalent diameter corresponding to the diameter of a sphere or circle with the same projected area as the particle) and crisp substrate surface at a surface-to-surface distance of separation of h is given by

$$F_{vdW} = \frac{A_{eff} R_p}{12h^2} \quad (18)$$

where A_{eff} is effective hamaker constant.

Calculation of electrostatic force (F_{el})

The electrostatic interaction between the seasoning particle and the crisp substrate can be considered as coulombic interaction between two oppositely charged particles situated on both sides of the surface and is given by (Bowling, 1988)

$$F_{el} = \frac{q^2}{48\pi\epsilon_0\epsilon_r(R_p + h)^2} \quad (19)$$

Where q is the net charge of the seasoning particle, ϵ_0 is permittivity of vacuum (electric constant), ϵ_r is the dielectric constant of the intervening medium (oil in this case), R_p is equivalent radius of particle and h is the surface-to-surface distance of separation.

Calculation of capillary force (F_{cap})

The pressure difference due to curvature of the oil layer between the particle and crisp surface is dependent on the surface tension of the oil and the principal radii of curvature of the oil interface. The excess outside pressure will exert an adhesive (attractive) force on the flavour particle and is given by (Bowling, 1988)

$$F_{cap} = 4\pi \frac{\sigma}{r} R_p \cos \phi \quad (20)$$

where σ is the surface tension of oil, r is the roughness factor which is the ratio of the actual surface area of interface (the rough surface) to the apparent area of the geometrical interface (the smooth surface), R_p is the equivalent radius of particle and ϕ is the contact angle of oil to the crisp surface.

Chutkowski and Petrus (2008) report that both the surface tension and dynamic viscosity of liquid applied are important parameters influencing the capillary adhesion forces. However, they have also state that surface tension is much stronger stimulant

(more than 600 times stronger). Therefore effect of viscosity is neglected in this PhD project.

The total adhesion force (F_{ad}) can be obtained from the following force balance:

$$F_{ad} = F_{vdW} + F_{el} + F_{cap} \quad (21)$$

$$F_{ad} = \frac{A_{eff} R_p}{6h^2} + \frac{q^2}{48\pi\epsilon_0\epsilon_r(R_p + h)^2} + 4\pi\frac{\sigma}{r} R_p \cos\phi \quad (22)$$

Enggalhardjo and Narsimhan (2005) used the mathematical formulas outlined above (Eq 5) to calculate the adhesion forces acting on flavour particles on tortilla chips. Due to similarities of material and substrate they used, same model without any modification was used directly in this study. The numerical values which are used in these mathematical formulas are outlined in Table 3-1 below.

Table 3-1. Numerical values used in calculation of adhesion forces

Symbol	Value	Source
A_{eff}	7.5×10^{-20} J (based on sodium borate spheres)	Zimon, 1969
q	1.38×10^{-16} C (for wood, sugar, soot and grain having 10 μ m diameter)	Bowling, 1988
ϵ_0	8.85×10^{-12} C ² /Jm (for soybean oil)	Enggalhardjo and Narsimhan, 2005
ϵ_r	3 (for soybean oil)	ASI Instruments, 2010
σ	0.034 N/m (for soybean oil)	Enggalhardjo and Narsimhan, 2005
r	1.18 (for tortilla chips)	Enggalhardjo and Narsimhan, 2005
ϕ	70° (soybean oil on rough chip surface)	Enggalhardjo and Narsimhan, 2005

Values of theoretical adhesion forces are outlined in Table 3-2. Two types of interaction including van der Waals and capillary forces increased with the particle size. However,

calculated electrostatic force decreased with particle size as can be seen in Fig. 3-1. As it can be observed clearly from the table that capillary force is much bigger in magnitude than others and it is driving force in total adhesion forces (Fig. 3-1).

Table 3-2. Calculated adhesion forces acting on particles

Particle size (μm)	van der Waals (N)	Electrostatic (N)	Capillary (N)	Total (F_{ad}) (N)
63	8.75E-15	5.50E-14	1.45E-06	1.45E-06
125	1.74E-14	1.98E-14	2.89E-06	2.89E-06
180	2.50E-14	1.08E-14	4.16E-06	4.16E-06
212	2.94E-14	8.13E-15	4.90E-06	4.90E-06
250	3.47E-14	6.07E-15	5.77E-06	5.77E-06

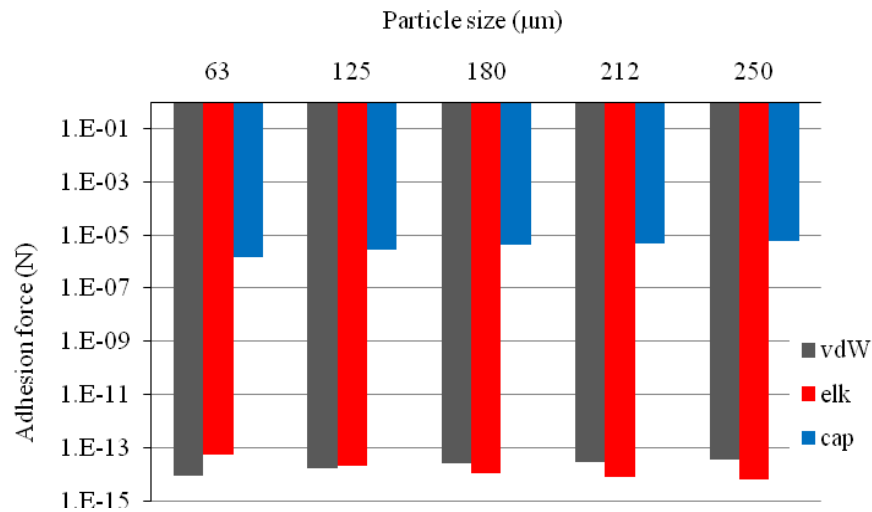


Figure 3-1. Log chart of adhesion forces acting on particles

The theoretical van der Waals force is in the range of 1×10^{-16} to 1×10^{-14} N. This magnitude is much smaller than the calculated total adhesion force. The theoretical electrostatic force (1×10^{-15} to 1×10^{-14} N) for different particle sizes is smaller compared with capillary force and hence with total adhesion force. The calculated capillary force, as shown in Table 3-2, is found to be of the order of 2×10^{-6} to 7×10^{-6} N, which is relatively larger compared with van der Waals and electrostatic forces. Therefore, only

the capillary force significantly contributes to the total adhesion force. The effect of particle size on total adhesion force can be seen in Fig. 3-2.

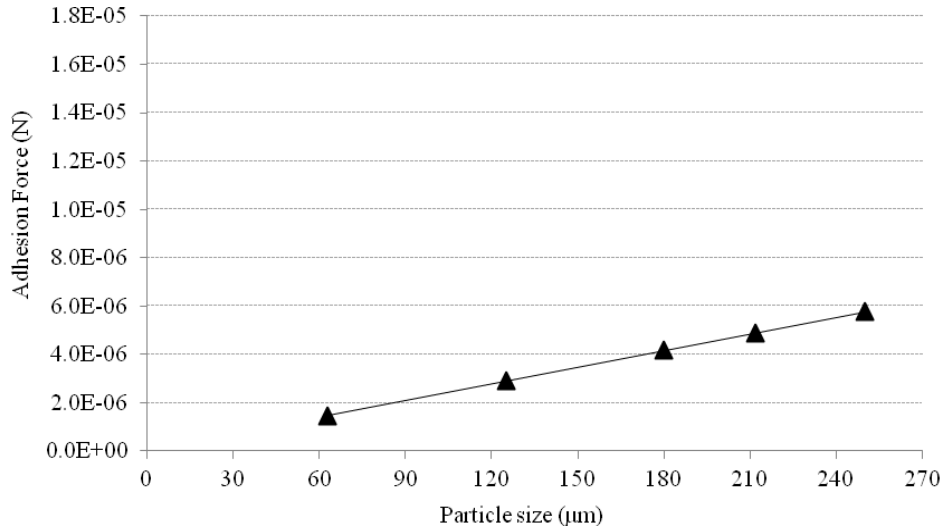


Figure 3-2. Calculated total adhesion forces versus particle size

3.2 Total force acting on particles during deceleration of plate of IAT

The mass of each particle of the powders used in this study was determined using Eq. 23.

$$m = \rho_p V_p \quad (23)$$

Where m is the mass of one particle, ρ_p and V_p represents its density and volume, respectively.

The estimation of the roughness of the particle surfaces was discussed elsewhere (Salazar-Banda et al, 2007). They used SEM micrographs of the particles. It has been reported that for each particle in the micrographs, an external and an internal circumference were drawn. They used these diameters to determine a mean diameter. Roughness was determined as the ratio between mean diameter and arithmetic diameter.

They have found that the estimated roughness was 11% and 4% for two powder materials they have used (phosphatic rock and manioc starch). This means that 11% and 4% of the diameter of particles are rugosities.

In this study, rugosities were neglected and particles were assumed to have shapes close to sphere. Therefore their volume was estimated using the equation used to determine the volume of a sphere, Eq. 24.

$$V_p = \frac{4\pi r^3}{3} \quad (24)$$

where r is the mean radius (obtained by sieve analysis) of the particle.

The calculated values of the particle masses obtained using Eq. 23 and Eq. 24 are presented in Table 3-3 for each size fraction studied.

Table 3-3. Mean mass of a single particle of powder materials used.

Mean diameter (μm)	Mean mass (kg)				
	Prawn Cocktail	Cheese and Onion	Salt and Vinegar	Salt	Glass
63	1.55E-09	1.62E-09	1.70E-09	2.26E-09	2.62E-09
125	1.21E-08	1.26E-08	1.33E-08	1.77E-08	2.05E-08
180	3.62E-08	3.77E-08	3.97E-08	5.28E-08	6.11E-08
212	5.91E-08	6.16E-08	6.49E-08	8.59E-08	1.01E-07
250	9.69E-08	1.01E-07	1.06E-07	1.41E-07	1.65E-07

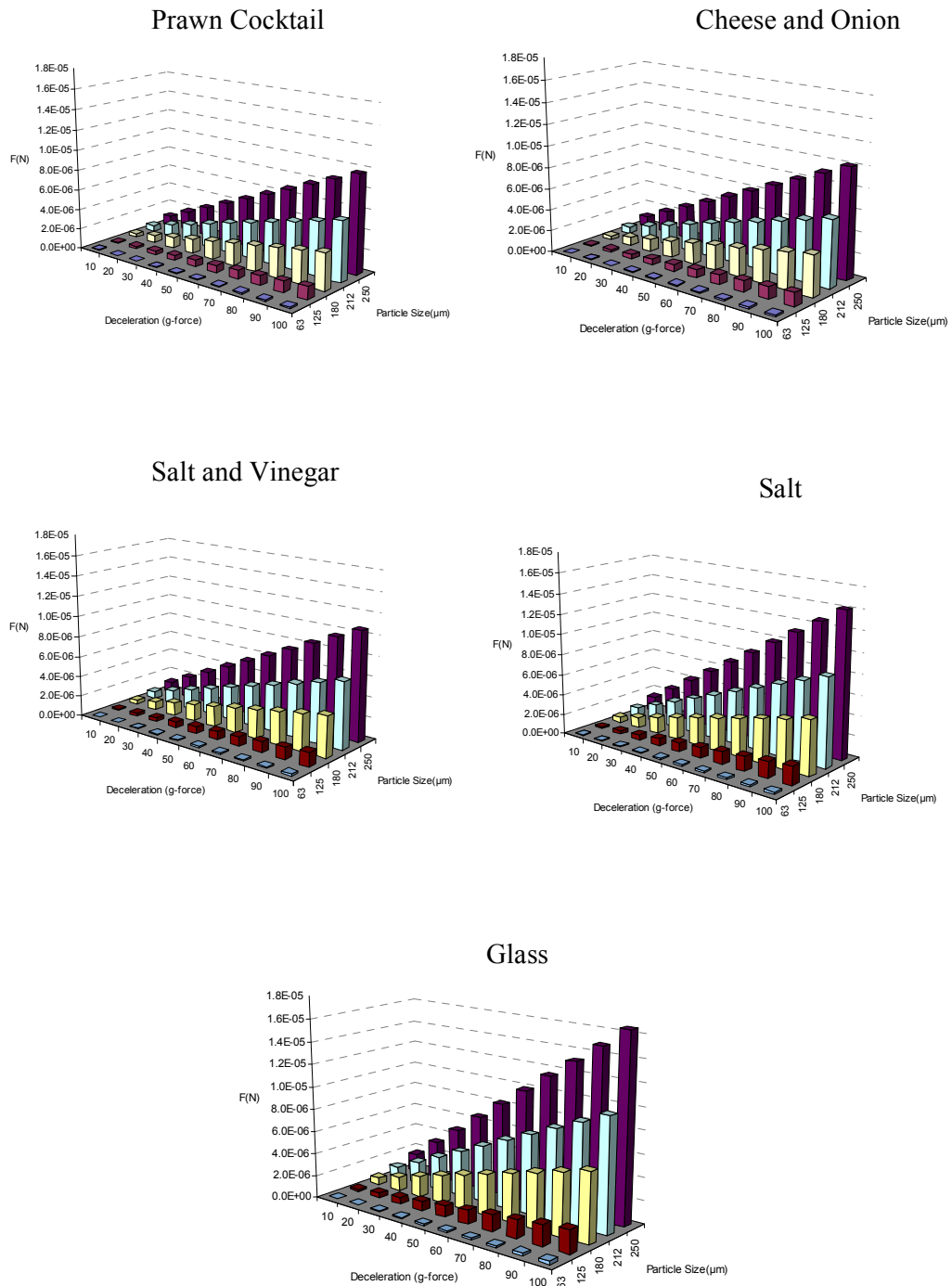


Figure 3-3. Experimental forces acting on particles for different powder material from experimental data.

The total force, which leads to detachment, acting on particles can be calculated by using Eq. 25 and the results can be seen in Fig. 3-3 for 5 different powder materials.

$$F = ma \quad (25)$$

where m is the mass of single particle and a is the deceleration in terms of g of plate of IAT measured by accelerometer.

3.3 Comparison of the theoretical adhesion force with the force acting on particles during deceleration

The inferred theoretical force of adhesion increases with particle size (Fig. 3-4), consistent with the total force acting on single particle during deceleration of the sample holder secured in the platen. Larger particle size had a greater effect on the total adhesion force. However, larger particles possess bigger forces acting on them due to their mass at same deceleration compared to fine particles of the same material. It can be stated that the force acting on particle due to deceleration of the platen is the driving factor of particle detachment. In other words, if the force acting on particle is bigger than total adhesion force, particle detachment takes place.

Fig. 3-4 shows a comparison between the theoretical inferred force of adhesion and forces acting on single particles during deceleration for different particle sizes at two different decelerations (10 and 100 g). The increase of magnitude of theoretical adhesion force versus particle size is smaller than that of experimental force for the given powders at 100 g deceleration. For the particles having average mean diameter less than 125 μm , the generated force on particles is less than theoretical adhesion force acting on particles while it is getting higher when the particles getting bigger than 125 μm . 10 g deceleration does not produce bigger force acting on particle than theoretical adhesion for five size fractions. One can say that particle detachment does not take place at 10 g deceleration for five size fractions and at 100 g deceleration for particles having smaller diameter than 125 μm because adhesion force is bigger than forces acting on particles.

The experimental results are interpreted in terms of total adhesion force between particles and surface assuming that particles leave the surface under a detaching mechanism as soon as the detachment force equals adhesion force. In case of

detachment, detachment force (F_{df}) needs to be equal or bigger than total adhesion force and can be expressed as:

$$F_{df} \geq F_{ad} \quad (26)$$

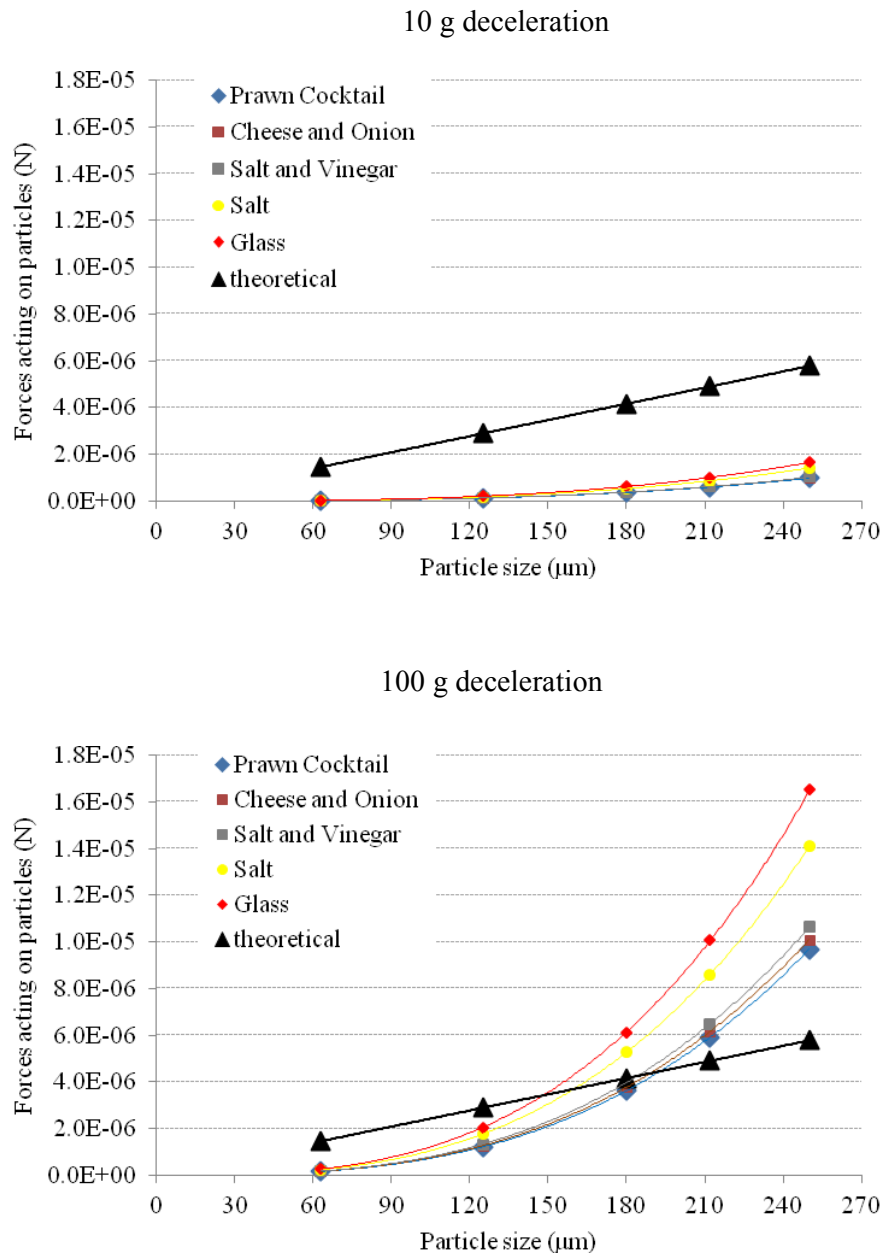


Figure 3-4. Comparison of theoretical total adhesion force to total forces acting on single particle (at 10 and 100 g decelerations) versus particle size.

According to Fig. 3-4 and Eq. 26, it is expected that all particles having average mean diameter bigger than 180 μm to be detached from crisp surface at 100 g deceleration but in fact, this doesn't happen as discussed in Chapter 4.

CHAPTER 4

RESULTS AND DISCUSSION

4.1 Results obtained

In order to achieve the main goals of the research project outlined in Chapter 1, a number of tasks had to be undertaken. These are outlined below:

- A literature review of past and present work associated with techniques and devices used for particle adhesion measurement, crisp production and flavour coating techniques.
- Planning, design and construction of a novel adhesion tester along with its experimental methodology.
- Physical characteristics (size, shape, powder density) of different powders and crisp substrate (surface structure) that have been used in the project have been identified.
- Assessment of particle adhesion in different process conditions by using IAT.
- Comparative analysis of data obtained from IAT, centrifuge technique and theoretical calculations (discussed in Chapter 3).

The results of each of these sections of work is summarised as followed.

4.1.1 Fracture test

Fracture strength of crisp samples was analyzed to be used in design stage of the tester. The material used for this purpose consisted Crinkly's crisp samples with oil as intervening media and without oil on the surface. The reason to choose Crinkly's crisp was due to its round and corrugated shape. The analysis was undertaken using a texture analyser (QTS 25, Brookfield Engineering, Inc) with a QTS 25 compression probe, moving at a speed of 10 mm/min.

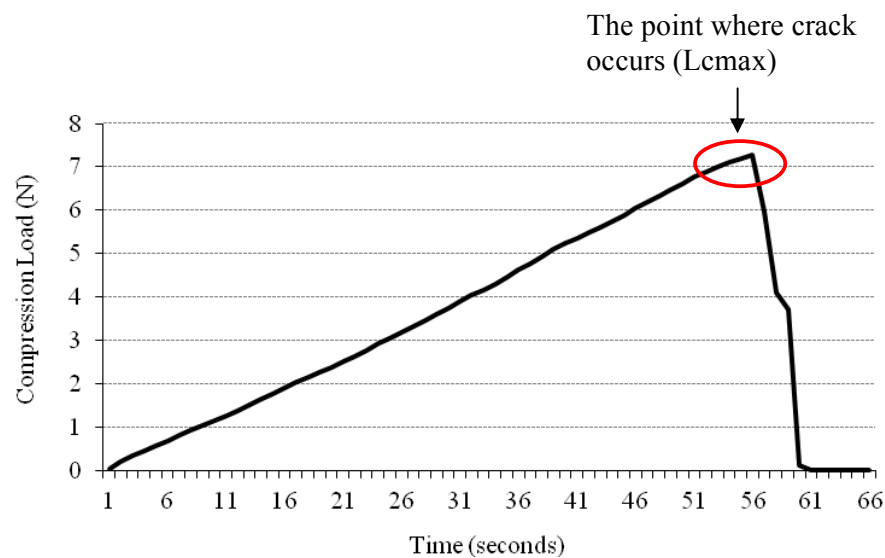


Figure 4-1. Force-deformation curve of crisp substrate

Fracture strength was measured in 20 repeat tests for oil coated and uncoated crisp samples. Maximum applied forces against a supported structure (L_{cmax}) were obtained from force-time curves (Fig. 4-1) and were adapted to a graph (Fig. 4-2).

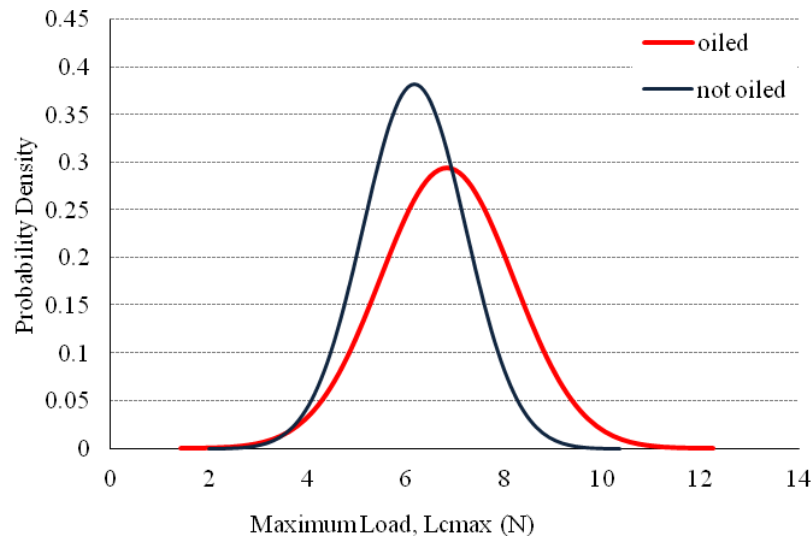


Figure 4-2. Normal distribution of fracture strength of different crisp substrates

The results obtained show that the crisp samples differed in resistance to the load forces. The moisture and oil content of the crisp and variation in shape characteristics might play important role in this differentiation. It can be stated that the presence of oil reduces the crack growth rate and the variation in curvature structure of corrugated crisp substrate may result in variation in crack growth rate.

Analysis of strength of crisp revealed a load peak during the movement of the compression probe. According to the method, the breaking load was determined by the higher peak.

The values of maximum load might be derivatives of different parameters (e.g., hardness, ductility of the sample, Young's modulus). The maximum load values were observed in the range of 5 and 8 N for most of the crisp samples. A few of them could resist to higher load values up to almost 10 N.

The mean force required to fracture the crisp substrate was calculated and found as 6.7 N. By using Eq. 25, the maximum applied force before fracture of crisp was calculated

as 6700 g¹ (average weigh of one crisp is 1 gram). This is quite high magnitude of force when it is compared to the deceleration values of IAT.

4.1.2 Impact force generation of IAT

The deceleration of the IAT plate dropped from different heights was measured using an accelerometer (2017AS10, VIP Sensors, USA) which was attached to a signal conditioner (5100IEPE, VIP Sensors, USA). The signals from the conditioner were processed by an oscilloscope (GDS-8205, INSTEC, USA) and its software (INSTEC Free Capture RS 232).

Small variations were obtained between measurements due to imperfect environmental and physical characteristics such as uneven surface of the colliding parts, slight differences or personal errors in adjusting drop heights. For that reason, the mean value of ten different peak values was taken for calculations and depicted as a deceleration curve versus drop height (Fig. 4-3)

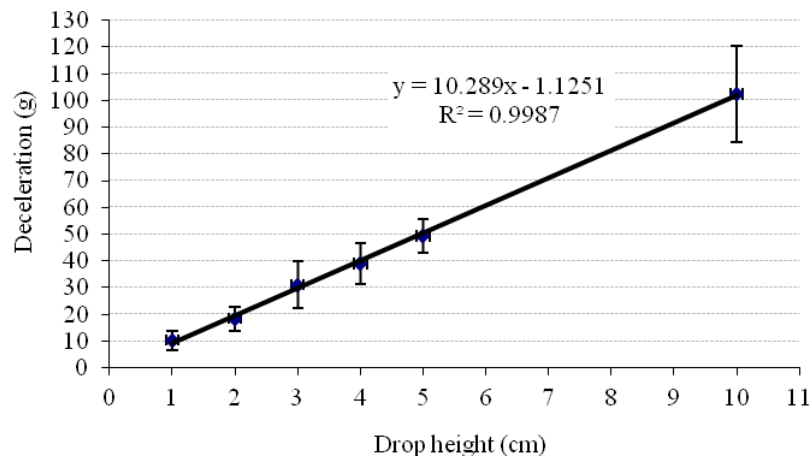


Figure 4-3. Impact force generation over drop heights

Fig. 4-3 shows a strong linear relationship ($R^2=0.993$) between deceleration and drop distance of the plate.

¹ See Appendix 6 for further information about deceleration of objects

Reproducibility of peaks of deceleration of platen can be seen in Fig. 4-4. The readings from oscilloscope screen were used to calculate g values. It has been reported that 100 mV output of the accelerometer is equal to 1 g unit (see calibration certificate in Appendix 7) which can also be expressed as $9.81 \text{ m}\cdot\text{s}^{-2}$ (VIP Sensors, USA). That means a 1 Volt peak on Oscilloscope screen equal to 10 g deceleration.

It can be seen in Fig. 4-4 that oscilloscope shows several shocks at the end of a drop. The first peak was taken into consideration to calculate the forces acting on particles and assumed that the shocks after first impact did not have effect on particle detachment.

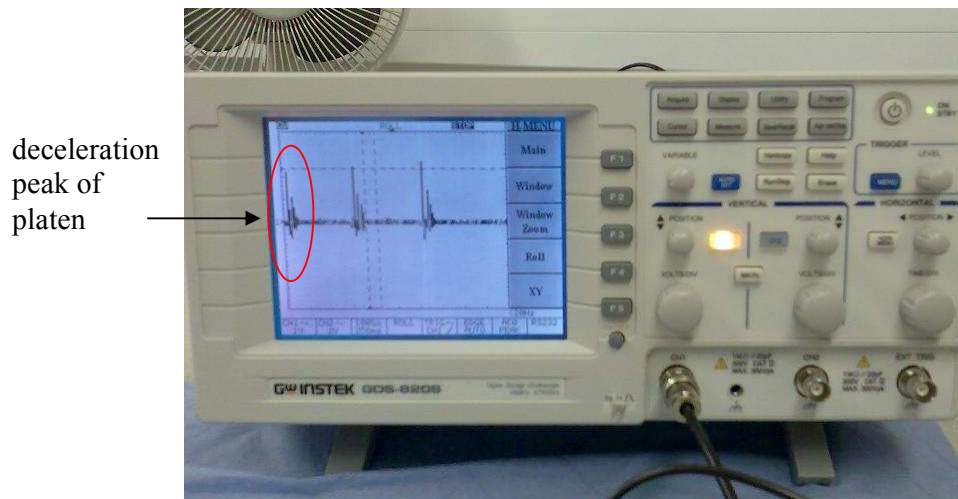


Figure 4-4. A snapshot from oscilloscope

Fig. 4-5 shows the deceleration peaks obtained by using a wireless data logger accelerometer. The platen was dropped from 1 mm distance and repeated several times to get an average value.

As it can be seen in Fig. 4-5, the average peak is around 1 g which is in agreement with the impact force generation curve in Fig. 4-3. The variation of peaks of different drops might be due to the sampling rate of data logger (100 Hz) and possible errors in adjusting the drop height of the platen.

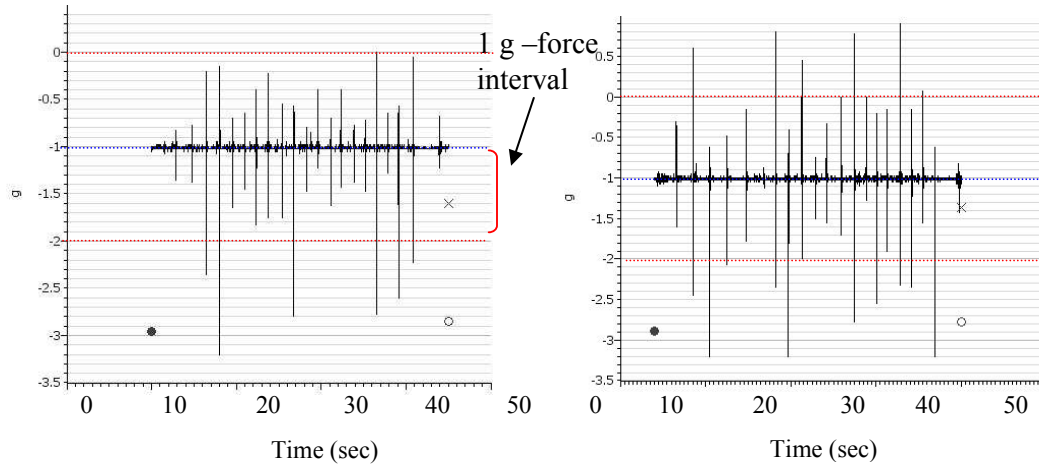


Figure 4-5. Deceleration peaks obtained by using Hobo wireless accelerometer from 1 mm drop distance.

4.1.3 Size analysis of the flavour powder systems

The size distribution of three different flavour powders, which are used in snack industry to coat the crisp surfaces, obtained on laboratory scale sieves (using mesh sizes of 53, 90, 150, 300, and 500 μm), is shown in Fig. 4-6. This figure shows that the flavour powders possess a wide size distribution and they have different size fractions.

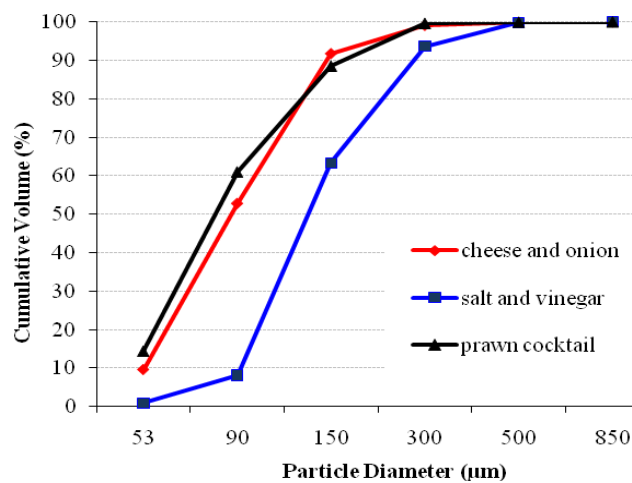


Figure 4-6. Cumulative size distribution of different flavour powders

From Fig. 4-6, it can be considered that the size distribution of flavour powder material can be divided into three categories such as 63-125, 125-180, and 180-250 μm for convenience of sieving. In order to investigate and understand the effect of particle size on adhesion strength of particles, salt powder had been chosen as a reference material. A mix of a salt powder was obtained from Kerry Ingredients, UK and sieved into these three size ranges for use in the experiments. The result of the experiment will be discussed in the following parts of the report.

4.1.4 Particle density

Particle density is an important parameter to calculate the weight of a single particle. To be able to measure particle densities, a gas picnometer (Micromeritics Accucyc 1330) was used get measurements for three flavour, three salt and four glass powders having different size distributions and the data obtained are outlined in Table 4-1.

Table 4-1. Particle densities of powder material

Material	particle density (g/cm^3)
Prawn Cocktail	1.482
Salt and Vinegar	1.626
Cheese and Onion	1.544
Salt (63-125 μm)	2.162
Salt (125-180 μm)	2.156
Salt (180-250 μm)	2.154
Crushed glass (150-180)	2.504
Crushed glass (212-250)	2.526
Glass sphere (150-180)	2.507
Glass sphere (212-250)	2.513

The difference in particle densities varies for different materials. However significant increase in particle size caused slight decrease in the value of particle density for the same group of powder. In general, from the results it can be stated that the particle density values of salt powders are higher than that of flavour powders and glass powders have higher particles density than salt powders. The difference might be

appeared to be somewhat related to physicochemical structure and fraction of expandable minerals in the material.

4.1.5 Effect of particle size on adhesion strength

The magnitude of flavouring particle loss relative to impact force should be less for particles subject to larger adhesion forces against the crisp surface. Typically adhesion force was found to be least for the relatively coarse particles used in this study (180 to 250 μm) and greatest for mid-range sized particles (125 to 180 μm). The adhesion force for fine particles (63 to 125 μm) was found to be in between that of coarse and middle sized particles (Fig. 4-10). This behaviour could be due to agglomeration of fine particles in presence of oil to form bigger particles thus smaller adhesion force and bigger losses. Agglomeration of micro- and nano-particles occurs naturally and easily because the surface forces such as van der Waals forces, capillary forces and electrostatic forces can overcome only against gravitational and inertial forces for particles. In most of cases these agglomerated small particles might have behaved similar to bigger particles because the particles stick together and form a bigger particle. In Fig 4-7 the behaviour of three salt fractions can be seen on a substrate surface under an optical microscope. The images show the agglomeration of fine particles and dispersion of other fractions on the surface.

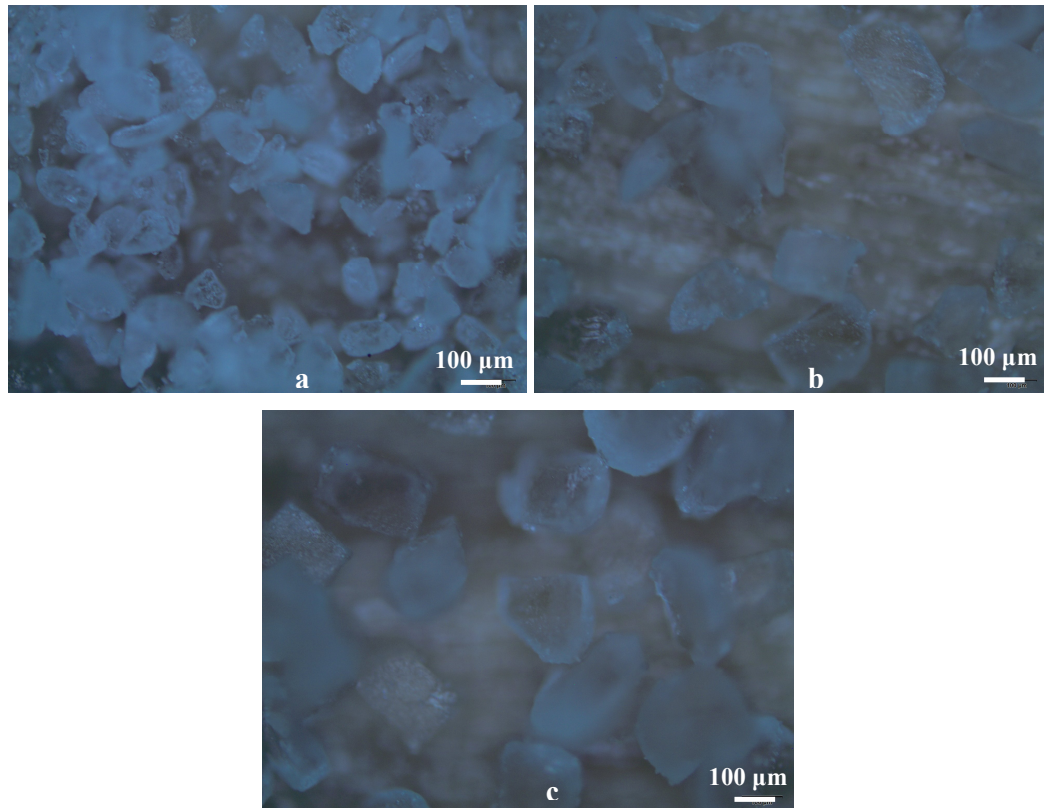


Figure 4-7. Salt particles under an optical microscope:
a, 63-125; b, 125-180; c, 180-250 μm

Fig. 4-10 shows the percentage mass of detached salt particles for three size fraction versus the force acting on particles at three different decelerations (48, 77 and 102 g). The results of the experiments were plotted in terms of the total amount of powder detached from each sample divided by the total amount of adhered powder as a function of impact force applied. It should be noted that the error bars correspond to standard deviation and show the spread and do not indicate a lack of confidence in the mean. Fig. 4-8 shows distribution of mean values versus number in sample and Fig. 4-9 shows how the individual substrates vary in terms of quantity applied, and how this affects amount of powder detached.

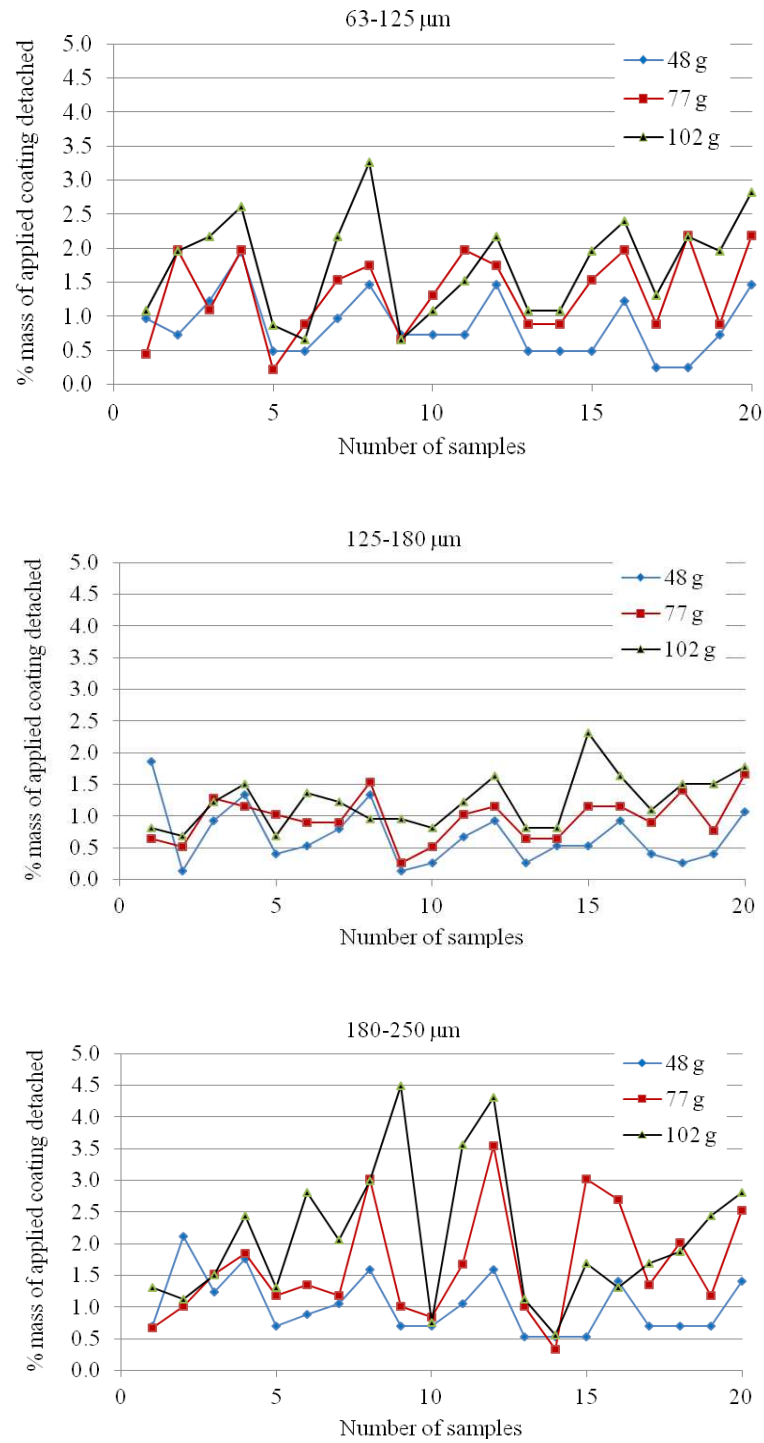


Figure 4-8. Distribution of mean value of % detached particles versus number in sample for different size fractions

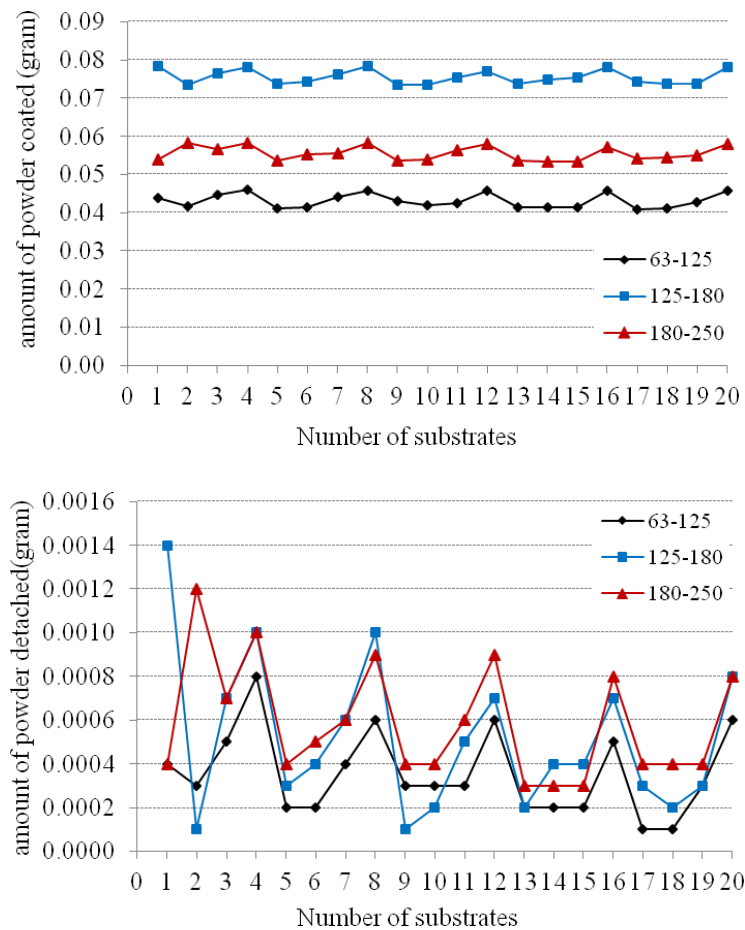


Figure 4-9. Distribution of mass of coated and detached particles versus number in sample for different size fractions

From Fig 4-10, it can be clearly seen that the average force acting on particles are different at same decelerations of the platen of IAT for different size fractions due to particle density. For instance, at 48 g deceleration, while the average force acting on particles is around 5×10^{-7} N for 63-125 μm , it is around 1.5×10^{-6} N for 125-180 μm size and around 5×10^{-6} N for 180-250 μm particles.

According to data given, it can be concluded that medium sized particles showed bigger adhesion strength then coarse and fine particles. This behaviour of fine particles may be linked to the change in particle density values of small particles when they form bigger particles as a result of agglomeration.

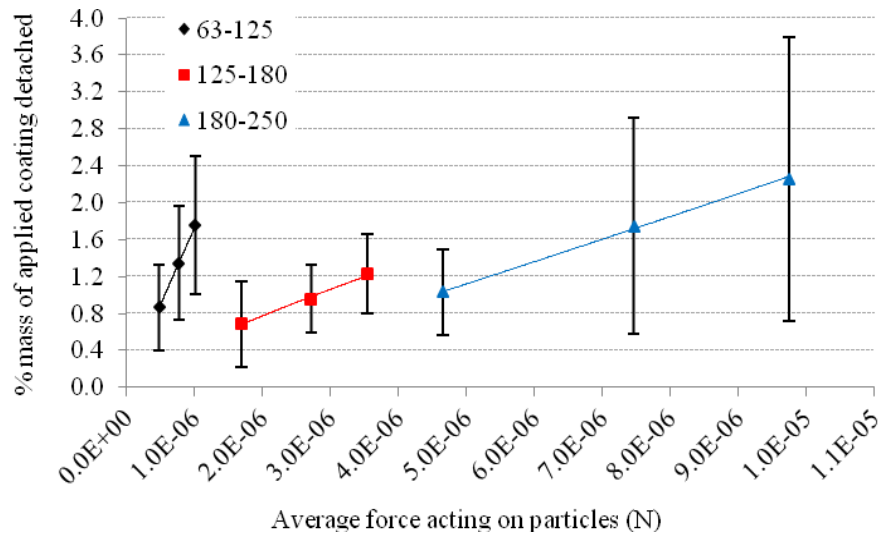


Figure 4-10. Percentage of salt particles detached as a function of particle size and force acting on particles (by using IAT)

The amount of particle loss versus impact force is expected to be smaller for larger adhesion force of particles onto substrate surfaces. It can be observed from the figures that similar values of forces acting on particles showed different effect on detachment of different size fractions. For instance, it can be observed from Fig. 4-10 that, while 1×10^{-6} N could detach 1.7% of fine particles, 1.7×10^{-6} N could detach 0.6% of medium size particles and 4.6×10^{-6} N about %1 for coarse particles. These data may give an idea of adhesion strength of different size fractions since the average forces acting on singles particle are close to each other. Fine particles were not expected to show weaker adhesion strength than other two fractions. The reason to that behaviour might be that: (i) it is possible that this behaviour could be due to the agglomeration of fine particles in presence of oil to form bigger particles resulting in weak adhesion force and more detached particles; (ii) the particles removed at lower decelerations may represent loosely held particles in a second or third layer (coincident particles).

The effect of increase in force acting on particle on detachment can also be observed from Fig 4-10. The increase in the percentage particle losses relative to deceleration of the platen was significant from 48 to 102 g (increased from 0.8% to 2.4%).

4.1.6 Effect of particle shape on adhesion strength

Fig. 4-11 shows the percentage of glass particles detached from the crisp substrate by using IAT. The effect of two different size fractions (150-180 μm and 212-250 μm) and two different shapes (crushed and spherical) on adhesion strength were investigated under two different decelerations and the results can be seen in Fig. 4-11.

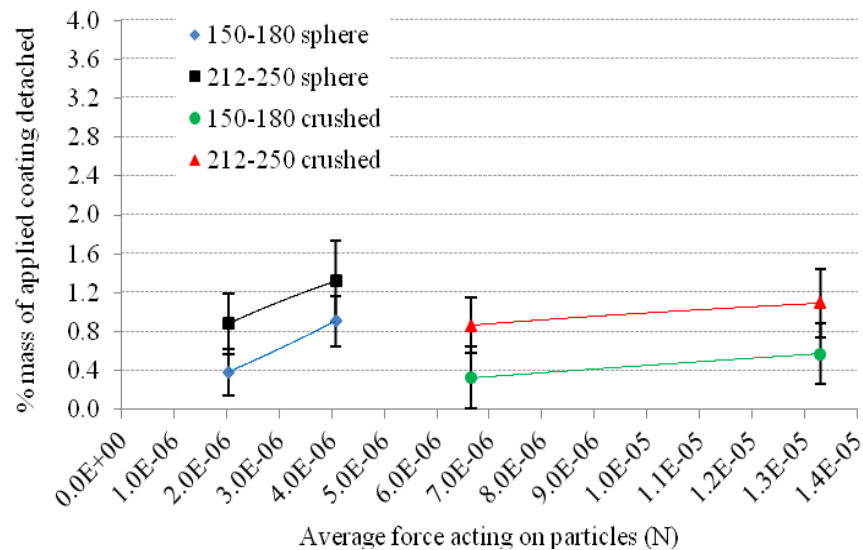


Figure 4-11. Percentage of glass particles detached as a function of particle size, particle shape and force acting on particles (by using IAT)

As expected, increases in the magnitude of force acting on particles increased the amount of detachment regardless of shape. The effect of shape on detachment can be observed from Fig. 4-11. For both size fractions, spherical shapes detached more than crushed particles even at smaller magnitude of force acting on spherical particles than on crushed ones. This difference in behaviour may be due to surface irregularities and hence larger contact area for crushed compared to spherical particles.

From the data obtained it can be stated that particle geometry plays a role in the adhesion force, decreasing in order for crushed glass and sphere of a given mass. When the shape of a particle is more rectangular, the adhesion force then becomes stronger as shown in the results. The reason comes from a larger contact area between particle and

surface. It is known that an increase in contact area results increasing adhesion force, hence less particles detached in presence of oil as intervening media.

4.1.7 Effect of the amount of surface oil on particle adhesion strength

The decrease in particle loss was higher at higher oil contents (Fig. 4-12). This implies that the adhesion force increases with oil content. The decrease in the rate of particle loss for coarse and middle sized particles versus 105 g impact force was significant when the surface oil content was increased from 0% to 1%. However, the decrease for fine particles was not so well defined (Fig. 4-12). Also the change in the rate of flavour loss was not significant between 1% and 2.5%. Therefore, the adhesion force increased as the oil content increased from 0 to 1% on the surface of the crisp. This behaviour could be due to larger hydrophobic interaction of the seasoning with the crisp surface at higher oil contents. However, further increase in oil content did not result in a further significant increase in the adhesion force.

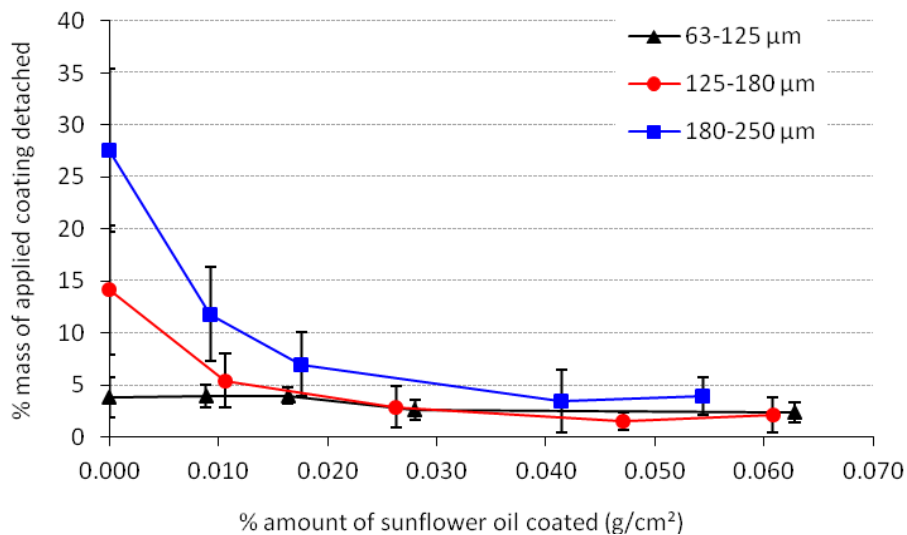


Figure 4-12. Effect of surface oil content on particle loss of salt (loaded 3 gram at 26 rpm for 20 seconds)

4.1.8 Effect of other process characteristics on particle detachment

Fig. 4-13 presents the percentage of particle losses of a given size from the crisp surface as a function of different laboratory process parameters (tumbler speed, retention time in tumbler mixer, and the amount of load of the powder into the tumbler mixer) at 105 g deceleration level for salt particles, respectively.

Fig. 4-13 shows the results for three size fractions of the salt particles. In that figure it can be observed that there is no significant change in particle loss rates with the increase of the angular speed for fine (63 to 125 μm) and medium sized (125 to 180 μm) particles. However significant varied results were obtained when the particles get bigger (180 to 250 μm). Additionally, while little variations were obtained in percentage of flavour loss by changing the feed quantity of the powder (3 to 6 gram per batch) and retention time (20 to 60 sec) in tumbler mixer for fine and medium sized particles, the variations are much higher for coarse particles.

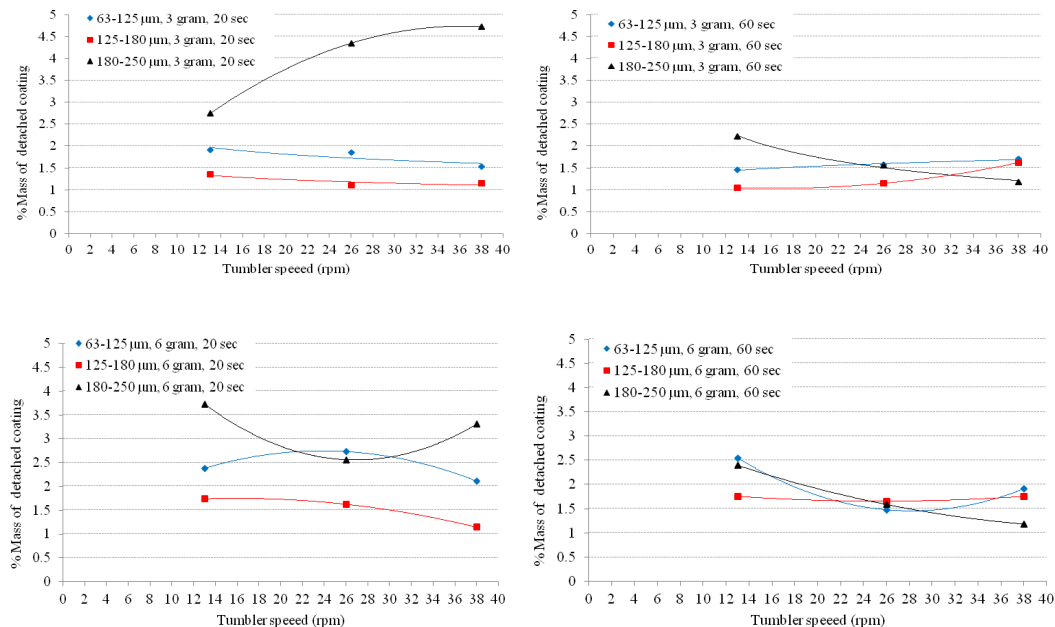


Figure 4-13. Effect of different process parameters on particle adhesion

The percentages of flavour loss for fine particles are in between 1.5%- 2.5%, for medium sized particles 1%-2% and for coarse particles 1% and 4.5%. These results show agreement with the results presented in Fig. 4-10 as the effect of particle size on the rate of particle loss.

4.1.9 Adhesion behaviour of different flavour powders

Fig. 4-14 shows the percentage of flavour particles detached from the crisp surface as a function of necessary force to detach them, for three different flavour powders studied. The applied detachment force was generated by Impact Adhesion Tester by free dropping motion of the plate of the tester from different heights. The data were obtained by loading 3 gram at 26 rpm for 20 seconds.

The adhesion force variation with different flavour powder observed in Fig. 4-14 can be explained by the difference in size distribution of powders, hence the size of the particles and by the nature of contact among contiguous bodies. During contact, a large particle will usually lead to a smaller contact area with crisp surface and be exposed to a bigger detachment force. Thereby, the larger adhesion force is due to the growth in contact area associated with an increment in the dimensions of the particle and the particle density.

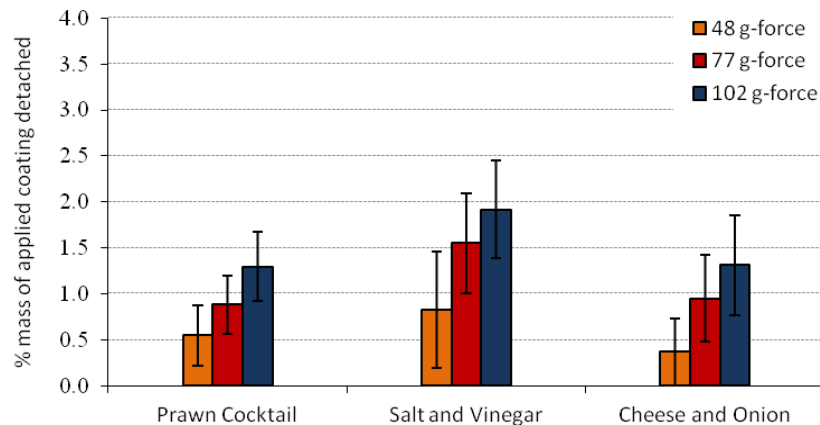


Figure 4-14. Percent particle loss of different flavour powders over deceleration forces

4.1.10 Reproducibility of the test procedure

Fig. 4-15 and Fig. 4-16 show data for two different retention times; 30 seconds and 60 seconds at deceleration force of 48 g and 105 g loading at 26 rpm. The powder used was salt in the particle size range from 180 to 250 μm .

The bars in Fig. 4-15 show very similar behaviour, at the same experimental conditions. However, there is a significant difference of the data obtained from the 3rd trial of detachments experiments, loading at 6 gram for 30 seconds. This might be caused by imperfect personal/ experimental variables.

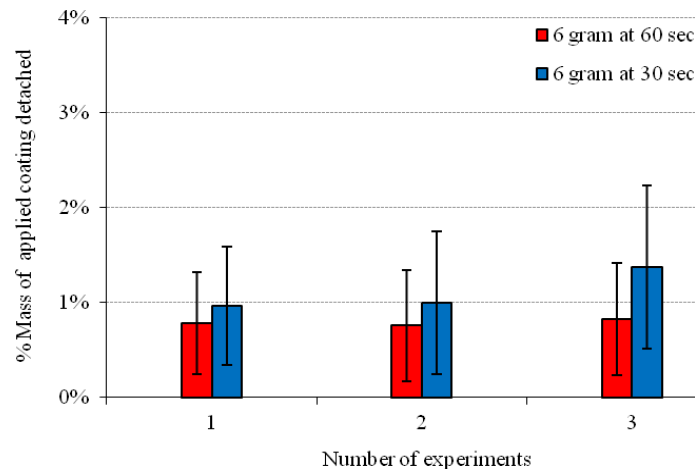


Figure 4-15. Repeatability results of % particle loss at 48 g

It can be observed from the Fig. 4-16 that, the data obtained fluctuates significantly and the percentage detached particles are higher than that of Fig. 4-15; around 0.8-1.5 % in Fig. 4-15 and increased to 1-2% in Fig 4-16. This may be because the adhesion behaviour of powder gets uneven when the impact force increases.

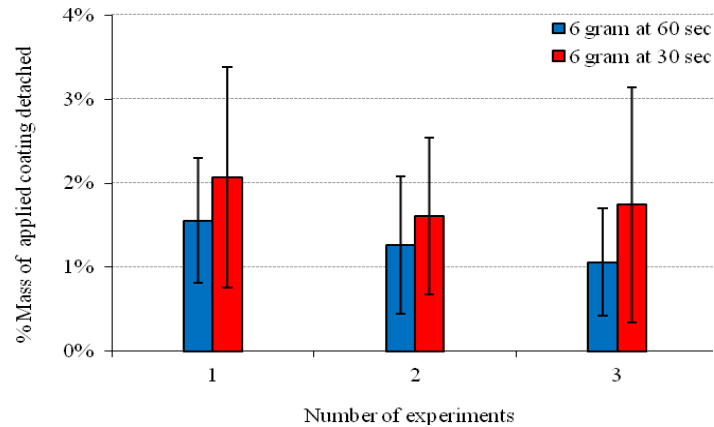


Figure 4-16. Repeatability results of % particle loss at 105 g

4.2 Comparison of results to centrifugal tester

An ultra-centrifuge was used as part of this PhD project to gather the data to be able to compare with the data obtained from IAT. Although the way the force acted on particles and working principles are different for these two techniques, it was decided that comparison might give some ideas about the validity of new tester and its experimental procedure.

Table 4-2. Calculated average force (N) acting on salt particles at different rotational speeds

Rotational speed (rpm)	63-125 μ m	125-180 μ m	180-250 μ m
300	5.44E-07	1.92E-06	5.28E-06
500	1.51E-06	5.34E-06	1.47E-05
1000	6.04E-06	2.13E-05	5.87E-05
1500	1.36E-05	4.80E-05	1.32E-04
4000	9.67E-05	3.42E-04	9.39E-04

Fig. 4-17 represents the percentage mass of applied coating (salt particles having three different size fractions) detached from wood chip surface as a function of applied centrifugal angular speed. Average forces acting on particles during centrifugation were calculated by using Eq (15) and the values are shown in Table 4-2. The average force

acting on particles varied from 5×10^{-7} to 9×10^{-4} N depending on centrifugal angular speed and particle size.

It can be observed from Fig. 4-17 that, with the increase in the average force acting on particles (a function of angular speed) the percentage of detached particles increased.

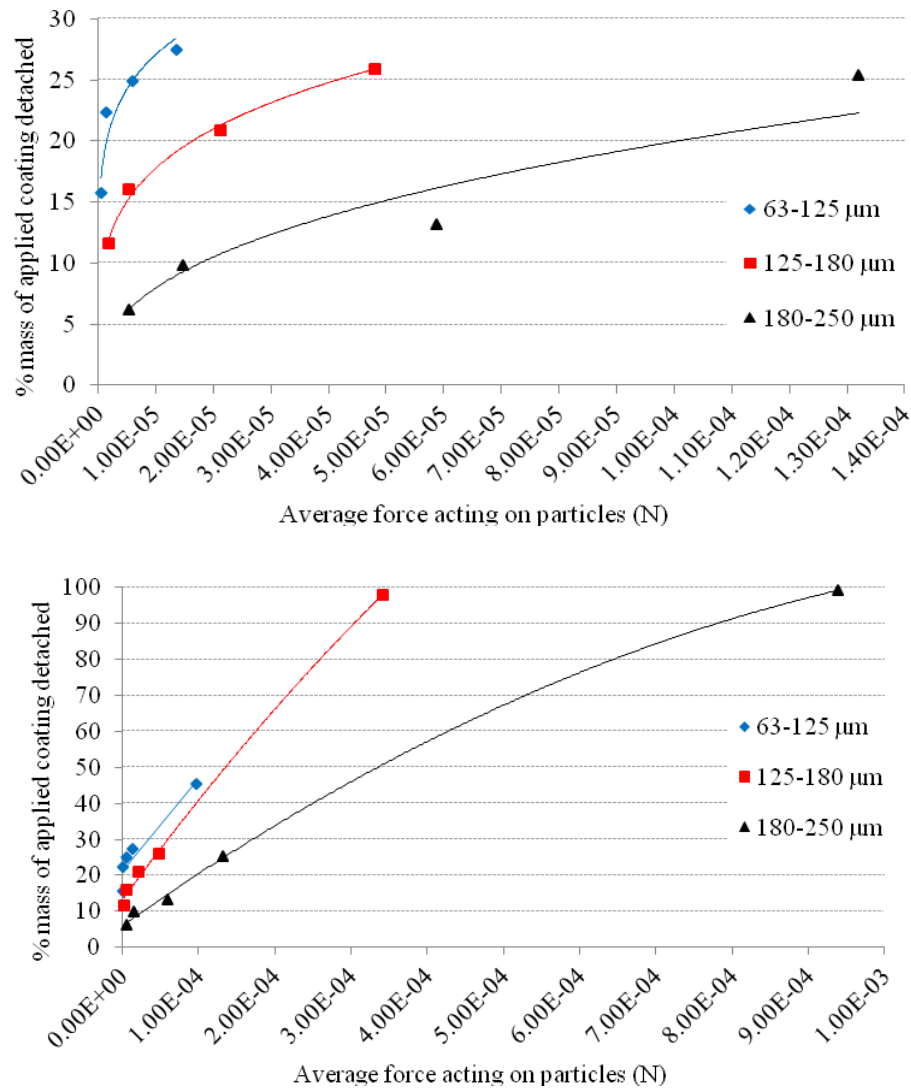


Figure 4-17. Percentage of salt particles detached as a function of particle size and force acting on particles (by using centrifuge)

For fine particles, the mass of particle loss is greater than that of medium and coarse particles at same average force. For instance, in the range of average force of 5×10^{-6} to 6×10^{-6} N, while the amount of detached particle is over 20% for fine particles, it is

below 20% for medium and below 10% for coarse particles. The possible reason to this behaviour may be agglomeration of fine particles to form a bigger size and thus weakening the adhesion strength. Bigger particles tend to adhere on the surface and show less agglomeration. Another reason may be attributable the shape of particles. Fine particles are more irregular than coarse particles and coarse particles have more regular cubic shape which may increase the contact area. Irregular particles possess less contact area and therefore weaker adhesion.

It can be observed from the Fig. 4-17 that the force needed to detach 100% of particles from substrate surface for medium size particles was found to be in the range of 5×10^{-5} to 4×10^{-4} N while it was found to be from 2×10^{-4} to 9×10^{-4} N for coarse particles.

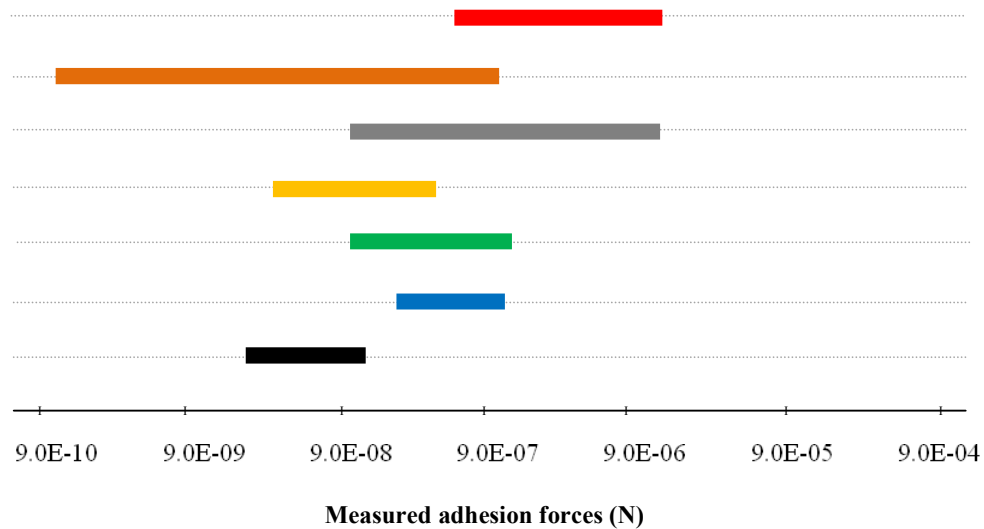
The findings of this study showed a good correlation to the results obtained by Salazar-Banda et al (2007) - who used phosphatic rock and manioc starch particles having mean diameter ranging from 13 to 45 μm using the centrifuge technique. They calculated the theoretical adhesion force and reported as varying from 3×10^{-7} to 7×10^{-7} N. They have also reported that there was significant loss of particles (more than 60%) after applying centrifugal force at around 1×10^{-6} N. According to Enggalhardjo and Narsimhan (2005), the experimental adhesion force and theoretical adhesion force showed a good agreement and varied from 1×10^{-9} to 1×10^{-7} for cheese seasoning particles on tortilla chips by using wind tunnel experiment.

At same magnitude of forces acting on particles, higher percentage of detachments was observed from centrifuge technique than IAT. For example, for fine particles, while around %1 of particles detached at 5×10^{-7} N when IAT was used, it was around %15 when centrifuge technique was used. For coarse particles, while it was recorded as %1 when IAT was used at around 5×10^{-6} N, it can be seen from Fig. 4-17 that it is around %5 when centrifuge technique is used. The difference might be due to the different surface of substrates used (crisps substrate has corrugated/inclined surface which may cause sliding friction unlike veneer surface which has a flat surface) and possible particle losses due to handling of substrate while placing into centrifugal tubes. It can also be stated that the forces acting on particles on both techniques are in different ways which are sustained force for centrifuge and short duration for IAT. Sustained force might be more effective in breaking a viscous force than a shock.

4.3 Discussion of different techniques and relevance of the data obtained to findings of this study

One problem of correlating the data between different techniques and IAT was that of how to display the comparative data. The major goal in this PhD project was to establish a new methodology to measure particle adhesion using a novel adhesion tester. Consequently, it was decided that the best way to compare the data and methods is direct comparison of the techniques have been used by other researchers and data that they have obtained with the findings of this PhD study (Fig. 4-18). The comparisons will be individually discussed below.

Enggalhardjo and Narsimhan (2005) used a wind tunnel to study the adhesion forces acting on flavour particles on tortilla chips by using air flow over the inclined surface. They have noted that there was a critical distance at which the drag force counterbalances the frictional forces since the air stream was applied parallel to the surface of substrate. In other words, the flavour particle will be in equilibrium at critical distance. The weight of particles removed may depend on the length of the substrate due to deposition of particles on the rest of substrate rather than being completely removed. This behaviour may not give representative results and measuring the critical distance may not be accurate. They have found that the % particle loss varied from 8% to 20% by increasing the air velocity from 0.5 to 1.2 m/s. They have reported that the estimated total theoretical adhesion forces increased from 2×10^{-8} N to 1×10^{-7} N with the increase of particle size from 48 to 240 μm . They have also reported that the inferred adhesion force based on experimental data is around 2×10^{-9} to 4×10^{-7} N. The findings of the study reported in this thesis are close to the data obtained by Enggalhardjo and Narsimhan (2005) but not exactly in a good agreement. For example, it was observed from the work undertaken in this thesis that 5×10^{-7} N could detach 15% fine particles (63-125 μm) when centrifuge technique is used while it is reported as around 20% by Enggalhardjo and Narsimhan (2005) for the similar magnitude of force.



- 48 to 240 µm flavour particles on tortilla chips by Enggalhardjo and Narsimhan (2005)
- 20-80 µm spherical glass particles on a silicon wafer by Hein et al (2002)
- 9-45 µm phosphatic rock, 11-27 µm manioc starch on a polished steel disc by Salazar-Banda et al (2007)
- 30 µm potato starch particles on a needle by Shimada et al (2003)
- 30-50 µm food powders on a glass plate by Otsuka et al (1988)
- 2.5 µm silica spheres on a silicon wafer by Paajanen et al (2006)
- data obtained from this PhD project

Figure 4-18. Comparison of adhesion forces reported in this PhD thesis to other researcher's findings.

Buck and Barringer (2007) conducted studies of the adhesion between salt particles and potato chip by measuring the vibration of a vibratory feeder. They have examined 3 major components and their attributes as they affected adhesion of salt onto potato chips: (i) amount of surface oil, time between frying and coating, and the use of different oils; (ii) physical attributes of salt particles such as size and shape; and (iii) use of electrostatic coating. They have noted that surface oil is the most important factor for adhesion since it leads to strong capillary force that dominates over other adhesion forces (vdW, electrostatic). According to Buck and Barringer (2007), the size of salt particles play 2nd most important role for adhesion. Smaller size was found to give better adhesion than larger particles of the same shape. They have also reported that

shape has little effect on adhesion. However, they have concluded that cubic shape salts adhered better than flake which adhered better than dendritic salt particles. This PhD work produced results which corroborate the findings of Buck and Barringer (2007) of a great deal. However, they have not calculated adhesion forces and therefore it has not been able to compare the particle adhesion based on magnitude of forces.

A paper by Hein et al (2002) presented vibration method for the measurement of adhesion forces between a particle (glass spheres) and a wall (silicon wafer). They have measured the acceleration of the vertical-sinusoidal vibrating surface, caused by its inertia, using a laser-scanning-vibrometer. They have used image analysis method to record particle re-entrainment and to correlate with acting acceleration. They have placed the vibrating surface in a flow channel and exposed to an air flow parallel to the surface. The contribution of air flow force to adhesion and inertial forces was neglected. There are some limitations with this method. These are limited achievable acceleration of the vibration system and limited optical acquisition of the particles when it is compared to IAT and its experimental procedure. This restricts the applicability to fine particles (smaller than 5 μm). They have reported the adhesion force varied from 2×10^{-7} to 9×10^{-7} for spherical glass particles in the range 20-80 μm . These values are roughly one decimal place lower than the calculated adhesion forces in this PhD thesis. This might be due variation of capillary forces acting on particles.

Salazar-Banda et al (2007) used centrifuge technique to study adhesion between phosphatic rock (9-45 μm , irregular form of shape) and manioc starch (11-27 μm , spherical) particles and a polished steel disk. They have used a tube and adapter constructed for inserting in the centrifuge. They have applied centrifugal rotations varying from 1000 up to 14000 rpm for 1 min. They have reported the % particles that remained adhered after applying centrifugal angular speeds. They have reported that the adhesion force needed to detach particles ranged from 1×10^{-7} to 1×10^{-6} . Their experiments show that the % particles remained adhered was around 60 (40% detached) at around 1×10^{-7} N for manioc starch particles while it was reported as around 20 (80% detached) for phosphatic rock particles at the same magnitude of force. It can be stated that findings of Salazar-Banda et al (2007) does not show a strong agreement with the finding of PhD project. The % of detached particles for fine powder (63-125 μm) was observed as 15% around 5×10^{-7} N, by using centrifugal technique, which is less than

40% and 80%. The reason to these differences might be due to difference in shape and size of particles, surface characteristics of substrate and intervening media used in experiments.

Shimada et al (2003) developed a new apparatus to measure the adhesive force between particles (corn starch, potato starch, lactose, and glass beads as spherical model) with a high resolution of approximately 2×10^{-9} N. They have measured the force directly by applying a pulling force to the particles with a contact needle. They have investigated the effect of humidity on particle adhesion. It has been reported that the adhesion force between different particles varied from 3×10^{-8} N to 3×10^{-7} N and an increase in moisture content from 10 to 30, increased adhesion force from 1×10^{-7} N to 5×10^{-7} N for potato starch particles (30 μm). It has been observed from this PhD work that 5×10^{-7} N could detach 15% when centrifuge technique used and around 1% when IAT used for fine powders (63-125 μm). It can be observed from these data that, particles adhered to surface needed bigger adhesion force than particles adhered to each other.

Otsuka et al (1988) studied determination of adhesive force between various food particles (30-50 μm) on a glass plate in a measuring cell which was fixed to the impact hammer of a pendulum shock testing machine. They have used an accelerometer to measure the impact acceleration generated. They have calculated the percentage of particles adhering to the substrate by counting the numbers of particles before and after impact. The adhesive force that they have reported varied from 1×10^{-7} to 1×10^{-5} N. They have reported that the percentage of detached particles varied from 20% to 90% at a range of forces acting on particles varied from 1×10^{-7} N to 1×10^{-5} N for various powder that have used in given size range. These values agree with the findings of theoretical calculations reported in this PhD thesis. The total adhesion force for fine particles were found around 1×10^{-6} N for fine particles (63-125 μm). Experimental data show that 1×10^{-6} N could detach 20% of fine particles which show agreement with the findings of Otsuka et al (1988).

Paajanen et al (2006) used an AFM to measure the humidity dependency of the pull-off force with spherical probes. They have investigated the adhesion of silica spheres (2.5 μm) on to silicon wafer under ambient pressure with different relative humidity up to 100%. Their data revealed an increase in adhesion with increasing humidity. The range

of pull-off force they have recorded varied from 1×10^{-9} to 8×10^{-7} N for different size of different particles at different RH%. George and Goddard (2006) have studied Atomic Force Microscopy to investigate the effect of surface roughness on particle adhesion. They have used model spherical glass beads having 20.6 μm size and uranium trioxide granules having 65 micron size on mica surface having different surface roughness (from 150 to 1500 nm). They have reported the force needed (pull-off force) to detach particles from surfaces varied from 1×10^{-7} to 3×10^{-6} N. These findings are in agreement with the findings derived from the work undertaken in this thesis in terms of effect of particle size on the magnitude of adhesion force.

Although the study of particle adhesion entered a new phase with the development of the Atomic Force Microscope (AFM) and the high sensitivity of this equipment enabled the measurement of nano-scale forces and separations between particles with diameters of only a few micrometers, some limitations have been reported as of AFM is that it can monitor adhesion of only single particle (Paajanen et al., 2006). Because flavour particles are irregularly shaped, there is a concern that the aspects of adhesion being monitored with AFM are not representative of the collection of flavour powder as a whole. Centrifugal, wind tunnel, vibration and impact adhesion testing monitor the adhesion of many particles and the outputs of these measurements are a distribution of all the flavour particles. However, AFM measures the adhesion of single particles with quite high precision and control (George and Goddard, 2006). There are number of applications this technique is involved in many fields of nanoscience and nanotechnology. One remarkable feature of AFM instrument is its ability to examine samples not only in ultra high vacuum but also at ambient conditions or even in liquids. AFM is capable of measuring three dimensional images of surfaces and studying the topography. Some examples to other possible applications of AFM can be given as substrate roughness analysis, grain size analysis, and studying changes in structure by in situ AFM analysis with changes in temperature.

CHAPTER 5

CONCLUSIONS AND FUTURE WORK

The objective of this research project was described in Chapter 1. The results of experimental work undertaken during this research project in order to attempt to address the original objective were discussed in Chapter 4. Broad conclusion to the work carried out in this project and suggestions for further work that could be undertaken to further improve the understanding of particle adhesion in industrial applications will be discussed in this chapter.

5.1 Introduction

A literature review was undertaken in order to determine the state of the technology in the field of particle adhesion. The literature research has shown that up to now a few studies have focused on direct measurement of adhesion strength of bulk material, which may be attributable to the lack of a standardized measurement technique for particle adhesion to substrates. Some of the techniques have been utilised are summarised and their findings are compared to the approach employed for this PhD project.

The primary aims of this project were to develop a bench size adhesion tester to infer flavour particle adhesion onto crisp surface and to prove or disprove any correlation between the data obtained from designed tester and from centrifuge adhesion tester as well as from other test methods used by other researchers previously. Additionally, it was anticipated that the technique could be rolled out into other scientific investigations relating to the adhesion strength of particles to substrates. The Impact Adhesion Tester (IAT) has been designed and constructed along with a tumbler mixer – both of which were successfully trialled at the Technical University of Munich and at Wolfson Centre for Bulk Solids Handling Technology at The University of Greenwich. The tester and its experimental procedure were found to be capable of quantitative adhesion force measurement for a variety of particulate material.

The secondary aims of the project were to prove or disprove the IAT's potential usefulness and determine whether there was a correlation between experimental data and inferred data from calculations derived from existing theory.

5.2 Development of an adhesion tester

After conducting a literature review, and as a consequence of the need to predict particle adhesion in bulk in food industry, a novel bench size adhesion tester was designed and constructed. This tester was designed to attempt to fulfil the need to better understand particle adhesion in industrial applications, quality control laboratories and related research fields. One of the requirements of this tester was that it could be light weight bench size tester to be able to carry to Technical University of Munich where the experiments were conducted or to any site for future use.

Investigation of the crack strength of the crisp substrates used in this study generated data from a number of them. However, it can be obtained from the data that the mean value of minimum load required to crack the substrates is around 6.7 N which means 6700 g roughly. The existence of oil on the substrate showed a slight increase in strength of the substrate.

In the design stage of the tester, it was aimed to construct a tester which would not generate higher g values than the mean crack strength of crisp substrate. The deceleration tests were carried out to investigate the deceleration values of the designed tester and it was found that the platen of the tester generated up to 100 g (from 10 cm) for different drop distances. It was obtained from the deceleration tests that there is a linear correlation between the drop distance and deceleration force generated.

5.3 Selection of a test substrate

The substrate used in this study is Crinkly's crisps as described in Chapter 2. Crinkly's crisps were chosen due to their uniform physical characteristics such as round shape, surface texture, size and rigidity. These features played important role in terms of repeatability of the experimental work and compatibility with the design characteristics of the tester.

5.4 Characterisation of flavour powders

The sieve analysis of the flavour powder indicated that different flavour powder showed different size distributions in a wide range from below 10 μm up to over 800 μm . It was decided that the size distributions of the flavour powders used in this study could be categorised into three main size ranges and these are 63 to 125 μm , 125 to 180 μm and 180 to 250 μm to be able to evaluate the effect of size on particle adhesion.

To be able to investigate the effect of particle shape on adhesion, crushed and spherical glass particles were studied.

5.5 Characterisation of adhesion strength of powders

Initial tests were undertaken to determine the major variables (as outlined below) associated with adhesion strength of flavour powders, salt and glass powders using the IAT. Further test work was conducted to prove a correlation between the IAT and centrifugal tester. Additionally, theoretical adhesion forces were calculated and the possible correlation between the results was investigated. The outcomes from these tests and calculations are discussed below:

Effect of surface oil

It was observed from the tests on determining the effect of oil that the adhesion strength increases at the presence of oil on the surface of crisp substrate due to strong capillary force. The effect of surface oil on particle adhesion generated data that demonstrated that with increases in oil content of the crisp substrate the particles adhered to the surface better. Further increase in surface oil content had no further effect on particle adhesion (the critical amount is around 1%).

It was confirmed that the presence of oil was the dominant factor affecting the adhesive force which is referred as capillary force. That means high surface oil content leads to strong capillary forces that dominate over van der Waals and electrostatic forces. It can be concluded that surface oil is the most important factor for adhesion.

Effect of particle size

From the tests conducted to investigate the effect of particle size on adhesion strength it was determined that particle size is the second most important factor for adhesion. While conducting these tests it was found that adhesion strength of medium size salt particles is greater than the fine salt particles. In theory, smaller size particles have better adherence than larger particles because of stronger van der Waals forces per unit of mass. However, in this study it has been observed that the adhesion strength was found to be slightly bigger for coarse salt particles (125-180 μm), in between for medium size particles (180-250 μm) and slightly smaller for fine particles (63-125 μm). To be able to detach 1% of particles, it was reported as the required magnitude of forces acting on particle are around 5×10^{-7} N, 2.8×10^{-6} N and 4.5×10^{-6} N from fine to coarse. It has been concluded that the reason why the experimental data is not in agreement with theory might be due to (i) agglomerations of fine particles to form bigger sizes and (ii) the particles removed at lower decelerations may represent loosely held particles in a second or third layer (coincident particles).

Effect of particle shape

The data obtained from the experiments show that the particle shape has significant effect on adhesion. It has been derived from the experiments that to be able to detach 1% particles, the required magnitude of forces acting on particle are around 2.5×10^{-6} N for spherical particles (212-250 μm), and around 6.8×10^{-6} N for crushed particles (212-250 μm). When there were differences in shape of the particles, crushed glass adhered better than spherical ones. It may be concluded that particle geometry plays an important role in the adhesion force, decreasing in order for crushed glass and sphere of a given mass. In other words, crushed glass particles adhere better than spherical ones for the particles having same weight.

Effect of process parameters and repeatability of experimental procedure

From the tests conducted to investigate the particle adhesion strength of different flavour powders it was obtained that they have showed different adhesion behaviour. This was concluded as due to difference in their size distributions, the growth in contact

area per unit mass associated with an increment in the dimensions of the particle and the particle density.

Investigation of process parameters such as amount of powder applied, residence time and rotational speed showed variations in the experimental results. It was obtained that increase (from 3 grams to 6 grams) in the amount of powder material used to coat the crisp substrate increased the per cent amount (from 2% to 2.8% at 26 rpm for fine particles) of particles detached. It was confirmed that increase in residence time (from 20 sec to 60 sec) in tumbler mixer decreased the amount of powder detached from the surface (from 2.8% to 1.6% at 26 rpm for fine particles) per unit mass of powder coated. However, change in rotational speed did not show a significant correlation to detachment even though different per cent amount of detached particles were observed for different rotational speeds.

The repeatability of the experimental procedure showed variations (approximately $\pm 0.3\%$) in the results. It can be concluded that variations may be due to imperfect experimental conditions and variations in physical/chemical characteristics of materials used.

It was observed that changing two of the coating process parameters affected the detachment of particles significantly as described in the previous paragraph. The differences observed are relatively high when compared to experimental error. Doubling the amount of powder fed into tumbler mixer caused an increase in the particle detachment by 0.8% and increasing the retention time in tumbler mixer three fold resulted in around 1% decrease in particle detachment. These figures tell us that the 1% difference in flavour particle loss would mean a huge amount when the daily usage of flavour powders is described as in tons.

These findings from these experiments show that it is possible to quantify the difference in the amount of particle detachment from substrate surface from altering some of the coating process parameters such as retention time and amount of powder used. This should be useful for industry in terms of calculating and predicting the flavour powder loss to optimise the process parameters. An example for utilising this analysis could be when coating crisp substrates in tumble mixer used in this study, changing the retention

time from 20 sec to 60 sec will give a decrease of 1.2% in detachment hence, less particle loss from the surface of substrate for fine powder material used in this study.

Comparison of experimental results to theoretical calculations, to centrifugal tester and to other researcher's findings

An empirical approach has been adopted involving the mathematical calculations by using the variables and constant values. This enabled calculations and predictions of magnitude of particle adhesion onto food surfaces over a range of particle size fractions, geometries and amount of surface oil. A possible correlation between experimental and calculated results has been explored. This procedure provides further understanding of particle adhesion and potential use of IAT along with its experimental procedure.

Theoretical calculations and experimental work using IAT and centrifuge technique showed that the magnitude of theoretical forces varied from 1×10^{-6} to 6×10^{-6} N for given size range and experimental adhesion forces varied from 5×10^{-7} to 1×10^{-5} N obtained by using IAT and from 5×10^{-7} to 9×10^{-4} N obtained by using centrifuge. The differences between all these values might be due to different type and design characteristics of sample housing used in two testers used in this study and experimental imperfections.

The research work that has been made has indicated that the concept of impact detachment as a mechanism by which adhesion performance can be assessed is valid. In addition to the proof of concept aspect of the work shows that such a test approach can be achieved without resorting to the use of expensive and physically very large equipment (aspects of most accepted scientific testers that precluded the adoption of such tests in many industrial QA laboratories).

Within the industrial context, the results from the detachment test and the tester with the analytical approach that has been developed can be used to provide useful information relating to better understanding and identification of flavour particle adhesion onto solid food surfaces.

To conclude, according to data obtained from experiments, to be able to get better adhesion, using an intervening media such as oil or an alternative low calorific media is

essential. Results showed that using fine powders in tumbler mixer gives better adhesion if the agglomeration is prevented. Increase in the size of salt particles used as carrier to the flavour powders increased the amount of particles detached. It can be stated that using flake shape particles adhere better than cubic and dendritic particles. Increasing retention time in tumbler mixer decreased the amount of particles detached. Using less amount of powder in mixer also decreased amount of particles detached. Based on the information obtained, to get better adhesion, flake shaped fine particles should be used in tumbler mixer at lowest amount possible and longest retention time possible as soon as these optimisations do not change the appearance of the product or make the final product's quality low.

The programme of work that has been undertaken within the Marie Curie Bio-powders RTN (Project No: EU MRTN-CT-2004-512247) has brought the dissemination of scientific measurement techniques to industry one step nearer, through the development of an economic tester that has the potential to provide quantitative test data for formulation scientists or quality assurance laboratories.

5.6 Recommendations and Future Work

The aims set for this project were successfully accomplished and the tests were conducted by using IAT. From the work carried out within the frame of the project, it was found that there are possibilities for further investigation to advance the understanding of particle adhesion onto food surfaces and for further evaluate the IAT. The following are some of the opportunities for further investigation that would benefit both academia and industry:

- Additional experimental work using more test materials is recommended. The additional work should focus on similar size range of the powder material that was used in this research project. The additional powder materials should be food originated and should be tried on different food surfaces which might enable to compare the results obtained. This should provide a more comprehensive study to be made of the calculations and analysis already produced in this project. This could extend to investigate the repeatability and validity of new tester along with its

experimental procedure as well as to further investigate the influence particle properties have on the adhesion strength.

- The particle adhesion onto food surfaces need to be investigated in much more detail, so that a better understanding of effects of parameters such as particle physical and chemical characteristics, substrate surface characteristics, environmental conditions at coating stage etc. to particle-surface, particle-particle adhesion is gained. This will enable the prediction of particle adhesion onto food surfaces to be improved.
- Effect of change in surface characteristics of substrate, change in type of oil and its physical characteristics, change of raw material such as using different potato varieties have not been studied in this project. These parameters might be useful to study to better understand adhesion of food powders.
- A mill can be used to disagglomerate particles instead of just feeding to the coating unit- this would enable more effective coating for finer particles. The adhesion behaviour of finer particles should also be examined after freezing them to prevent agglomeration during coating.
- In this research project, data obtained from IAT was compared with the data obtained from centrifugal tester. Comparison with an additional adhesion tester would be beneficial as data from two testers showed differences. The understanding of the influence of different techniques on particle adhesion measurement needs to be improved.
- Further research work is required to improve IAT in terms of its design, repeatability and reliability along with its experimental procedure to overcome variations and errors occurring during experiments. A fixed stop can be employed to ensure precisely repeatable drop height and a stainless steel cylinder can be used to avoid rusting. Additionally a metal spring instead of a rubber stopper can be used to avoid the rubber material gets hard over the time.
- The IAT is then needed to be evaluated by industrialists and experts to investigate the possible use and to validate the experimental procedure.

- The theoretical approach is advised to be further studied to better evaluate the results and better understand the adhesion behaviour of different powders.
- It may be possible to commercialise IAT after improving the design and validating its reliability by other researchers and industrialists. Other substrates having different shapes and sizes can also be tested with IAT as far as the sample holder is redesigned based on substrate's physical characteristics. Then it will be only the substrate holder to be changed with the change of substrate. This is an important point because there is a wide range of different sizes and shapes of snacks and snacks produced by food industry.
- There are other applications outside the food industry to which the understanding of powder adhesion and understanding of particle - surface forces would apply. Powder coating in chemical/mineral industry, powder adhesion in pharmaceutical industry such as tablet making and cleaning of particle sediments from production equipment can be given as examples.

REFERENCES

- Ahmadi, G., Guo, S., Zhang, X. 2007. Particle adhesion and detachment in turbulent flows including capillary forces. *Particulate Science and Technology*, 25:59-76.
- Ahmadi, G, Guo, S. 2007. Bumpy particle adhesion and removal in turbulent flows including electrostatic and capillary forces. *The Journal of Adhesion*, 83:289-311.
- ASI Instruments, 2010. Dielectric constant reference guide. Houston: ASI Instruments. Available from: <http://www.asiinstr.com/technical/Dielectric%20Constants.htm>. Accessed June 14, 2010.
- Bailey, A.G. 1998. The science and technology of electrostatic powder spraying, transport and coating. *Journal of Electrostatics*, 45(2): 85-120.
- Barbosa-Canovas, G., Ortega-Rivas, E., Juliano, P., Yan, H. 2005. Food Powders: Physical Properties, Processing and Functionality. Kluwer academic/Plenum Publishers, New York.
- Barringer, S.A., Abu-Ali, J.M., Chung, H. 2005. Electrostatic powder coating of sodium erythorbate and GDL to improve colour and decrease microbial counts on meat. *Innovative Food Science and Emerging Technologies* 6:189-193.
- Berry, R.J., Bradley, M.S.A. 2007. Investigation of the effect of test procedure factors on the failure loci and derived failure functions obtained from annular shear cells. *Powder Technology*. 174:60-63.
- Berard, V., Lesniewska, E., Andres, C., Perduy, D., Laroche, C., Pourcelot, Y. 2002. Dry powder inhaler: influence of humidity on topology and adhesion studied by AFM, *International journal of pharmaceutics* 232: 213-224.
- Biehl, H.L., Barringer, S.A. 2003. Physical properties important to electrostatic and nonelectrostatic powder transfer efficiency in a tumble drum. *Journal of Food Science*, 68: 2512-2515.
- Bieth, H.L., Barringer, S.A. 2003. Physical properties important to electrostatic and nanoelectrostatic powder transfer efficiency in a tumble drum. *Journal of Food Science: Food Engineering and Physical Properties* 68(8): 2512-2515.
- Biggs, S., Spinks, G. 1998. Atomic force microscopy investigation of the adhesion between a single polymer sphere and a flat surface. *Journal of Adhesion Science and Technology* 12:461-478.
- Bourne, M.C., Moyer, J.C., Hand, D.B. 1966. Measurement of food texture by a Universal Testing Machine. *Food Technology* 20:170-174.
- Bowen, W.R., Hilal, N., Lowitt, R.W. and Wright, C.J. 1998. A new technique for membrane characterisation: direct measurement of the force of adhesion of a

- single particle using an atomic force microscope. *Journal of Membrane Science* 139: 269-274.
- Bowling, R.A, 1988. A theoretical review of particle adhesion. In: Mittal KL, editor. *Particles on surfaces*. Vol. 1. New York: Plenum Press. p:129-142.
- Brennan, J.G. 2006. *Food Processing Handbook*. WILEY-WCH, Weinheim, Germany.
- British Standards Institute 1796: Part1: 1989, ISO 8156:1988, *Test Sieving*.
- Brown, R. L. and Richards J. C. 1970. *Principles of powder mechanics: Essays on the packing and flow of powders*. Pergamon Press, London, England.
- Buck, V. E., Barringer, S. A., 2007. Factors dominating adhesion of NaCl onto potato chips. *Journal of Food Science*, 72: 435-441
- Burns, R.E., Fast, R.B. 1990. Breakfast cereals and how they are made. *American Association of Cereal Chemistry Inc.* Ch. 7, 195-220.
- Butt, H.J., Jaschke, M., Ducker, W.A., 1995. Measuring surface forces in aqueous solution with the atomic force microscope. *Bioelectrochem. Bioenergy* 381:91-201.
- Caixeta, A. T., Moreira, R., Castell-Perez, E., 2002. Impingement drying of potato chips. *Journal of process engineering* 25: 63-90.
- Capella, B., Dietler, G. 1999. Force-distance curves by atomic force microscopy. *Surface Science Reports*. 34: 1-104.
- Cardot, J., Blond, N. and Schmitz, P. 2001. Adhesion and removal of particles from surfaces under humidity controlled air stream. *Journal of Adhesion* 75: 351-368.
- Carr, R. L. 1965. Classifying flow properties of solids, *Chem. Eng.*, 72, 3:69-72
- Carr, R.L. 1976. Powder and granule properties and mechanics. In *Gas Solids Handling in the Processing Industries*, Morchello, J. M. and Gomezplata, A. (eds.), Marcel Dekker, Inc., New York.
- Christison 1991. *Equipment Catalogue*, Albany Road, East Gateshead Industrial Estate, Gateshead, England.
- Chutkowski, M., Petrus, R. 2008. Empirical model of adhesion force induced by a liquid bridge inside a powder bed in a pendular state. *Chemical and Process Engineering* 29:75-86.
- Cooper, K., Gupta, A., Beaudoin, S. 2000. Substrate morphology and particle adhesion in reacting systems. *Journal of Colloid Interface Science* 228:213-219.
- Derjaguin, B.V., Zimon, A.D. 1961. Adhesion of powder particles to plane surfaces. *Kolloidnyi Zhurnal* 23-5: 544-552.

- Derjaguin, B. V., Muller, V. M., Toporov, V. J. 1975. Effect of contact deformations on the adhesion of particles. *Colloid Surf. A-Physicochem. Eng. Asp.* 53:314-326.
- Denis, C., Hemati, M., Chulia, D., Lanne, J.Y., Buisson, B., Daste, G., Elbaz, F. 2003. A model of surface renewal with application to the coating of pharmaceutical tablets in rotary drums. *Powder Technology* 130: 174-180.
- Dreier, W. 1991. The nuts and bolts of coating and enrobing.
http://findarticles.com/p/articles/mi_m3289/is_n7_v160/ai_11427836.
Access date: 20 Nov 21008
- Eichenlaub, S., Gelb, A., Beaudoin, S. 2004. Roughness models for particle adhesion. *Journal of Colloid and Interface Science*, 280: 289-298.
- Elayedath, S., Barringer, S.A. 2002. Electrostatic powder coating of shredded cheese with antimycotic and anticaking agents. *Innovative Food Science and Engineering Technologies* 3: 385-390.
- Endevco technical paper: Acceleration levels of dropped objects.
http://www.endevco.com/resources/tp_pdf/TP321.pdf. Accessed on September 10, 2007.
- Enggalhardjo, M. and Narsimhan, G. 2005. Adhesion of dry seasoning particles onto tortilla chip. *Journal of Food Science* 70(3): E215-E222.
- Feddema, J.T., Xavier, P., Brown, R. 2001. Micro-assembly planning with van der Waals force. *Journal of Micromechartronics*. 1.2: 139-153.
- Fitzpatrick, J.J., Ahrne, L. 2005. Food powder handling and processing: industry problems, knowledge barriers and research opportunities. *Chemical Engineering and Processing* 44: 209-214.
- Freitas, A. M., Sharma, M. M. 1999. Effect of surface hydrophobicity on the hydrodynamic detachment of particles from surfaces. *Langmuir*, 15: 2466-2476.
- Fuji, M., Machida, K., Takei, T., Watanabe, T., Chikazawa, M. 1998. Effect of surface geometric structure on the adhesion force between silica particles. *Journal of Physical Chemistry B*102: 8782-8787.
- Garcia, A. M., Reche, A. S., Jimenez, C. C., Martinez, J. M., 2005. Influence of the particle size of CaCO₃ on the adhesion of filled EVA materials. *Macromol. Symp.* 221: 23-32.
- Geldart, D., Abdullah, E.C., Hassanpour, A., Nwoke, L. C., Wouters, I. 2006. Characterisation of powder flowability using measurement of angle of repose. *China Particuology*, 4: 104-107.
- George, M., Goddard, D.T., 2006. The characterisation of rough particle contacts by atomic force microscopy. *Journal of Colloid and Interface Science* 299: 665-672.

- Gotzinger, M., Peukert, W. 2003. Dispersive forces of particle-surface interactions: direct AFM measurements and modelling. *Powder Technology* 102-109.
- Gould, W. 1999. *Potato Production Processing and Technology*. CTI Publications, Timonium, MA. pp. 145-156.
- Gould, W. 2001. Potatoes and potato chips. In *Snack Foods Processing* (E.W. Lusas and L. W. Rooney, eds.). Technomic Publishing Co., Lancaster, PA. pp. 227-246.
- Grandison, A.S., Lewis, M.J. 1996. *Separation Processes in the Food and Biotechnologies Principles and Applications*. Woodhead Publishing.
- Greenwood, J.A., Tripp, J.H. 1967. *Journal of Applied Mechanics*, 67:153-159.
- Guy, R., 2001. *Extrusion Cooking, Technologies and Applications*. Woodhead Publishing Limited.
- Hausner, H. H. 1967. *Int Powder Metall.* 3:7-13
- Halim, F., Barringer, S. A. 2007. Electrostatic adhesion in food. *Journal of Electrostatic* 65(3): 168-173.
- Hamaker, H.C. 1937. The London-van der Waals attraction between spherical particles. *Physica IV* 10: 1058-1072.
- Hayes, G.D. 1987. *Food Engineering Data Handbook*, Longman Scientific and Technical, London.
- Hein, K, Hucke, T., Stintz, M, Ripperger, S. 2002. Analysis of adhesion forces between particles and wall based on the vibration method. *Part. Part. Syst. Charact.* 19: 269-276.
- Hui, Y.H. 2006. *Handbook of Food Science, Technology, and Engineering*. CRC Press.
- Israelachvili, J.N. 1992. *Intermolecular and surface forces*. Academic Press, London.
- Jiang, Y., Matsusaka, S., Masuda, H., Qian, Y. 2008. Characterisation the effect of substrate surface roughness on particle-wall interaction with the airflow method. *Powder Technology*, doi:10.1016/j.powtec.2007.11.041.
- Johnson, K. L., Kendall, K., Roberts, A.D. 1971. Surface energy and the contact of elastic solids. *Proc. R. Sco. London, Ser. A* 324:301-313.
- Juliano, P., Barbosa-Canovas, G.V. 2009. Food powders flowability characterisation: theory, methods, and applications. *The Annual Review of Food Science and Technology* 11:3: 211-239.

-
- Kappl, M., Butt, H.J. 2002. The colloidal probe technique and its application to adhesion force measurement. *Part. Part. Syst. Charact.* 19:129-143.
- Karl, A. K., Johan, G. W., Dirk, T. 1991. Particle sizing by laser diffraction spectrometry in the anomalous regime. *Appl. Opt.* 30, 4839-4847.
- Katainen, J., Paajanen, M., Ahtola, E., Pore, V., Lahtinen, J. 2006. Adhesion as an interplay between particle size and surface roughness. *Journal of Colloid and Interface Science*, 304: 524-529.
- Katz, E.E., Labuza, T.P. 1981. Effect of water activity on the sensory crispness and mechanical deformation of snack food products. *Journal of Food Science* 46:403-409.
- Kerr, W.L., Ward, C.D., McWatters, K.H., Resurreccion, A.V.A. 2001. Milling and particle size of cowpea flour and snack chip quality. *Food Research International* 34: 39-45.
- Kippax, P. Measuring particle size using modern laser diffraction technique. Malvern Instruments Ltd. <http://www.chemie.de/articles/e/61205/>. Access date: 23rd September 2009.
- Knowlton, T.M., Carson J.W., Klinzing, G.E., and Yang, Y.C., 1994. The importance of storage, transfer and collection. *Chemical Engineering Progress*, 90: 44-54.
- Krokida, M.K. and Maroulis, Z.B. 1997. Effect of drying method on shrinkage and porosity. *Drying technology* 15 (10): 2441-2458.
- Kulkarni, P. A., Berry, R. J., and Bradley, M.S.A. 2010. Review of the flowability measuring techniques for powder metallurgy industry. Proceedings of the Institution of Mechanical Engineers, Part E: *Journal of Process Mechanical Engineering* 2010 224:159.
- Kunzt, L. A. 1996. Seasoning secrets for salty snacks. <http://www.foodproductdesign.com/archive/1996/0196DE.html>. Access date: 28 Feb 2004, Northbrook, Weeks Publishing Co.
- Lam, K.K., and Newton, J.M. 1991. *Powder Technology* 65:167.
- Larsen, R.I. 1958. The adhesion and removal of particles attached to air filter surfaces. *Am. Indust. Hygiene J.* 19:265-270.
- Leniger, H.A. and Beverloo, W.A. 1975. Food Process Engineering, Reidel, Dordrecht.
- Li, Q., Rudolph, V., Peukert, W., 2006. London-van der Waals adhesiveness of rough particles. *Powder Technology*, 161: 248-255.
- Lusas, E.W. and Rooney, L.W. 2001. Snack Foods Processing. CRC Press.
Can be previewed from:
http://books.google.co.uk/books?hl=en&lr=&id=W_5wlzckPkMC&oi=fnd&pg=P

R14&dq=lusas,+rooney&ots=sf9rBsfO9i&sig=OoGXJU60McAqawxIS91xX9dB
Djk#PPP1,M1.

- Maugis, D. 1992. *Journal of Colloid Interface Science*, 150: 243-269.
- Mayr, M. B., Barringer, S. A., 2006. Corona compared with triboelectric charging for electrostatic powder coating. *Journal of Food Science* 71(4): 171-177.
- Mazumder, M.K., Wankum, D.L., Sims, R.A., Mountain, J.R., Chen, H., Pettit, P., Chaser, T. 1997. Influence of powder properties on the performance of electrostatic coating process. *Journal of Electrostatics*, 40&41: 369-374.
- McCave, I.N., Syvitski, J.P.M., 1991, Principles and methods of geological particle size analysis, *in* Syvitski, J.P.M., ed., Principles, Methods and Applications of Particle Size Analysis: New York, Cambridge University Press, p. 3-21.
- Melton, S. L., Trigiano, M. K., Penefield, M. P., Yang, R. 1993. Potato chips fried in canola and/or cottonseed oil maintain high quality. *Journal of Food Science* 58(5): 1079-1083.
- Michalski, M.C., Desobry, S., Hardy, J. 1997. Food materials adhesion: a review. *Crit. Rev. Food Sci. Nutr.* 7(7): 591-619.
- Mittal, K.L. 1997. Role of interface in adhesion phenomena. *Polym. Eng. Sci.* 17(7): 467-473.
- Moreira, R., Sun, X., Chen, Y., 1997. Factors affecting oil uptake in tortilla chips in deep-fat frying. *Journal of Food Engineering* 31 (4): 485-498.
- Nedderman, R. M. 1992. Statics and kinematics of granular materials. University Press, Cambridge, England.
- Newton, J.M., Lam, K.K. 1992. Effect of temperature on particulate solid adhesion to a substrate surface. *Powder Technology* 73: 267-274
- Miller, M. J., Barringer, S. A., 2002. Effect of sodium chloride particle size and shape on nonelectrostatic and electrostatic coating on popcorn. *Journal of Food Science* 67(1): 198-201.
- Mittal, K.L. 1991. Particles on Surfaces: Detection, Adhesion and Removal, Vol 1-3. Plenum Press, New York.
- Niman, C. E. 2000. In search of the perfect salt for topping snack foods. *Cereal Foods World* 45(10): 466-469.
- NIST Guide for the Use of the International System of Units (SI) Special Publication 811, (1995) page 51.
- Oliveira, R. 1997. Understanding adhesion: a means for preventing fouling. *Experimental Thermal and Fluid Science*, 14:316-322.

- Otsuka, A., Iida, K., Danjo, K., Sunada, H. 1988. Measurement of the adhesive force between particles of powdered materials and a glass substrate by means of the impact separation method. III Effect of particle shape and surface asperity. *Chem. Pharm. Bull.* 36(2): 741-749.
- Paajanen, M., Katainen, J., Pakarinen, O.H., Foster, A.S., Lahtinen, J. Experimental humidity dependency of small particle adhesion on silica and titania. *Journal of Colloid and Interface Science* 304: 518-523.
- Packham, D.E. 1996. Work of adhesion: contact angles and contact mechanics. *Journal of Adhesion and Adhesives*, 16: 121-128.
- Pedreschi, F., Moyano, P., 2005. Effect of predrying on texture and oil uptake of potato chips. *Lebensmittel Wissenschaft Technology* 38(6): 599-604.
- Peleg, M. 1978. Flowability of food powders and methods for its evaluation-a review. *Journal of Food Process Engineering* 1:303-328.
- Peleg, M. 1983. Physical Characteristics of Food Powders. In Physical properties of foods (Ed Peleg & Bagley). The AVI Publishing Company, Inc, Westport, Connecticut.
- Podczek, F. 1998. Particle-particle adhesion in pharmaceutical powder handling. Imperial College Press, London, Great Britain.
- Podczek, F. 1999. Investigations into the reduction of powder adhesion to stainless steel surfaces by surface modification to aid capsule filling. *Int. J. Pharm.* 178: 93-100.
- Quesnel, D.J., Rimai, D.S., Sharpe, L.H. 2001. Particle Adhesion: Applications and Advances. Taylor and Francis, New York.
- Quevedo, R., Aguilera, J.M. 2004. Characterisation of food surface roughness using the glistening points method. *Journal of Food Engineering* 65: 1-7.
- Ratanatriwong, P., Barringer, S. 2007. Particle size, cohesiveness and charging effects on electrostatic and nonelectrostatic powder coating. *Journal of Electrostatics*, 65: 704-708.
- Rennie, P. R., Chen, X. D. and Mackereth, A.R. 1998. Adhesion characteristics of whole milk powder to a stainless steel surface. *Powder Technol* 97: 191-199.
- Ricks, N.P., Barringer, S.A., Fitzpatrick, J.J. 2002. Food powder characteristics important to nanoelectrostatic and electrostatic coating and dustiness. *Journal of Food Science*, 67:2256-2263.
- Rimai, D.S., DeMejo, L.P., Verrland, W. 1992. *Journal of Applied Physics*, 71:2253-2258.

- Ripperger, S., Hein, K. 2004. Measurement of adhesion forces between particles and rough substrates in air with the vibration method. *KONA* 22:121-133
- Polke, R. 1969. Adhesion of solids at elevated temperatures. *Adhesion et Physico-Chimie des Surfaces Solides* 51-54.
- Ranade, , M.B. 1987. Adhesion and removal of fine particles on surfaces. *Aeresol Science and Technology*, 7: 161-176.
- Rennie, P.R., Chen, X.D., Mackereth, A.R. 1998. Adhesion characteristics of whole milk powder to a stainless steel surface. *Powder Tech.* 97:191-199.
- Russ, B. E., Talbot, J. B. 1998. A method for measuring the adhesion strength of powder coatings. *Journal of Adhesion* 68: 257-268.
- Russ, B.E. 1997. A study of the adhesion of electrophoretically deposited phosphors, Ph.D. Dissertation, University of California, San Diego.
- Salazar-Banda, G.R., Felicetti, M.A., Goncalves, J.A.S., Coury, J.R. and Aguiar, M.L. 2007. Determination of the adhesion force between particles and a flat surface, using a centrifuge technique. *Powder Technology* 173: 107-117.
- Sandadi, S., Pandey, P., Turton, R. 2004. In situ, near real-time acquisition of particle motion in rotation pan coating equipment using imaging techniques. *Chemical Engineering Science* 59: 5807-5817.
- Segnini , S., Dejmek, P., Oste, R., 1999. Reproducible texture analysis of potato chips. *Journal of Food Science* 64: 309-312.
- Shaefer, D. M., Carpenter, M., Reifenberger, R., Demejo, L.P., Rimai, D.S. 1994. Surface force interactions between micrometer-size polystyrene spheres and silicon substrates using atomic force techniques. *Journal of Adhesion Science and Technology* 8: 197-210.
- Shaun H., Campbell, S.N., Brian D. R., Steve C., Maurice W. W. 2001. Effect of mica on particle-size analyses using the laser diffraction technique. *Journal of Sedimentary Research* 71-3: 507-509.
- Shimada, Y, Yonezawa, Y., Sunada, H. 2003. Measurement and evaluation of the adhesive force between particles by the direct separation method. *Journal of Pharmaceutical Sciences*, 92: 560-568.
- Shrankel, K. R. 2004. Safety evaluation of food flavourings. *Toxicology* 198:203-211.
- Shubert,H., 1987. Food Particle Technology, Part I: Properties of particles and particulate food systems, *Journal of Food Engineering*, 6: 1-32.
- Soltani, M, Ahmadi, G. 1995. *Phys. Fluids*, 7A:647-657.

- Sonnenberg, J. P., Schmidt, E., 2005. Numerical calculation of London-van der Waals adhesion force distributions for different superquadric shaped particles. *Part. Part. Syst. Charact.* 22: 45-51.
- Strumpf, D.M. 1986. Selected particle size determination techniques, *Manufacturing Confectioner*, 66, 111-114.
- Sumawi, H., Barringer, S.A. 2005. Positive vs. negative electrostatic coating using food powders. *Journal of Electrostatics* 63:815-821.
- Takeuchi, M. 2006. Adhesion forces of charged particles. *Chemical Engineering Science* 61: 2279-2289.
- Tang, J., and Busnaina, A.A. 2000. The effect of time and humidity on particle adhesion and removal. *Journal of Adhesion* 74: 411-419.
- Teunou, E., Fitzpatrick, J.J., 1999. Effect of relative humidity and temperature on food powder flowability. *Journal of Food Engineering* 42: 109-116.
- Teunou, E., Fitzpatrick, J.J., Synnott, E.C., 1999. Characterisation of food powder flowability. *Journal of Food Engineering* 39: 31-37.
- Tillman D.A. 2000. Biomass cofiring: the technology, the experience, the combustion consequences. *Biomass & Bioenergy* 19: 365-384.
- Tisai, C.J., Pui, D.Y.H., Liu, B.Y.H. 1991. *Journal of Aerosol Science and Technology*, 15: 239-255.
- Vasquez, D., Cecil, J., Shashikanth, B. 2005. An investigation of van der Waals forces in the assembly of micro devices. *Proceedings of the 2005 Annual IERC*, Atlanta, GA.
- Walz, J.Y. 1998. The effect of surface heterogeneities on colloidal forces. *Adv. Colloid Interface Sci.* 74: 119-168
- Willing, G. A., Ibrahim, T. H., Etzler, F. M., Neuman, R. D. 2000. New approach to the study of particle-surface adhesion using atomic force microscopy. *Journal of Colloid Interface Science* 226:185-188.
- Wong, D.C.Y., Adams, M.J., Seville, J.P.K. and Fryer, P.J. 2005. A computational model of flavour deposition onto food surfaces. *Food and Bioproducts Processing* 83(C2): 99-106.
- Yousuf, S, Barringer, S.A. 2007. Modeling nonelectrostatic and electrostatic powder coating. *Journal of Food Engineering*, 83: 550-561.
- Yu, H., MacGregor, J.F. 2003. Multivariate image analysis and regression for prediction of coating content and distribution in the production of snack foods. *Chemometrics and Intelligent Laboratory Systems* 67: 125-144.

Zimon, D. 1982. Adhesion of dust and powder. 2nd ed. New York.

Zimon, A.D., 1969. Adhesion of dust and powder. New York, Plenum Press, p: 424.

APPENDICES

Appendix 1. Dimensions of platen of IAT

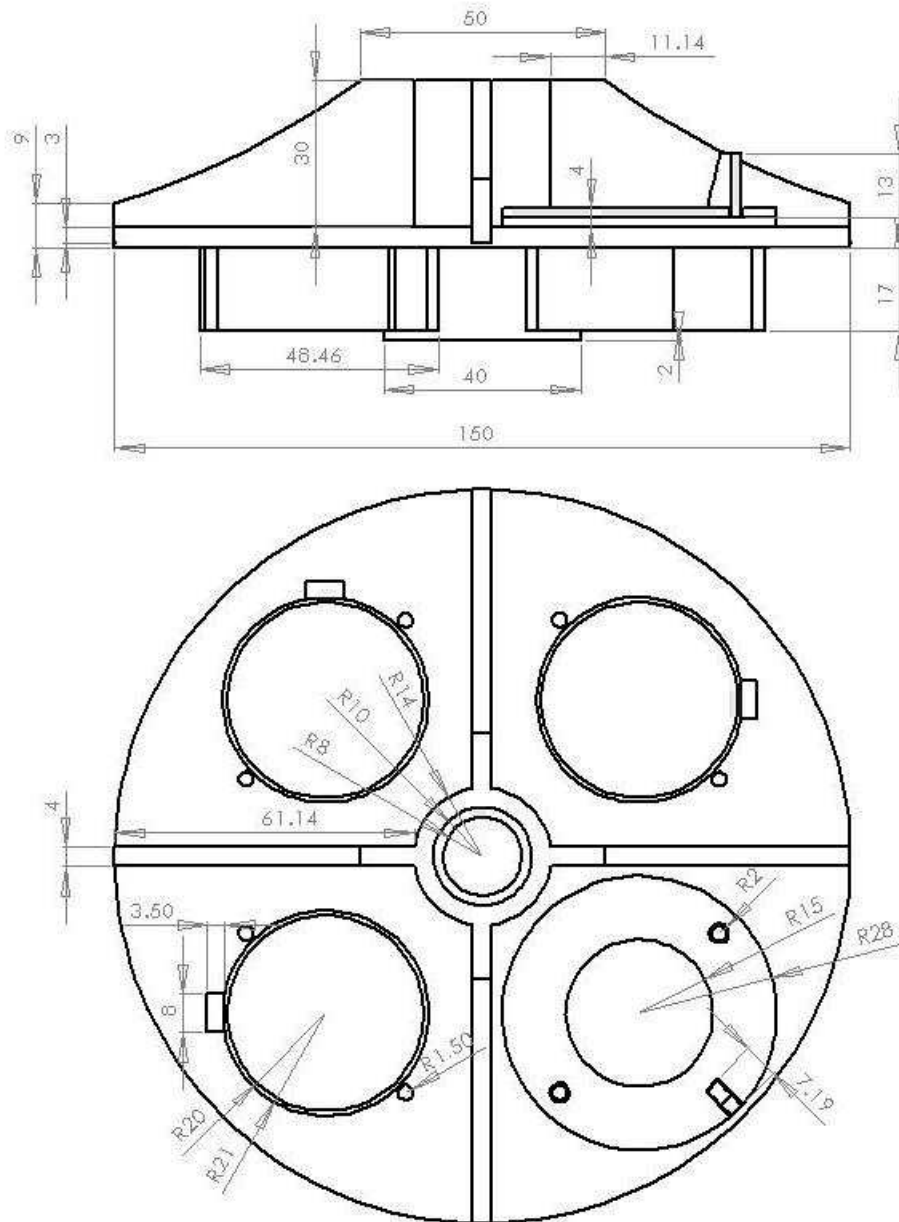
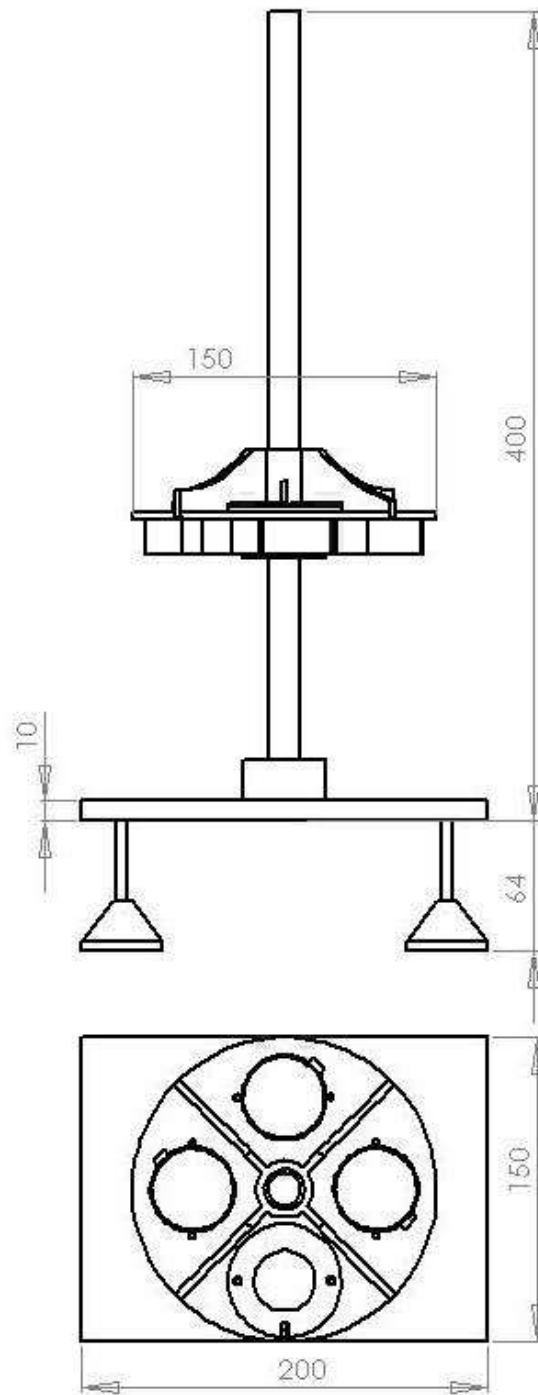


Figure A-1. Dimensions of IAT platen (mm)

Appendix 2. Parts of IAT and their dimensions

Table A-1. Components of IAT are shown in Appendix E

Item name	Quantity	Dimensions (mm)
Cylindrical shaft	1	16 x 200
Steel plate	1	150 x 200
Adjustable foot	4	D=4, h=65
Stopper	1	D=30 h=20
Platen	1	D=150 thickness=3
Ball bearing	1	ID= 16, OD= 24, h=30
Sample holder upper part	4	ID=30, OD=60, thickness=2, h=8
Sample holder bottom part	4	ID=30, OD=60, thickness=2, h=8
Plastic Petri dish	4	ID= 35, thickness=15, h=10
Screw	8	3x10 (M3)
Bubble level	1	-
Tweezers	1	-
Substrate placing tool	1	-
Ruler	1	300

Appendix 3. Dimensions of IAT**Figure A-2.** Dimensions of IAT (mm)

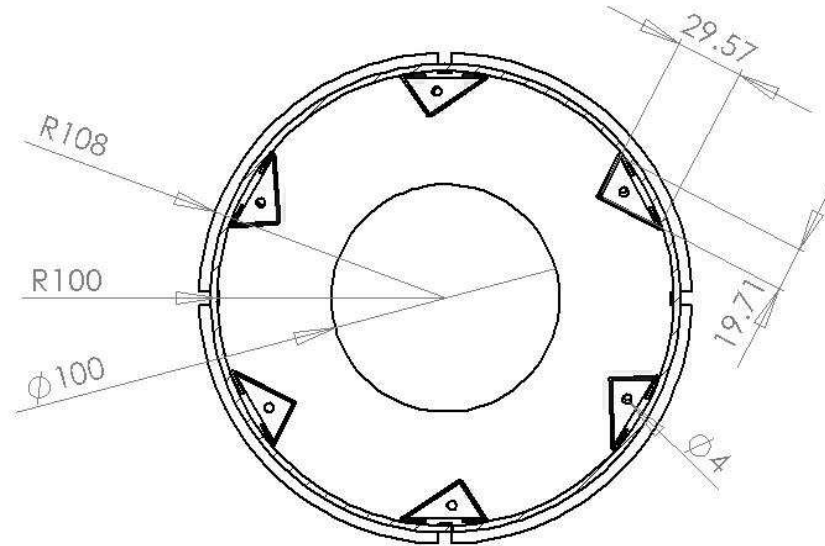
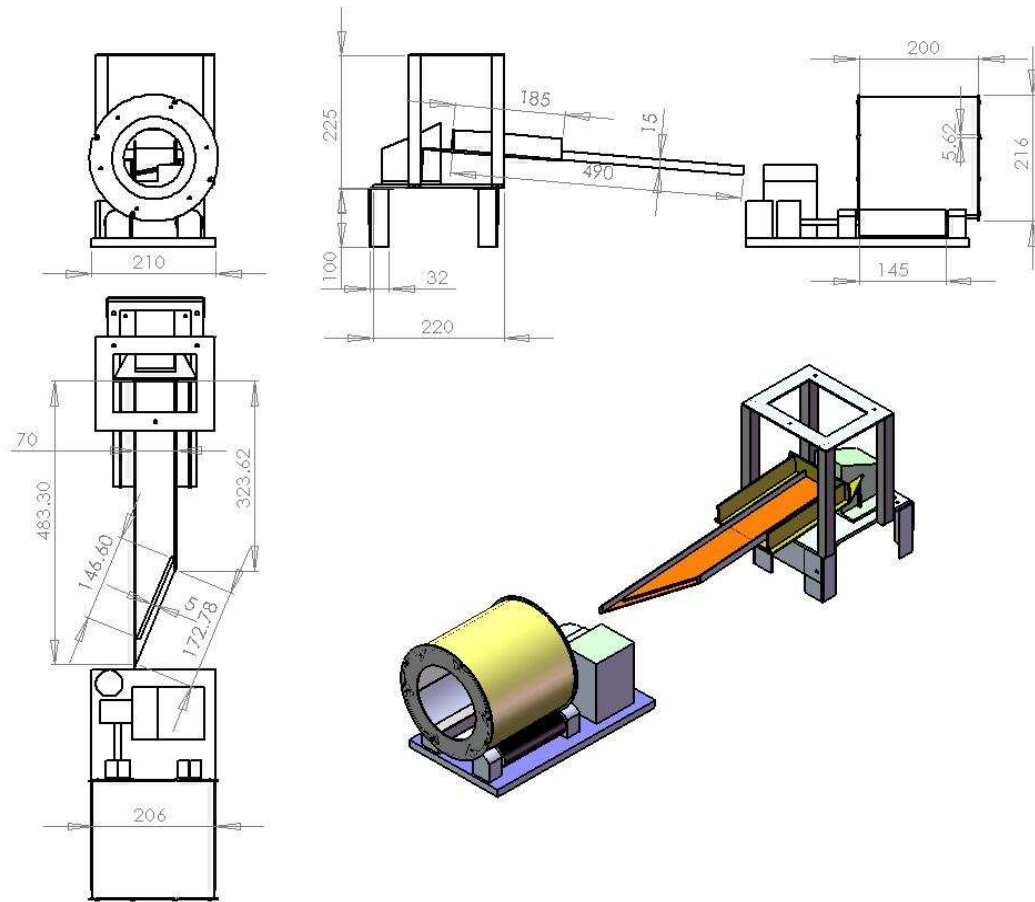
Appendix 4. Dimensions of tumbler mixer

Figure A-3. Dimensions of tumbler mixer (mm). Length: 200 mm

Appendix 5. Dimensions of vibratory feeder**Figure A-4. Dimensions of powder feeder unit (mm)**

Appendix 6. Acceleration of dropped objects

Acceleration is the time rate of change of velocity and is measured in $(m/s)/s$. A ‘g’ unit is a unit of acceleration equal to Earth’s gravity at sea level ($9.81 m/s^2$).

It has been reported that the objects may impact rigid surfaces with very large accelerations when dropped from a height of one meter. Lower mass objects tend to result in greater accelerations (Endevco, 2007). The amount of acceleration of a dropped object is proportional to the square root of the drop height, and the inverse of the pulse width (Endevco, 2007).

The dropping object onto a horizontal surface starts at rest, and free-falls to impact a rigid surface after travelling a distance, d_1 , as shown in Figure A5. After impact, the object rebounds upward to some height d_2 .

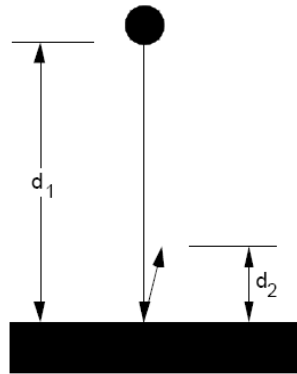


Figure A-5. Free-fall of and object

A constant acceleration due to gravity acts on an object in free-fall, and the velocity increases in the downward (negative) direction as

$$v(t) = gt \tag{A1}$$

The distance travelled is

$$d(t) = \frac{1}{2}gt^2 \quad (\text{A2})$$

These two equations may be combined to determine the velocity of the object immediately prior to impact

$$v_1 = -\sqrt{2gd_1} \quad (\text{A3})$$

Just before impact, the object is still in free-fall. During impact, the object must stop its downward course, and reverse its direction. This is where the high level acceleration occurs. Acceleration is, by definition, the rate of change of velocity. The faster the object changes from downward velocity to upward velocity, the greater the acceleration.

$$a = \frac{\Delta v}{\Delta t} \quad (\text{A4})$$

In general, more massive objects take more time to rebound. While the change of velocity of more massive and less massive objects is equal when they rebound from a horizontal surface, the more massive object takes more time to rebound (and has a longer pulse width), so Δt is greater, resulting in less acceleration as shown by equation 4. Because of this, lighter objects will tend to exhibit shorter pulse widths and greater acceleration levels.

The wave shape referred to as a half sine is used to describe the output of an accelerometer during a drop shock. The half sine can be used as a model to predict the behaviour of drop shock phenomena. A plot of acceleration versus time of a half sine shock will look something like that shown in Figure A6.

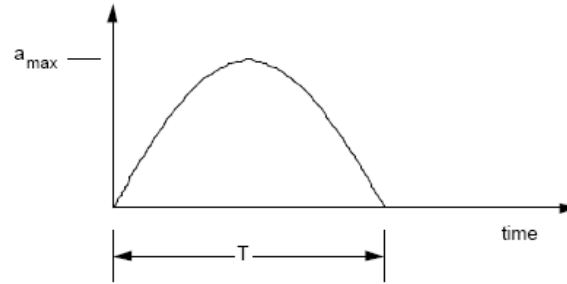


Figure A-6. The half sine of a dropped object

The velocity is the integral of the acceleration, plus an integration constant. Integrating the half sine results in a ‘half cosine’, and would look something like that shown in Figure A7, below.

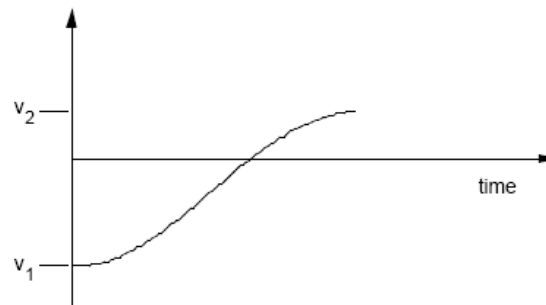


Figure A-7. Half cosine of a dropped object

To set the boundary conditions of the velocity curve, v_1 is simply the velocity immediately before impact and v_2 is the velocity immediately after impact.

The peak acceleration in a drop shock is primarily depend on two things: (i) The inverse of pulse width. Shorter pulse widths result in higher accelerations. (ii) The square root of the drop and rebound distance. Assuming minimal rebound, doubling the drop height result in a 41% higher shock (Endevco, 2007).

$$a_{peak} = \frac{\pi}{T} \sqrt{\frac{g}{2}} (\sqrt{d_2} + \sqrt{d_1}) \quad (A5)$$

$$g_{peak} = 0.71 \frac{\sqrt{d_2} + \sqrt{d_1}}{T} \quad (A6)$$

Where d_1 and d_2 are in meters and T in seconds. The pulse width T is dependent on the shape and material properties of the dropped object and the impact surface.

For generalization purposes, let say dropped object a solid mass of some material and when impacts a rigid surface, the object deforms (compresses), and may rebound back upwards. The acceleration can be expressed as:

$$a = \sqrt{\frac{EAgd_1}{hm}} \quad (A7)$$

Where E is the elasticity modulus, A is the area being compressed, h is the compressed height, g is the gravity, d_1 is the rebound distance, and m is the mass of the object. From this basic equation, a number of conclusions can be deduced.

- Greater acceleration levels will be achieved when the surface area, A , is increased. Flat-on-flat impacts generates greater accelerations than sharp corner impacts.
- Higher drop distance produce greater acceleration.
- Lower mass objects cause greater acceleration.
- Stiffer object (higher modulus) achieve greater acceleration.

Some estimated peak acceleration levels are given in Table A2 (various drop height and pulse width)

Table A-2. Estimated peak decelerations

Pulse width (msec)	cm	15	30	60	90	120	150
	0.010	28000	39000	55000	68000	78000	87000
0.013	21000	30000	42000	52000	60000	67000	
0.016	17000	24000	34000	42000	49000	55000	
0.020	14000	20000	28000	34000	39000	44000	
0.025	11000	16000	22000	27000	31000	35000	
0.032	8600	12000	17000	21000	24000	27000	
0.040	6900	10000	14000	17000	20000	22000	
0.050	5500	7800	11000	14000	16000	17000	
0.063	4400	6200	8800	11000	12000	14000	
0.079	3500	4900	7000	8600	10000	11000	
0.100	2800	3900	5500	6800	7800	8700	
0.13	2200	3100	4400	5400	6200	6900	
0.16	1700	2500	3500	4300	4900	5500	
0.20	1400	2000	2800	3400	3900	4400	
0.25	1100	1600	2200	2700	3100	3500	
0.32	870	1200	1700	2100	2500	2800	
0.40	690	1000	1400	1700	2000	2200	
0.50	550	780	1100	1300	1600	1700	
0.63	440	620	870	1100	1200	1400	
0.79	350	490	690	850	1000	1100	
1.0	280	390	550	680	780	870	
1.3	220	310	440	540	620	690	
1.6	170	250	350	430	490	550	
2.0	140	200	280	340	390	440	
2.5	110	160	220	270	310	350	
3.2	87	120	170	210	250	280	
4.0	69	100	140	170	200	220	
5.0	55	78	110	130	160	170	
6.0	46	65	90	110	130	150	
8.0	34	49	69	84	100	110	
10	28	39	55	68	78	87	
12	23	33	46	56	65	73	
16	17	25	35	43	49	55	
20	14	20	28	34	39	44	
25	11	16	22	27	31	35	
32	9	12	17	21	25	28	
40	7	10	14	17	20	22	
50	6	8	11	13	16	17	
63	4	6	9	11	12	14	
79	4	5	7	9	10	11	
100	3	4	6	7	8	9	

Selecting a right accelerometer and signal conditioner affects the quality of measurement. There are points need to be considered before selection:

- Size and shape of the object to be measured
- Type of accelerometer mounting
- Type of measurement
- Dynamic characteristics of accelerometer
- Transfer characteristics of amplifier
- Frequency range and resolution of analog-to-digital conversion

Some typical accelerometer applications are:

- Tilt/Roll
- Vibration detection
- Vehicle skid detection
- Impact detection
- Feedback for active suspension control system

Eq. A8 can be used to calculate the inferred deceleration of objects

$$g_{peak} = 0.71 \frac{\sqrt{d_1} + \sqrt{d_2}}{T} \quad (A8)$$

d1: drop distance (m)

d2: jump distance (m)

T: pulse width (s)

Appendix 7. Calibration certificate of IEPE accelerometer

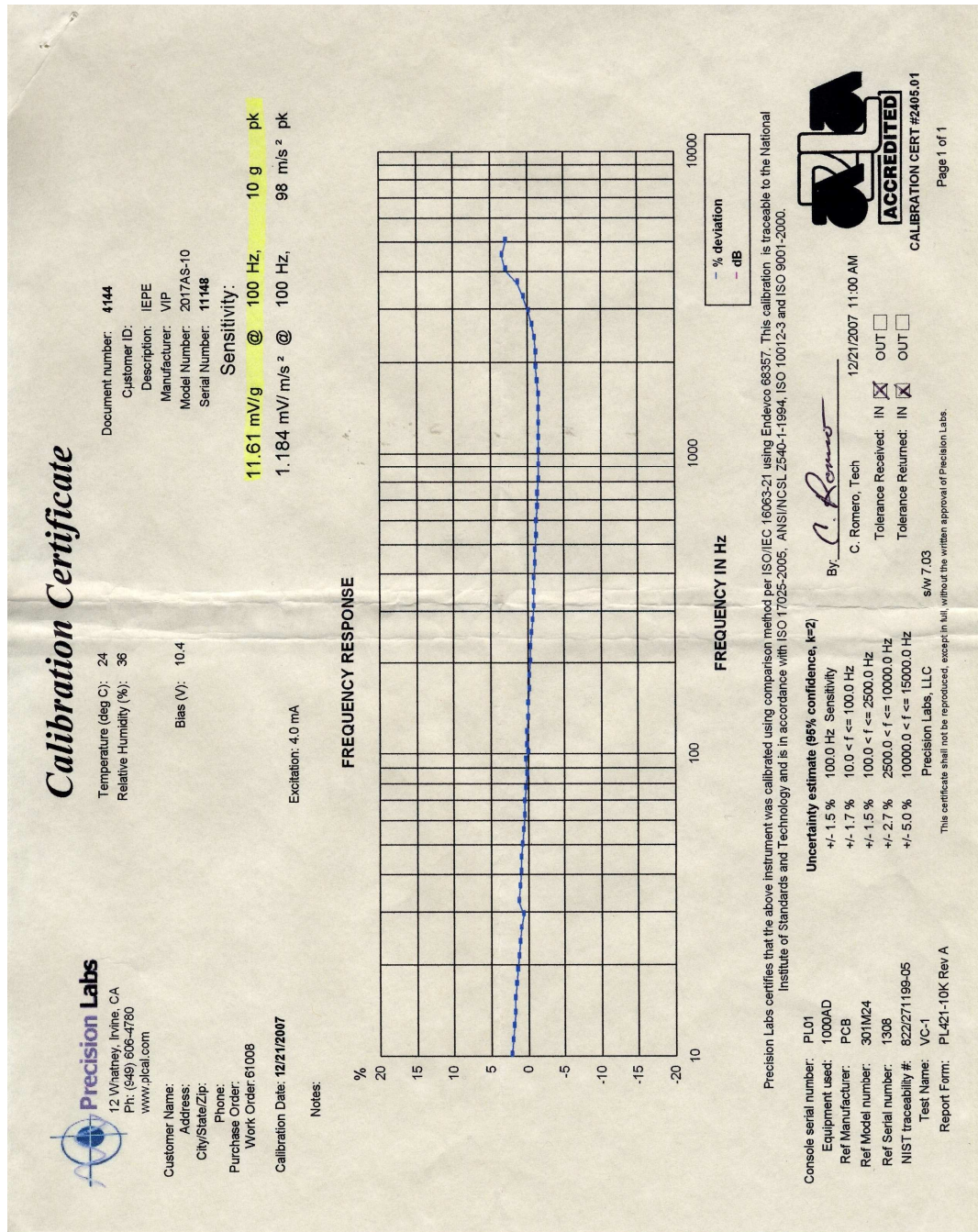
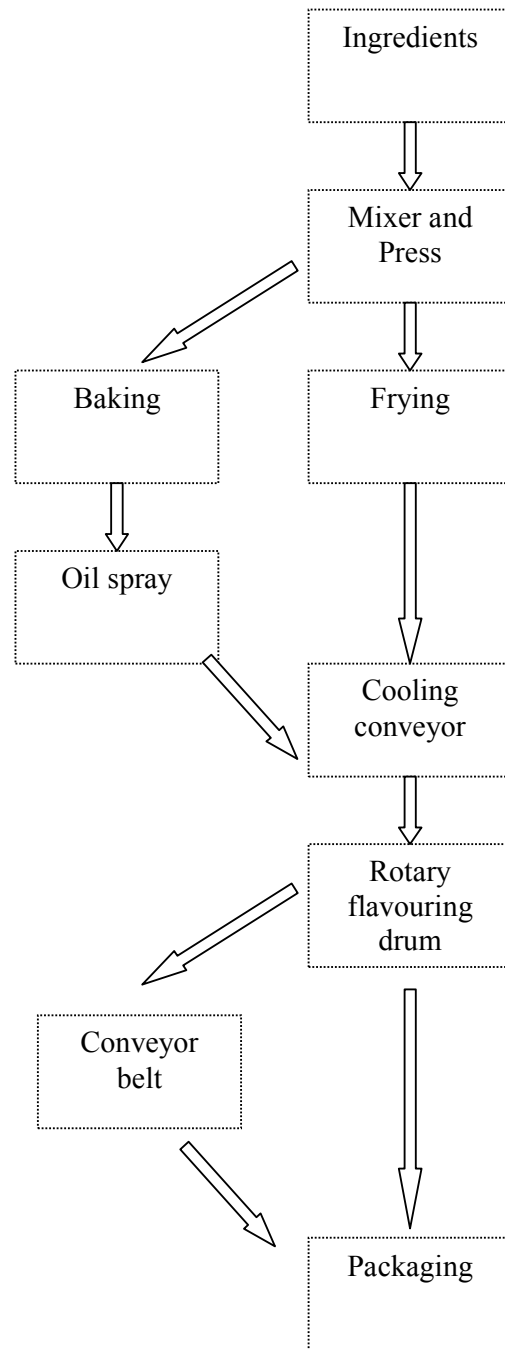


Figure A-8. Calibration certificate of IEPE accelerometer

Appendix 8. Crisp production process flow diagram**Figure A-9.** Crisp production flow diagram